Doctoral Thesis

Modeling of Radiation-induced Dimensional Instability of Metals and Alloys in Nuclear Systems: Improved Understanding of the Stress and Alloying Elements Effects by Rate Theory

Sang Il Choi

Department of Nuclear Engineering

Graduate School of UNIST

2019

Modeling of Radiation-induced Dimensional Instability of Metals and Alloys in Nuclear Systems: Improved Understanding of the Stress and Alloying Elements Effects by Rate Theory

Sang Il Choi

Department of Nuclear Engineering

Graduate School of UNIST

Modeling of Radiation-induced Dimensional Instability of Metals and Alloys in Nuclear Systems: Improved Understanding of the Stress and Alloying Elements Effects by Rate Theory

A thesis/dissertation
submitted to the Graduate School of UNIST
in partial fulfillment of the
requirements for the degree of
Doctor of Philosophy

Sang Il Choi

12/06/2018
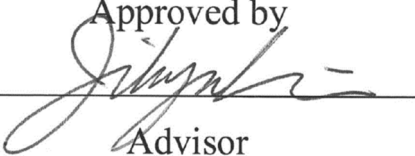
Approved by

_____

Advisor
Prof. Ji Hyun Kim
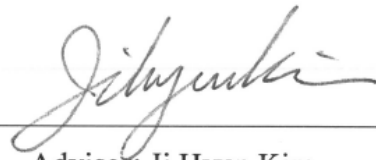
Modeling of Radiation-induced Dimensional Instability of Metals and Alloys in Nuclear Systems: Improved Understanding of the Stress and Alloying Elements Effects by Rate Theory
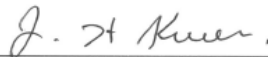
Sang Il Choi

This certifies that the thesis/dissertation of Sang Il Choi is approved.
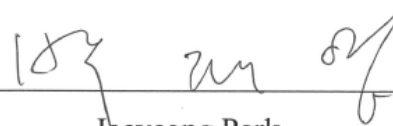
12/06/2018

_____
Advisor: Ji Hyun Kim

_____
Junhyun Kwon

_____
Chi Bum Bahn

_____
Sangjoon Ahn

_____
Jaeyeong Park

Abstracts

Historically a rate theory is one of the most favorite modeling methodologies to simulate the radiation effects on structural materials for nuclear reactors. The easy usability of rate theory, caused by various simplification, could help many researchers to grasp fundamental the understanding. However, simplification in rate theory gives not only easy accessibility but also inaccurate information. Various effect such as alloying element, stress, and cascade effect were neglected because lattice distortion could not be directly considered. Hence, in this paper, to overcome the simplification of rate theory, two approaches had been applied to enhance the performance of the rate theory. In the first approach, detail behavior of defect, which is derived by the state of art simulation tools, were adopted in diffusion coefficient under the stress and alloying element condition. In the second, cascade effect on sink annihilation was considered by a fitting method from the experimental observation.

The stress effect on interstitial diffusivity also recently studied by MD simulations. C. Kang and M. Banislaman show that migration energy of interstitial and its clusters is reduced by applied stress in iron. Hence in this study, irradiation swelling, and creep is predicted by considering the recent calculation result. In ultra-long fuel cycle condition, hoop stress could be nearly up to 600 MPa. By MD simulation it was observed that diffusivity of interstitial has 8.437×10^{-5} cm^2/s at 873 K. This value was 11 times higher than non-stress applied condition (7.414×10^{-6} cm^2/s).

In detail, M. Christensen reveals that Nb decreases the interstitial diffusivity nearly 1/5.64 at 500 K and 1/5.88 at 700 K with 0.5 % Nb in zirconium. Also, the same method was applied to account the Sn effect. Sn shows the high dependency with temperature and relatively less effect than Nb. Interstitial diffusivity is decreased about 1/4.05 at 500 K and 1/1.38 at 700 K with 2.5 Sn. This information was adopted in rate theory and then irradiation growth was predicted. By adding 0.5 % Nb in cold-worked zirconium, 0.2 % strain is obtained whilst cold-worked pure zirconium shows nearly 0.3 % strain at 10 dpa. Since there was no experiment about irradiation growth of Zr-0.5Nb, Zr-2.5Nb experimental result was compared with simulation results.

In case of cascade annihilation of sinks, there is no study including theoretical method. However, by F. Garner, it was experimentally observed that network dislocation density of iron-based alloy is saturated nearly 10^{11} cm^2 no matter how fabrication process is applied to the specimen. Hence by the fitting method, sink annihilation rate by cascade is adopted in rate theory. As results, irradiation swelling rate is decreased by nearly 30 % compared with non-considering the cascade annihilation of sink case.

Until now, three representative types of rate theory were developed in the research area of radiation effect; these are SRT, CDM, and PBM. In case of SRT and CDM, there is no big difference except the consideration of cluster number density. However, there is a large gap between PBM and SRT/CDM because 1-D reaction kinetics, caused by mobile interstitial cluster, is accounted in PBM.

Since the purpose of this dissertation is an improvement of scientific understanding of the RIDI behavior within rate theory frames, there was attempting to verify the stress and alloy element effect between SRT and PBM in zirconium, and between CDM and PBM in iron. However, unfortunately, in case of zirconium, PBM could not be carried out because many parameters for cluster such as migration, formation, and binding energy are not discovered. Hence, stress and alloy element effect were verified only in SRT. In case of an iron-based alloy, since there was significant progress about study of defect behavior, stress and alloy effect could be examined in between CDM and PBM.

There was also a conventional way to account the stress and alloy element effect. To improved scientific understanding, the result of the conventional method and results of this work are compared in the discussion chapter. Therefore, the result of this study could enhance the fundamental understanding of radiation effect on structural materials because various effects were considered within various rate theory frame.

To My Mother, Do Young Lee

Table of Contents

List of figures

List of tables

Abbreviation

1-D: One dimensional

3-D: Three dimensional

CDM: Cluster dynamic modeling

CP-3: Chicago pile-3

DAD: Diffusion anisotropy difference

FBR: Fast breeder reactor

NRL: Northern research laboratories

MSD: Mean square displacement

PBM: Production bias modeling

PWR: Pressurized water reactor

RIDI: Radiation-induced dimensional instability

SIPG: Stress-induced preferred growth

SPIA: Stress preferential induced attraction

SPIN: Stress induced preferred nucleation

SRT: Standard rate theory

TDE: Threshold displacement energy

UKAEA: Atomic energy authority in UK

I   Introduction

I.1   Research background:

In nuclear engineering history, aluminum, zirconium, and iron are firstly considered as cladding materials. Until now, these materials are still used for cladding because the properties of each material are optimized in various aspects. There were numerous attempts to development a new advance alloy system over the 70 decades. As a result, Oxide dispersion-strengthened alloy, high entropy alloy, functional grade materials and Sic composite are considered as candidate materials for cladding of next-generation nuclear reactor. However, despite these efforts, there are limitations to replace the conventional materials by new alloy system because verification is needed to confirm that new alloy system could maintain adequate properties such as ductility, compatibility, weldability, toughness, mechanical, corrosion resistant, irradiation resistant and thermal conductivity.

In this circumstance, a fundamental understanding of the radiation effect on conventional materials could be a valuable study in an engineering point of view. Among the various radiation effects on materials, Radiation-Induced Dimensional Instability (RIDI) is one of the most important factors for a design principle. Therefore, the objective of this thesis dissertation is the improvement of the scientific understanding of the RIDI behavior of cladding and structural materials in various reactor conditions for the development of a prediction model of RIDI.

In specifically, the RIDI behavior of zirconium and its alloys were investiged for pressure tube condition in CANDU reactor. In case of iron and its alloys, environmental condition were assumed as that of Fast Breeder Reactor (FBR). Irradiation growth and creep of Zr-2.5Nb pressure tube determine the life of the CANDU reactor. Hence simulation result of this study could contribute to the safety analysis of CANDU rector with fundamental understating. Not only zirconium and its alloys but also iron and its alloys are important issued as cladding materials in FBR. Hence this study could contribute the safety analysis of cladding materials.

Until now, many types of researches about RIDI have been carried out. There are significant progress about rate theory including the development of Production Bias Modeling (PBM) [1], Diffusion Anisotropy Difference (DAD) [2], and Cluster Dynamic Modeling (CDM) [3]. Nevertheless, there is no general model to explain RIDI because too many parts of defect behavior remain with un-known. In detail, the scientific understanding of defect reaction kinetics should be defined in various environment situations. However, only limited information about alloy element and stress effect on defect behavior is revealed in irradiation situation. Moreover, cascade effects on defect generation or

sink annihilation had not been studied extensively. Hence in this study, to grasp the improved the fundamental understanding, RIDI was calculated by combining between various rate theory and the recent results of state of art simulation tools.

I.2   First discovery of RIDI

The first historical discovery of RIDI is from the fissile material such as uranium and plutonium. Radiation-induced anisotropic swelling was firstly confirmed in uranium rod in the 1950s and then subsequently degradation of cladding materials was also found in 1960s [4]. Before the radiation-induced degradation is discovered, those kinds of the phenomenon are already predicted by Wigner who is famous for the symmetry principle in quantum physics physic. It was an obviously predictable phenomenon because the high energy particle destroys the lattice ordering [5]. In order to confine the characteristic of uranium deformation, a single crystal of uranium metal was tested. Form the test results, it was confirmed that the uranium matrix is elongated by <010> direction and shorten by <100> direction.

Subsequently, irradiation creep and growth of cladding materials were discovered and then other structure materials for nuclear power plants could gain research interest. In the early 1960s, RIDI of iron-based materials was firstly confirmed by an experiment. In 1967, the swelling phenomenon of stainless steel was firstly figured by Cawthorne [6]. From a few nanometers up to more 150 nanometers, the cavity was founded by an electron.

In case of fuel materials, the degree of radiation damage is much more severe than cladding material because not only neutron but also fission fragments bombard the lattice ordering. Hence irradiation swelling is unavoidable phenomena in nuclear fuel system [7]. However, in the case of cladding materials, depend on based metal, the volume could be conserved, i.e. irradiation swelling could not occur. By experimental observation, it was confirmed that there are three representative dimensional changes by radiation in cladding materials [8]. Those are irradiation growth, swelling, and creep. These dimensional changes are classified by volume and stress.

1.   Irradiation growth is volume conservative distortion without applied stress;

2.   Irradiation swelling is the isotropic volume expansion without any applied stress;

3.   Irradiation creep is the volume conservative distortion by the applied stress.

I.3   A brief history of development of cladding materials

The first modern type cladding was an aluminum alloy in Chicago pile-3 (CP-3) because aluminum has fairly good properties as structural materials at low-temperature condition (However, the poor corrosion properties of aluminum lead to its replacement at CP-3 condition) [9]. The advantages of aluminum as structural materials include low mass density, low neutron reaction cross section, high thermal conductivity, and high specific heat. Hence aluminum cladding is still used for research reactor condition. However, irradiation swelling occurs, and heat conductance is decreased by the accumulation of radiation damage.

The iron-based alloy was chosen as cladding material because chrome element could increase corrosion resistant with high mechanical strength in high-temperature condition. From the experimental result of Chicago pile-1, researchers confirmed that neutron chain reaction could be sustainable and controllable. And then, researchers focus was moved on the development of a new type of reactor, where fissile materials could consistently be generated for its power resource, i.e. breeding of fissile materials. As result concept of FBR was developed. Since one of the most important characteristics of FBR is using the fast neutron, cladding material is exposed in a harsh radiation condition. SS 316 shows severe irradiation creep and swelling behavior. Depending on materials properties, irradiation swelling occurred from 5 % to 30 %. Which give motivation for the researcher to develop a new iron-based alloy. Subsequently advanced iron-based alloy is developed for cladding candidate materials in FBR. Since in the FBR condition, cladding candidate materials must maintain corrosion resistant property and reasonable mechanical strength, ferritic martensitic stainless steel was chosen for cladding material. As results, various type of high chrome steel were tested in Experiment Breeder Reactor-II [10]. HT-9 maintain its dimensional integrity until 200 dpa.

Early in 1970s navy admire H. Rickover designed the Pressurized Water Reactor (PWR) system to prevent sodium and water reaction in seawater [11]. Simultaneously, the Kroll process was developed, and then nuclear grade pure zirconium could be generated. Hence nuclear graded zirconium-based alloys were chosen for PWR because of excellent corrosion resistant and high neutron resistant property. After the 1970s, FBR program lost its driving force and then PWR became most dominant nuclear reactor, hence, a research about the zirconium cladding materials had been overwhelming more than 4 decades in the cladding research area. However, despite their excellent properties as structure materials, unlikely iron-based alloy, zirconium has anisotropy properties as hcp structure hence zirconium shows irradiation growth and creep.

I.4   Anisotropy materials: Zirconium alloy

The typical RIDI of anisotropic materials (i.e. zirconium or titanium) is expansion in the a-direction and contraction in the c-direction, i.e. irradiation growth.

The research history about irradiation growth of zirconium is started by Buckely who firstly suggest quantitative irradiation growth mechanism by the atomic move in 1969 [12]. After that, principle researches had been done by Fidleris [13] and Adamson [14]. In 1980s irradiation growth are systemically organized researched extensively by Northerm Research Laboratories (NRL) of Atomic Energy Authority in UK (UKAEA). For the understanding of the environment (fluence and temperature) effect on zirconium, three key parameters (temperature, fluenece and materials properties) are controlled by researchers [15-18]. In detail, experiment had been done by varying the interest factor while other factors are fixed.

Specifically, to figure out the texture effect on the growth mechanism, researchers examined the irradiation growth of single crystal. After the analysis of single crystal data, polycrystalline zirconium and its alloy were also researched with same environment condition. To maintain consistency of neutron spectrum, irradiation tests were carried out by same reactor, i.e. DIDO reactor

From these experiments, quantitative information was obtained by major parameters. Moreover, sink morphology change is researched by microstructure analysis, and then the qualitative mechanism was suggested. Up to now, several experiments of irradiation growth and creep also have been done for pressure tube [19].

I.5   Isotropy materials: Iron-based alloy

For isotropic materials, irradiation swelling is typical RIDI behavior because 3-D vacancy sink is generated, i.e. void nucleation and growth. There is three distinguished regimes for irradiation swelling. First stage is void nucleation stage. In this stage, there is no swelling because the relaxation volume of cluster is very high. However, after this stage, void growth induced the high swelling rate with exponential form. In the finally stage, steady-state volume expansion occurs because sink density is saturated.

Historically, RIDI of iron had been independently researched by many different laboratories in various countries such as U.K, France and U.S.A etc. Representative researchers and laboratories are E.A.little of UKAEA in UK [20], D.S. Gelles of Hanford Laboratory, F. A. Garner of Pacific Northwest National Laboratory in USA [10, 21], and D. Gilbon & P. Dubuisson of CEA in France [22].

Unlike zirconium alloy, there was no systemically organized experimental project for iron-based alloy because iron-based alloy has many different phases with various alloy composition and fabrication process. Hence, many laboratories independently investigate the environment or manufacturing effect on RIDI of the iron-based alloy. With this tendency, void swelling of the iron-based alloy was examined by alloying element, fabrication process, and environment conditions. For example, the swelling degree was simply researched by depending on Cr concentration or temperature change or degree of cold work. Also, austenite and the ferritic material are directly compared to figure out why ferritic steel has high swelling resistance rather than austenite steel. Lately, it was revealed that the relaxation volume of bcc ferrite for self-interstitial is larger than that of fcc austenite. Large relaxation volume means unstable configuration and it induces high mobility. Specifically, it is believed that migration energy of vacancy in bcc iron has only 0.55 eV whilst that of fcc austenite lattice has 1.4 eV [23].

I.6 History of radiation effect modeling

Like any other theory, the history of rate theory is started from the experimental observation. Development of fission reactor gives chance to think about radiation interaction with materials. In detail, to understand RIDI phenomena, point defect reaction with solid are studied. As result, Kinchin & Pease and NRT model were suggested for the quantification of defect generation. And then, rate theory which is based on mean field approximation was adopted to predict RIDI. Mansur [24] and Sizmann [25] are compressively organized the point defect reaction mechanism. Temperature and fluence effect on dimensional instability were calculated and analyzed. Since the reaction kinetics between the defect and lattice atom is the heart of chemistry, it was natural that rate theory was adopted to explain irradiation degradation.

However, in this formulation, which is based on point defect modeling, various radiation-induced phenomena could not be explained. For example, high swelling rates in low dislocation density, void swelling near grain boundary, and void lattice formation. The new approach had been introduced by Woo and Singh to solve these problems. At the first time, the migrating dislocation effect was only considered. In this approach, interstitial clusters are the only generation and assumed vacancy cluster are annihilated. Hence this model is named by production bias method. However, it was revealed that interstitial cluster is mobile itself. Hence 1-D reaction kinetics have been developed and the more realistic formulation is suggested to replace the traditional rate theory. Although, there were some limitations of the PBM frame, i.e. swelling saturation or void lattice ordering, Barash and Goloubov attempt to solve those limitation [26].

Before Mansur and Sizmann summarized and generalized the rate theory, theoretical model of general reaction kinetic is already developed for various application such as stellar system and biosystem. Reaction probability could be derived from general reaction kinetic, and then rate theory could be established. Hence particle reaction kinetics, the central idea of general reaction kinetics, is reviewed.

I.6.1 Particle reaction kinetics

After observation of severe RIDI in cladding materials, rate theory became the most powerful approach to understand the RIDI. As particle reaction kinetics is the basis of rate theory, prediction or analysis of radiation defect behavior totally depend on calculated results from particle reaction such as capture efficient and diffusivity.

Until the 1950s, particle reaction kinetics had been exclusive properties of physics of chemistry or bioengineering. However, after observation of severe radiation degradation of dimensional instability,

this particle reaction kinetics became the most powerful research tool for prediction or analysis of radiation defect behavior.

The first quantification approach published in 1917 by Smoluchowski and then Waite expanded his accomplishment with elegant expression [27]. Gosele and Woo are most representative researchers in reaction kinetics of irradiation defect [2, 28]. Gosele found the generalized reaction formula of radiation defect. After several years woo development methodology to reflect diffusion anisotropy of non-cubic structure by changing the normal coordinate system. Also, He successfully predicts irradiation growth and creeps phenomena base on Gisele's works. Diffusion anisotropy effect on defect reaction with each type of sinks was systemically organized. Hence behavior of dislocation loop which is representative radiation sink in zirconium materials had been analyzed with a change of dimensional instability.

The reaction between the extended sink and mobile defects is one of a special case in particle reaction kinetics. Hence reaction probability is the most generalized problem and important concern of reaction kinetics. From Fick's second law to Smoluchowski boundary condition, simplified mathematical treatments are well organized. Particle concentration is one of the most important result which calculated from reaction probability. In the non-production situation, Concentration is simply decreased isotopically to the other molecular. In the non-cubic system, reaction kinetics need to be modified probability density

I.6.1.1 Formulation of particle reaction kinetics

In 1957 Waite formulate the general equation for reaction kinetics in condensed materials system [27]. Reaction probability was expressed by define probability distribution as follow

$$\rho_{Ai(Bj)}(r_A, t; r_B)dV_A/V \qquad \text{Equation I.6.1}$$

Where $\rho_{Ai(Bj)}$ is probability that A_i is in the volume element dV_A at r_A, t given that B_j is at r_B

$$\frac{\partial \rho_{ij}}{\partial t} = \left(\frac{\partial \rho}{\partial t}\right)_{chem} + D_A \nabla_A^2 \rho_{ij} + D_B \nabla_B^2 \rho_{ij} \qquad \text{Equation I.6.2}$$

The average number of pairs having the A in dV_A at r_A, t given that B_j is in dV_B at r_B, t

$$C_{AB}(r_A, r_B, t)dV_A dV_B = 1/V \sum_{i}^{NA^0} \sum_{i}^{NB^0} \rho_{ij}(r_A, r_B, t)\, dV_A dV_B \qquad \text{Equation I.6.3}$$

From this problem, a general solution is derived with complicate mathematics by the change of Cartesian coordinate and new variable

$$\frac{\partial C_A}{\partial t} = \frac{\partial C_B}{\partial t} = 4\pi r_0^2 D C_A^0 C_B^0\, \rho_{ij}(r, t) \qquad \text{Equation I.6.4}$$

There is three representative boundary condition, one is about equilibrium probability, two is an initial condition, third is reaction radius condition:

$$\rho_{ij} \to 0 \; as \; t \to 0, \rho_{ij}(r, t = 0) = h(r), \rho_{ij}(r = r_0, \; t) = 0 \qquad \text{Equation I.6.5}$$

Therefore, the unique solution to this problem is $(C_B = C_A)$

$$\frac{1}{C_A} = \frac{1}{C_B} = \frac{1}{C_{A^0}} + k \left[\frac{2r_0}{(\pi D t)^{\frac{1}{2}}} \right] C_A C_B \qquad \text{Equation I.6.6}$$

Therefore, the unique solution to this problem is $(C_B \neq C_A)$

$$C_A = \frac{(C_A^0 - C_B^0)C_A^0}{C_A^0 - C_B^0 \exp\left\{ -k(C_A^0 - C_B^0)\left[1 + \frac{2r_0}{(\pi D t)^{\frac{1}{2}}} \right] \right\}} \qquad \text{Equation I.6.7}$$

I.6.2 Defect reaction rate theory

The simplest defect rate equation was made by Sizmann [25], from this balance equation model, it could be calculated that defect concentration in a matrix which could be expressed by three terms. K_o is defect production rate. It could be calculated from G_{NRT} term by considering cascade relaxation. K_{iv} is recombination rate which mean vacancy and interstitial are combine and go to perfect lattice atom, the last term K_{vs} & K_{is} means that total sink strethe ngths of all the extended defects in the material. C_i and C_v are defect concentration of interstitial and vacancy. And C_s^T is total sink strength of matrix.

9

$$\frac{dC_v}{dt} = K_o - K_{iv}C_iC_v - K_{vs}C_vC_s^T \qquad\qquad \text{Equation I.6.8}$$

$$\frac{dC_i}{dt} = K_o - K_{iv}C_iC_v - K_{is}C_iC_s^T \qquad\qquad \text{Equation I.6.9}$$

Defect rate equation is the mathematical expression of radiation-induced defect quantity and quality. Hence quantification of radiation-induced defect concentration is the essential part of theoretical irradiation growth modeling. Therefore, defect rate equation is must need to irradiation growth modeling. It is researched from uranium to structure materials.

II   Problem statement

II.1   Limitation of radiation damage quantification

All of radiation-induced phenomenon (creep, segregation, growth and swelling) could be characterized by two classified parts. The first part, which is called as primary radiation damage, is occurred below than 10^{-11} sec [29]. In this time scale, radiation-induced cascade is created and recovered. This part composed with two sequences. The first sequence could be only explained by collision theory because neutron has high energy and speed. In detail, the interaction between neutron and matrix generate the primary knock on atom (PKA). And then PKA interact with the other atom in the lattice matrix. And then, secondary knock on the atom, ternary knock on the atom are generated. This phenomenon seems like quite simple. However, lately it will be dealt with NRT model in the next section, the interaction between atoms is a complex mechanism which includes all radioactive phenomenon such as electron excitation, Compton scattering, and photoelectronic effect etc. In view point of displacements, the energy which is not used for displacements could be referred to as inelastic scattering. And then in the second sequence, cascade relaxation or cascade cooling phenomenon is occurred from 10^{-11} sec up to 10^{-8} sec when most of the defects are annihilated. The difficulty to calculated survive defect is similar to that of the first sequence, because cascade relaxation is also too fast, and the atom is fluctuated in a various potential field. In this sequence, the most defect will be directly or spontaneously annihilated to stabilize each atom's energy state because atoms are entangled. Hence the quantification of surviving defect is the hardest part in radiation damage research and study. Therefore, research about quantitative analysis of RIDI would be valuable work only if each part could be calculated by probable approach and methodology.

The second part is thermal migration of defects which phenomenon is occurred from 10^{-8}. In this region, rate theory finally could be used for RIDI. Recombination, clustering, and sink absorption and & emission occurred by a thermal diffusion mechanism. The relatively second part has been researched many years than first parts hence many research results are compiled with a systemically organized approach.

The Defects concentration could be characterized by time which criteria was firstly suggested by Sizmann. In Figure II.1.1. the reaction mechanism is visualized by time sequence.
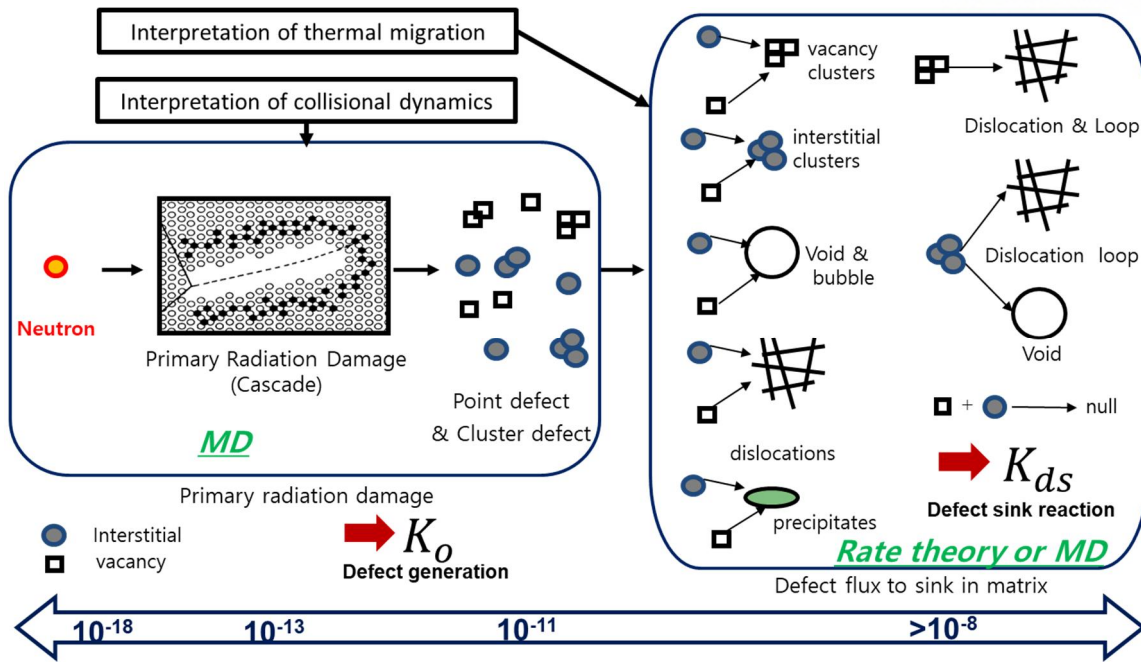
Figure II.1.1 Visualization of the reaction mechanism of each time sequence

II.1.1 Primary radiation damage

There are many factors to occur the RIDI, the fundamental input parameters are environment variables. Hence the irradiation effect on materials could be analyzed by three environmental parameters (fluence, stress and temperature) and materials properties. Among these three parameters, the fluence is a most important parameter in radiation damage because it is the origin all of radiation-induced phenomena. Hence to quantify the primary radiation damage, the neutron spectrum is fundamental input information. And then, finally, radiation damage could be quantitively expressed by using threshold energy and collision theory model, surviving defects could be calculated. There are various models for radiation damage from NRT to Kinchin and Pease. Nowadays NRT model is most accepted in world-wide.

II.1.1.1 Limitation of Neutron spectrum calculation

To calculate the primary radiation damage which is occurred up to 10^{-11} sec, firstly neutron fluence should be quantified by neutron spectrum. However, this information is beyond of material science and engineering. The neutron spectrum could be calculated from the research group of the nuclear reactor physic. There are many codes for neutron physics which in include McCARD and MCNP. Fortunately, these codes also use Monte Carlo transport method and the calculation result is very accurate. Therefore, it is obvious that the discrepancy of radiation damage between reality and simulation does not depend a neutron spectrum.

II.1.1.2 Limitation of Threshold displacement energy (TDE)

Next step to calculate radiation damage is derived the threshold displacement energy (TDE). TDE is minimum energy to generate defect. This value is change depending on the material. By considering TDE and neutron spectrum, finally, radiation damage could be quantified. However, it is not an easy way to determine the exact value of TDE. The state of art technic to calculate the exact value of TDE must consider all parameters such as the direction of PKA, thermal vibration, and cell size of simulation etc. This methodology is well described in B. Mosab's paper [30]. However, only TDE of pure materials could be calculated and there is no comprehensive study about TDE. Hence world-wide literature study is needed.

II.1.1.3 Limitation of NRT model

In 1972, NRT model was proposed and until now this model is using as international standard [31]

$$v(T) = \frac{k(E - S_e)}{2E_d}(NRT)$$

Equation II.1.1

Where E is the total energy of the PKA, Se is the energy lost in the cascade by electron excitation, E_d is damage energy. From the above equation, a total number of defect created by PKA could be deduced. And then dpa could be derived by dividing by a total number of the atom. However, to calculate over all neutron effects, we have to calculate the average cross section of the neutron spectrum. Below equation is about the average neutron cross-section.

$$\sigma_D(E_i) = \int_{\check{T}}^{\hat{T}} \sigma_D(E_i, T) v(T) \, dT = \int_{\check{\phi}}^{\hat{\phi}} \sigma_D(E_i, \phi) v(T) \, d\Omega$$

Equation II.1.2

$\sigma_D(E_i, T)$ is the probability that a particle of energy E_i impart a recoil energy T to a struck lattice atom, $v(T)$ = the number of displaced atoms. After calculating the average cross section of the various neutron spectrums, finally, total number of the defect could be calculated.

$$R_d = N \int_{\check{E}}^{\bar{E}} \phi(E_i) \sigma_D(E_i) \, dE_i$$

Equation II.1.3

$$G_{NRT} = N \int_{\check{E}}^{\hat{E}} \Phi(E_i) \sigma_D(E_i) \, dE_i$$

Equation II.1.4

where N is the lattice atom density, $\Phi(E_i)$ is the energy-dependent particle flux, $\sigma_D(E_i)$ is the energy-dependent displacement cross-section. This equation could be simplified after some mathematical calculation. In these days, SPECTER code [39] is most widely used by many researchers.

As referred, all-atom interaction mechanism which includes all radioactive phenomenon such as electron excitation, Compton scattering, and photoelectronic effect etc are hard to be considered. Hence simplification of NRT model is the main problem. Mechanism of the neutron and matrix is complex to analyze. There is four mechanisms (elastic, inelastic, (n, γ), (n, α)) to occur displacement. However, there is no tool to analyze all reaction kinetics. In MD simulation, neutral collision kinetics could be calculated but, ionic interaction is neglected. In the case of SRIM code, electron excitation could be considered but neutron interaction does not consider. Hence the simplification NRT model should be modified by considering all reaction kinetics.

II.1.1.4 Limitation of quantification of cascade relaxation

As referred, radiation damage is classified as two parts. In second phase, most of the defect is recombined by the corruption of cascade and thermal recombination. However, until now, these phenomena are not systemically organized. There are too many energy groups in the neutron spectrum, grouping method and functional analyze are an essential part. The similar approach or methodology could be fined in neutron physic because neutron physics researcher should use various grouping method to calculate the neutron reactivity. However, in case of neutron physics, reactivity is so much important for a nuclear reactor to maintain sustainable fission reaction, hence unlikely radiation damage research, it was systemically organized. Even if it obvious that organizing the primary radiation damage is the major problem of rate theory, there is no research group which has enough capacity to generate the cascade recombination phenomenon.

II.2   Limitation of rate theory

Traditionally, the modeling of RIDI was derived by simplified rate theory based on diffusion's limited reaction and MD simulation [32]. Technically depending on three factors i.e., sink density, defect flux, and bias factor, RIDI is calculated. However, various assumption and limitation is still a barrier to understand the fundamentals of radiation effect on materials. Especially, limitations of rate theory are clearly revealed when it compared with MD simulation about reaction kinetics. Among the various limitation, major issues are treated in this section.

II.2.1 Mean-field approximation

First, the rate theory is based on a deterministic method based on the mean field which means that rate theory could not consider the heterogeneous generation and growth of sinks and defects in the matrix. Hence sink size and morphology are uniform and stochastic sink development could not be accounted.

The second limitation is about bias factor or capture efficiency. Obviously capture efficiency is not constant because sink morphology and density are changed, and other environments are applied. However, until now, there is no research about bias fact, which could consider the all variation. Obviously, all researcher also assume that capture efficiency is constant. Despite this recognition, there was no general approach or systemically method to analyze capture efficiency.

Third, modification of diffusion coefficient in stress applied condition is needed more sophisticated analytic treatment. In Braisford model, stress-induced diffusion coefficient is calculated by ideal volume of lattice atom and applied stress [33]. Although the more theoretical approach is already developed by Woo and Gosele for prediction of irradiation creep [2, 34]. These study results have never been verified. Moreover, there is no theoretical study about bimolecular reaction kinetics in a radiation environment after Woo's study. Recently ab-initio simulation takes the place the position of this analytical method [35].

Lastly, the role of the alloy also un-clear in rate theory. From experimental results, it was clear that alloy has an effect on irradiation swelling and growth [36]. As stress effect, diffusivity characterization could be a solution to this problem. However, few literature studies about alloy effect on defect diffusivity had been carried out [37].

II.2.2 New research trend for limitation of rate theory

Not only rate theory but also various simulation tools were adopted to analyze the RIDI. Molecular dynamic simulation, ab-initio and kinetic Monte Carlo simulation are representative simulation tools.

Alloy element and stress effect is a region where new methodology application could be effectively used. In case of MD simulation or first principle method, each atom position could be detected. Hence, near the alloy element, point or cluster defect could be analyzed their displacements.

In rate theory, single diffusivity value is adopted to express the point defect diffusivity. However, until now this value is adopting by fitting the experiment result or only useful for the pure metal. Hence recently point defect diffusivity is calculated by using MSD. It was revealed that Nb act trap for interstitial hence its diffusivity is dramatically decreased in zirconium. Just as an alloy element case, stress effect on diffusivity could be clearly confirmed by MD simulation. In this case, also the MSD method is used for calculating the diffusivity of point defect. One thing is different is only strain commend is added in input script. In this case not only point defect case but also a cluster defect could be analyzed by C.W. Kang's results [37].

Although, significant progress of computer simulation performance (i.e. MD simulation and ab-initio), rate theory is still a favorite option to simulate radiation effect on materials because this method can give an instinctive understanding of irradiation behavior with short computation time. Moreover, scale of simulation time and simulation length is large enough to satisfy the engineering point of view whilst other simulation method still need a lot of limitation of time and length scale. Therefore, it is important to organize the pro and cons of each tool's characteristic.

In conclusion, since rate theory must use average value in a various terms such as defect generation, recombination rate, and sink absorption rate, hence each term should be verified by MD simulation or ab-initio method. However, it is hard to calculate that each term characteristic because there are too many things, which has to be considered. For example, to calculate absorption rate of just one type of sink, such as dislocation, not only direction of dislocation but also stress applied degree should be considered with various alloy element effect. However, the only limited human and financial resource could be available to consider all parameters effect with organized test matrix. Therefore, fragment knowledge on the specific condition where MD simulation or ab-initio simulation have been adopted, should be organized, summarized and combined for rate theory.

III Rationale and Approach

III.1 Research goal

This chapter describes the research goal and approach. For life extension and improved safety analysis of cladding candidate materials in nuclear reactor condition, my research aims to establish the physical model.

Until now many experimental fitting models are used for safety analysis. However, these modelings have fundamental limitation without an experimental database. Moreover, to suggest the new idea for radiation resistant materials, the physical model should be an essential part.

There were many attempts to explain radiation damage and effect by the physical model. However, as referred in introduction and problem-statements chapters, there is blank part to filled with new results which are calculated by new methodology and tools such as MD simulation, kinetic monte carlo and ab-initio method.

Not only new methodology but also traditional rate theory has been developed to explain various phenomenon such as void lattice ordering, the high swelling rate with low dislocation density and high swelling rate change depend on grain boundary.

Therefore, in this study, state of art results about specific topics such as stress effect or alloy effect on defect behavior and cascade effect on defect generation will be adopted in advanced rate theory. Finally, calculated results will be verified with other simulation results or experimental results.

III.2 Research tools

Historically, quantitative evaluation of defects generated by neutron irradiation has been internationally carried out. Unfortunately, sixty years ago, there was no generalized tool for quantitative analysis. Hence quantitative evaluation of primary radiation damage and sinks development were calculated by using an analytic equation.

For this reason, theoretical evaluation of nuclear materials has been developed since the 1960s and various studies have been conducted to derive fundamental mechanisms for various phenomena that have not been clarified yet.

Rate theory is the most important results of the theoretical study. Reaction probability was calculated by solving the diffusion equation. In rate theory, defect generation, recombination and absorption rate could be derived. At firstly only point defects were considered and cluster defects were neglected. As referred in introduction chapter, Mansur [24] and Sizmann [25] systemically organized the fluence, temperature and sink effect on materials in an early stage. Recently rate theory had been developed up-to CDM and PBM to consider the cluster defect behaviors [1, 38].

However, even theoretical and analytical method could give hint to interpret radiation damage and effect phenomena, many studies about the predicting the life expectancy had been carried out through the experimental results rather than theoretical approach because the theoretical basis still has a lot of immature parts.

Nevertheless, this certain limitation, the reason of why much research on the degradation behavior has been made on the theoretical basis is there is no way to directly examine the high-level radiation effect on microstructure in an experimental manner. Although there are few studies about the in-situ observation of radiation effect on materials in low temperature with electron source [39].

Hence, recently, state of art simulation tools are adopted in the field of nuclear materials society, i.e. ab initio, MD, and kMC, which are recognized as key to solve the limitation of rate theory [40, 41]. These three methodologies could cover the microstate of atomic behavior, which rate theory could never consider.

III.2.1 Cluster dynamic modeling

The fundamental of rate theory, which is including approach and methodology, are well-described in Fundamental of radiation materials science [8] and Brailsford papers [32] where reaction kinetics were summarized, and reaction probability is calculated by SRT. In this chapter, simple characteristics are represented. The SRT is not integrated method, number density is needed as input data. Hence to derive number density of sinks, i.e. vacancy and interstitial cluster, the master equation should be extended up-to unlimited number. There is two representative methods to obtain cluster distribution. The one is Kritani method [42] which is originally to calculate the vacancy distribution in quenching. The other is Goloubov method [43] to consider transmutation effect on cluster effect. Unfortunately, these methods are needed specialized numerical ODE solver and simulation time. However, the form of the master equation itself is simple as following equations.

$$\frac{dC_i}{dt} = K_o - K_{iv}C_iC_v - \sum_n \rho_n Z_n^i C_i D_i + \left(E_i^2 + \beta_v^2 \right)C_{2i} + E_i^3 C_3 + E_i^4 C_{4i} \qquad \text{Equation III.2.1}$$

$$\frac{dC_{2i}}{dt} = \eta G_{dpa} \frac{f_{icl}^2}{2} + \beta_i^1 C_i / 2 + \left(\beta_v^3 + E_i^3 \right)C_{3i} - \left(\beta_v^2 + \beta_i^1 + E_i^1 \right)C_{2i} \qquad \text{Equation III.2.2}$$

$$\frac{dC_{3i}}{dt} = \eta G_{dpa} \frac{f_{icl}^3}{3} + \beta_i^2 C_2 + \left(\beta_v^4 + E_i^4 \right)C_{4i} - \left(\beta_v^3 + \beta_i^3 + E_i^3 \right)C_{3i} \qquad \text{Equation III.2.3}$$

$$\frac{dC_{4i}}{dt} = \eta G_{dpa} \frac{f_{icl}^4}{4} + \beta_i^3 C_{3i} - \left(\beta_v^4 + \beta_i^4 + E_i^4 \right)C_{4i} \qquad \text{Equation III.2.4}$$

Where $C_{xv \ or \ xi}$ is vacancy or interstitial cluster concentration in the iron matrix (cm^{-3}), K_0 is the defect generation rate (cm$^{-3}s^{-1}$), which means vacancy and interstitial are combined to be a perfect lattice atom. G_{dpa} is the cluster defect generation rate (cm$^{-3}s^{-1}$), f_{cl}^x is the fraction of cluster, η is the cascade efficiency, K_{iv} is the recombination rate (cm^3s^{-1}), ρ_n is the density of sink of n type in the iron matrix (cm^{-2}), $Z_n^{v \ or \ i}$ is the vacancy or interstitial bias factor of sink on n type in the iron matrix, which is a dimensionless number, β is the point defect absorption constant, E is the point defect emission constant, ρ_n is the density of a specific sink such as dislocation line, dislocation loop, and void. Figure III.2.1 and Figure III.2.2 show the fundamental mechanism of cluster dynamic theory. Each cluster could be growth or dissolved by absorption of point defect.
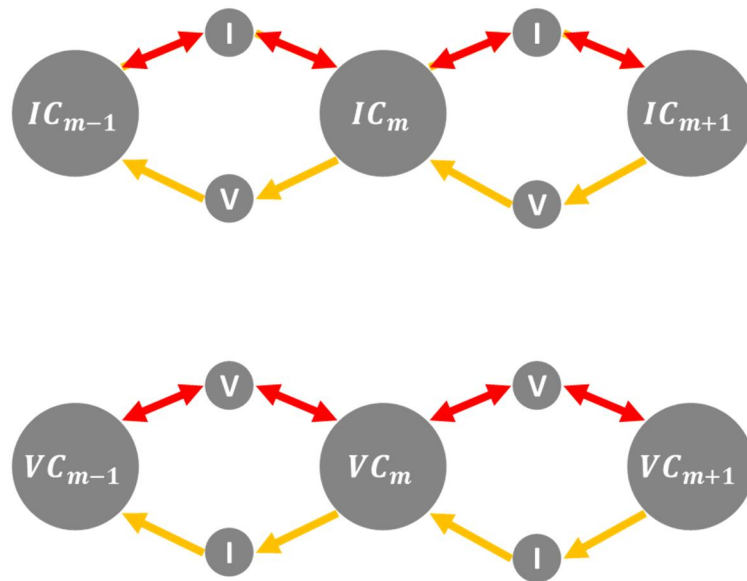
Figure III.2.1 Schematic of cluster dynamic modeling

Hence defect concentration equation of any size cluster (it is denoted by m size cluster) could be understood as shown Equation III.2.1. If m-1 size cluster absorbs same type point defect, it will be m-size cluster. In case of m-size cluster, any absorption or emission of point defect will decrease the concentration of m-size cluster.
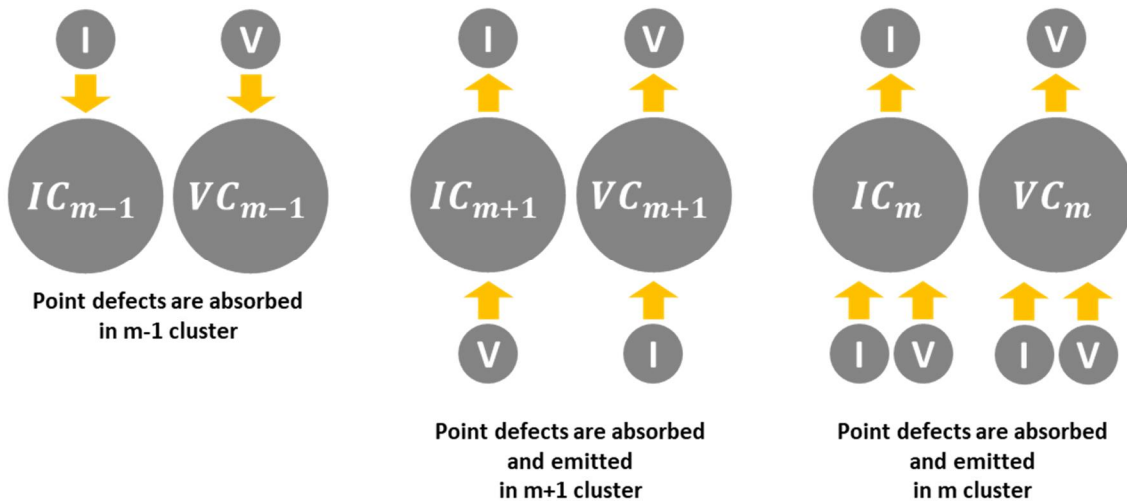
Figure III.2.2 Schematic of cluster evolution

$$\beta_{i\,or\,v}^{\mathrm{m}} = \frac{z_{i\,or\,v}^{m}}{a_0^2} D_{i\,or\,v} C_{i\,or\,v} = 4\pi(R_p + R_C)(D_p + D_C)$$

Equation III.2.5

$$E_i^{\mathrm{m}} = \frac{D_i}{a_0^2}\exp(-\frac{E_j^B}{kT}) = 4\pi(R_C)(D_C)\exp(-\frac{E_j^B}{kT})$$

Equation III.2.6

The physical meaning of the first term on the right hand of Equation III.2.1 is defect generation rate; the second is recombination rate; the third is the vacancy absorption rate of any sink in the iron matrix; the rest term is about cluster growth and dissolve. In Equation III.2.2, first term show cluster generation rate and the rest term represent cluster behavior. The rate theory of vacancies follows the same method as that of interstitials in Equation III.2.2 ~ Equation III.2.4.

Among these various terms in the Equation III.2.1, sink absorption rate is the most interesting factor in the point of view to calculate dimensional instability because it determines the accumulation rate of defect on the sinks. The integral of accumulating defect rate to sink directly induced dimensional instability in mean field rate theory assumption.

III.2.2 Production bias modeling

As referred, simple rate theory, i.e. CDM was not enough to explain some phenomenon. It was obvious that a new approach is needed. In 1997 Singh published the paper which is well formulated and organized about cascade effect on microstructure [1]. After then, various papers about the reaction kinetics are published. For example, in 2000, Goloubov summarize these limitations and explain the discrepancy between bcc and fcc structure [44]. However, there is no big change in 1997's frame. Therefore, the original frame of Singh's paper in 1997 is still important and enough to understand core ideas.

The key idea of Singh's paper is the mobile interstitial cluster is generated and reacted with other sinks. Hence the modified master equation of simple rate theory is necessary. Moreover. the new equation about mobile interstitial cluster should be formulated. The theoretical basis of the one-dimensional approach is described in Borodin's work approach [45]. The noticeable point in Singh approach is that only the mobile interstitial cluster and sink reaction was considered in Equation III.2.7.

$$\frac{dC_g}{dt} = K_g(t) - D_g C_g k_g^2$$

Equation III.2.7

here C_g is the mobile interstitial number density concentration, K_g is the generation rate of mobile interstitial, D_g mobile interstitial diffusion coefficient and K_g^2 sink strength. In the Equation III.2.7 equation about sink strength is

$$k_g = \frac{\pi \rho d_{abs}}{4} + \sqrt{\frac{2}{l(2R_g - l)}} + \sigma_v N_v$$

Equation III.2.8

here d_{abs} is effective interaction diameter, R_g is grain radius, l is the distance from the grain boundary, σ_v are the cross-section clusters with size. From the Equation III.2.7, master the equation should be modification because mobile interstitial cluster has always positive effect on interstitial cluster number density whilst mobile interstitial cluster has negative effect on vacancy cluster.

$$\frac{dC_x}{dt} = K + \beta_i^{x-1} C_{x-1i} - \left(\beta_v^x + \beta_i^x + E_i^x\right) C_{xi} - \beta_{MIT}^x C_{xi} + \beta_{MIT}^{x-x_g} C_{(x-x_g)i}$$

Equation III.2.9

here β_{MIT} is absorption rate of mobile interstitial cluster with extended sinks. As shown in Figure III.2.3.

23
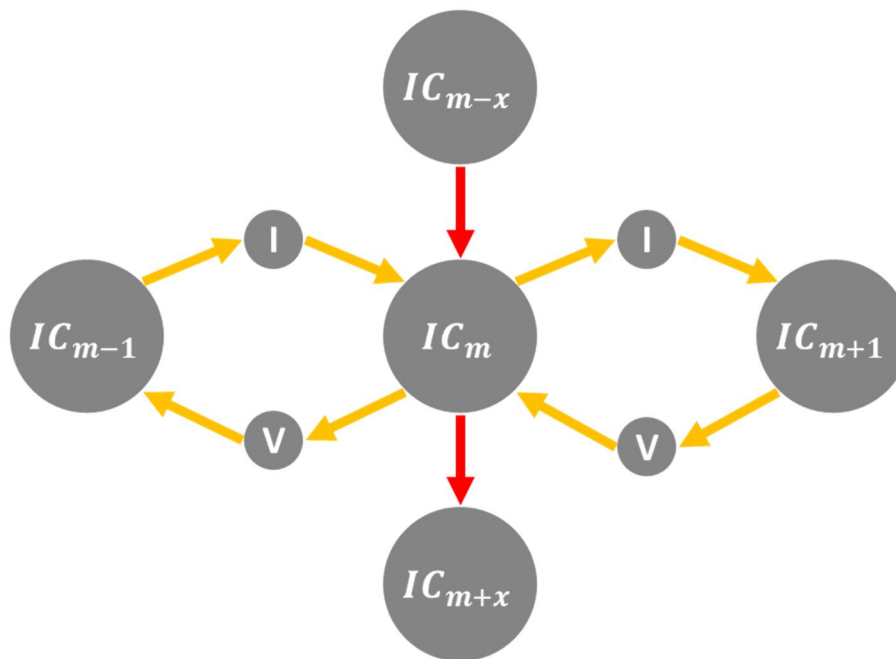
Figure III.2.3 Schematic of production bias modeling

III.2.3 MD simulation & First principle

The thermal dynamic is about equilibrium. In the past, there is no way to precisely analyze the atomic behavior. But by creating the concept of entropy, the phase of materials is predicted hence all kind of thermal dynamic approach is based on experimental results. Nowadays, the research trend turns from the thermodynamic to kinetics, because of development of first principle method. As implied by the name, the first principle needs nothing from experimental results because the first principle is the law to consist the all of matter in the universe. However, in order to solve the wave equation for electron structure, the various assumption should be applied, moreover, many-body problem needs a lot of computer simulation power. Nevertheless, ab-initio and MD study give a lot of information about atomic behavior which has never revealed before. Therefore, nowadays, we are in the phase transition of academic tools for analyzing the materials behavior. In the past, thermodynamic is only ways, however, nowadays first principle and MD simulation are the major issues in nuclear materials academia. Specifically, radiation-induced phenomena are occurred in wide time and length scale because neutron has high energy. The range of time scale is started from femtoseconds to decades and the range of dimensions is started from the angstrom to meter scale, that has more than 13 orders of magnitude. Therefore, to accurate analysis of atomic behavior, MD simulation and ab-initio tools have to be used.

MD simulation is about the solution of Newton equation which about the position, velocity, and acceleration. By using the initial positions and potential field, find the lower energy states with a small-time interval. What makes MD simulation to be important is methodology or algorithm to solve the many-body problem and computer capacity which makes MD simulation is possible. In the past, the idea is already has been suggested. However, there is no way to solve many-body system without a computer. Not only algorithm and computer capacity but also potential is the most important factor in MD because, without potential, MD is useless. Recently potential is calculated by the first principle or is fitted by experimental results.

To calculate the interatomic potential of the atom, the first principle had been suggested. This method is a memorial invention which is developed form the state of art physical model. There are many underlings physic and mathematic to consist the first principle method. The art of this simulation is not just solution of wave equation, but, the various logical assumptions to solve wave equation. Wave

equation itself is not a hard problem because it is second order PDE which solution is well known. However, wave equation is only available in a simple case such as hydrogen model. In case of transient metal, there are so many electrons exist hence variable is too many. There is history to solve the complex system. However, this modeling development is out of this study range.

III.3 Approach and Method

In rate theory, RIDI was calculated by reaction probability between defects and sinks hence sink size and number density should be derived. Traditionally sink strength is a useful concept to calculate the reaction probability and it induced sink size change. In this section, it will be explained that how to derive the sink strength and how to connect between RIDI and sink strength. Finally, as referred in problem state chapter, traditional calculation of sink strength could not consider the stress and alloy effect. Hence in this section, methodology to consider the stress and alloy effect is described.

III.3.1 Definition of the diffusion

Before to derive sink strength, it is necessary to define the diffusion coefficient because what is dealt with in this study is almost kinetics of atomic behavior. Before directly derive the diffusion coefficient in 3-Dimension, it is easy to derive in lower dimension, i.e. 2-Dimension. In 2-Dimension, one point can move each step δ, hence if let x_n be position of after the $k'th$ step then

$$x_k = x_{k-1} \pm \delta$$

Equation III.3.1

the average value of each step will be zero, hence by using mean squared position

$$x_k^2 = x_{k-1}^2 \pm 4\delta x_{k-1} + 4\delta^2 = x_{k-1}^2 + 4\delta^2$$

Equation III.3.2

from the above equation, displacement from zero point could be expressed

$$x_n^2 = 6n\delta^2 = 4\left(\frac{\delta^2}{\tau}\right)t = 4Dt$$

Equation III.3.3

therefore, diffusion coefficient can be defined as a tool for expression the displacement in a mean square position. Now, turn into a 3-Dimensional problem, it is very simple because mean square displacement is linearly increasing with time
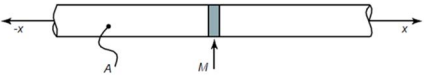
$$x_n^2 = 6n\delta^2 = 6\left(\frac{\delta^2}{\tau}\right)t = 6Dt \qquad\qquad \text{Equation III.3.4}$$

III.3.2 Normal distribution of particle

It must be easier to understanding sink strength if normal distribution is understood. Because both problems are dealing with second-order PDE. There are many ways to solve second order PDE. There is a general solution and specific solution. As literature, the general solution is a most general way to solve PDE. From this method, it could be determined that the solution is existance or not. However, in this study, the only specific solution will be treated because the general solution is needed furrier transform which is beyond of this study scope. As shown in Figure III.3.1, Fick's second law is a second order PDE problem.

$$P_t(r) = \frac{1}{(4\pi Dt)^{\frac{3}{2}}} exp\left(-\frac{r^2}{4Dt}\right) \qquad\qquad \text{Equation III.3.5}$$

Diffusion equation(second order linear PDE)

$$\frac{\partial C}{dt} = D\frac{\partial^2 C}{dx^2}$$

- **How to second order linear PDE could be change by ODE form**

- To use dimensional analysis, we must consider all the parameters that control the solution.

- Table summarizes the dependent and independent variables for our problem. there are m = 5 parameters and n = 3 dimensions. dimensionless groups was suggested in order to simplification $\pi_1 = f(\pi_2)$

$\pi_1 = \frac{C}{M/(A\sqrt{Dt})}$ dependent variable

$\pi_2 = \frac{x}{\sqrt{Dt}}$ independent variable

$C = \frac{M}{A\sqrt{Dt}} f\left(\frac{x}{\sqrt{Dt}}\right)$ where $\eta = x/\sqrt{Dt}$

Table 1.2. Dimensional variables for one-dimensional pipe diffusion.

	Variable	Dimensions
dependent variable	C	M/L^3
independent variables	M/A	M/L^2
	D	L^2/T
	x	L
	t	T

Figure III.3.1 Problem of 1-dimension diffusion

To obtain the normal distribution of some particle position, a new variable is suggested, and the separation of variable technic is used. Finally, particle concentration could be derived.

General form of joint probability
- Consider the six-dimensional hyperspace formed by the combination of the Cartesian laboratory coordinates of Ai and Bj

- Chain rule to compute $\dfrac{\partial C}{dt}$

$$\frac{\partial C}{\partial t} = \frac{\partial}{\partial t}\left[\frac{M}{A\sqrt{Dt}}f(\eta)\right] = \frac{\partial}{\partial t}\left[\frac{M}{A\sqrt{Dt}}\right]f(\eta) + \frac{M}{A\sqrt{Dt}}\frac{\partial f}{\partial \eta}\frac{\partial \eta}{\partial t}$$

$$= \frac{M}{A\sqrt{Dt}}\left(-\frac{1}{2}\right)\frac{1}{t}f(\eta) + \frac{M}{A\sqrt{Dt}}\frac{\partial f}{\partial \eta}\left(-\frac{\eta}{2t}\right) = \frac{M}{2At\sqrt{Dt}}\left(f + \eta\frac{\partial f}{\partial \eta}\right)$$

- Similarly, we use the chain rule to compute $\dfrac{\partial^2 C}{dt^2}$ as follows

$$\frac{\partial^2 C}{dt^2} = \frac{\partial}{\partial t}\left\{\frac{\partial}{\partial t}\left[\frac{M}{A\sqrt{Dt}}f(\eta)\right]\right\} = \frac{\partial}{\partial t}\left[\frac{M}{A\sqrt{Dt}}\frac{\partial f}{\partial \eta}\frac{\partial \eta}{\partial t}\right] = \frac{M}{ADt\sqrt{Dt}}f(\eta)\frac{\partial^2 f}{\partial \eta^2}$$

$$\therefore \frac{\partial C}{dt} = D\frac{\partial^2 C}{dx^2} \rightarrow \frac{M}{2At\sqrt{Dt}}\left(f + \eta\frac{\partial f}{\partial \eta}\right) = D\frac{M}{ADt\sqrt{Dt}}f(\eta)\frac{\partial^2 f}{\partial \eta^2}$$

Figure III.3.2 Solution of 1-dimension diffusion problem

III.3.3 Sink strength

As shown in the normal distribution problem, traditional method to describe the atomic behavior i.e., kinetics is mass conservation equation [8]. Sink strength is also derived the same methodology. Defect generation, loss, and diffusion term are expressed as the balance equation. depending on the geometric characteristic of sink case, the coordinate system should be changed as cartesian, spherical, and cylindrical system. In the case of the void, as shown in figure expressed as spherical system whilst dislocation has a cylindrical system.

(Defect flux at x) $-$ (Defect flux at $x + \Delta x$) $+$ (Rate of defect generation) $=$
(Rate of change of the defect of the element)

$$J_r - J_{r+\Delta r} + \dot{K} = \frac{\Delta C}{\Delta t}$$

$$\frac{J_r - J_{r+\Delta r}}{A\Delta r} + \frac{\dot{K}}{A\Delta r} = \frac{\Delta C}{\Delta t A\Delta r}$$

$$\frac{1}{A}\frac{J_r - J_{r+\Delta r}}{\Delta r} + \dot{k} = \frac{\Delta C}{\Delta t}$$

$$\lim_{\Delta x \to 0}\frac{1}{A}\frac{J_r - J_{r+\Delta r}}{\Delta r} + \dot{k} = \lim_{\Delta t \to 0}\frac{\Delta C}{\Delta t}$$

$$\lim_{\Delta x \to 0}\frac{J_r - J_{r+\Delta r}}{\Delta r} = \frac{\partial J}{\partial r} = \frac{\partial}{\partial r}\left(DA\frac{\partial C}{\partial r}\right)$$

$$\frac{1}{A}\frac{\partial}{\partial r}\left(DA\frac{\partial C}{\partial r}\right) + \dot{k} = \frac{\partial C}{\partial t} \quad \text{Cartesian coordinate system}$$

$$\frac{1}{r^2}\frac{\partial}{\partial r}\left(Dr^2\frac{\partial C}{\partial r}\right) + \dot{k} = \frac{\partial C}{\partial t} \quad \text{Spherical coordinate system}$$
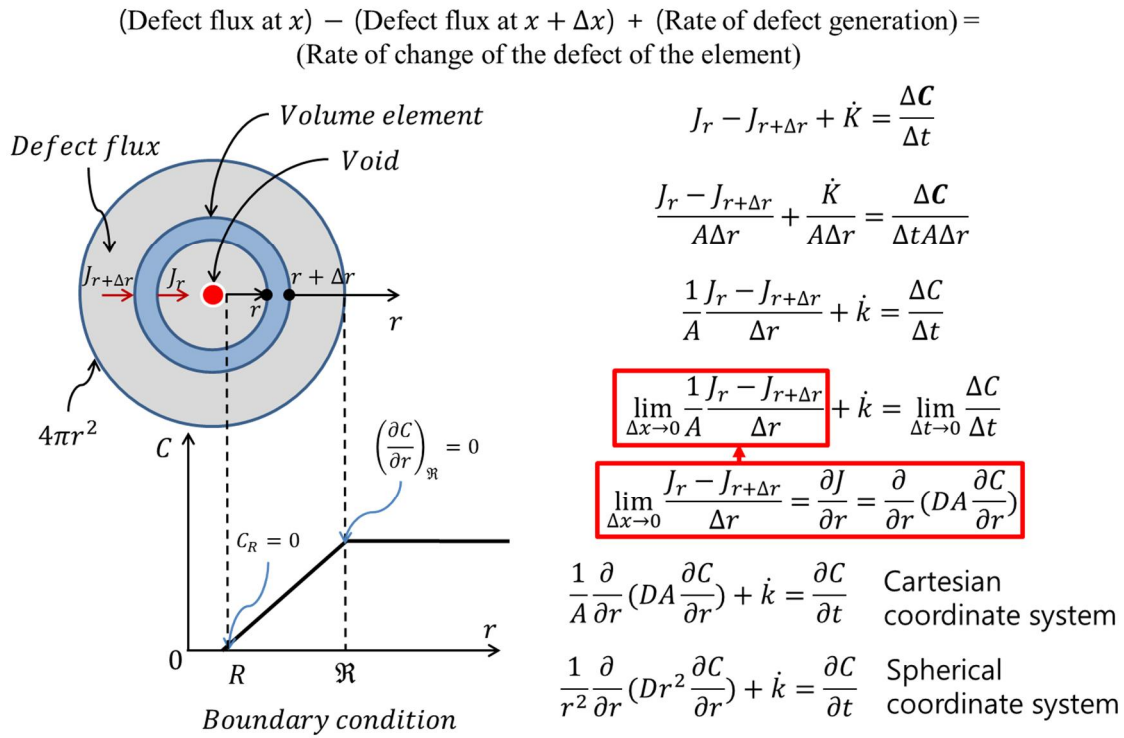
Figure III.3.3 Spherical mass balance system for void sink strength

Since PDE problem is not easy to solve, it was assumed steady-state condition. Hence PDE problem converts into ODE problem. Fortunately, second-order non-linear homogeneous ODE is a well known problem hence solution to this problem is well described in the textbook of engineering mathematics. the solution is

$$C(r) = C_R + \frac{K_0}{6D}\left[\frac{2\mathcal{R}^3(r - R)}{rR} - (r^2 - R^2)\right] \qquad \text{Equation III.3.6}$$

(Defect flux at x) $-$ (Defect flux at $x + \Delta x$) $+$ (Rate of defect generation) $=$
(Rate of change of the defect of the element)

$$J_r - J_{r+\Delta r} + \dot{K} = \frac{\Delta C}{\Delta t}$$

$$\frac{J_r - J_{r+\Delta r}}{A\Delta r} + \frac{\dot{K}}{A\Delta r} = \frac{\Delta C}{\Delta t A\Delta r}$$

$$\frac{1}{A}\frac{J_r - J_{r+\Delta r}}{\Delta r} + \dot{k} = \frac{\Delta C}{\Delta t}$$

$$\lim_{\Delta x \to 0}\frac{1}{A}\frac{J_r - J_{r+\Delta r}}{\Delta r} + \dot{k} = \lim_{\Delta t \to 0}\frac{\Delta C}{\Delta t}$$

$$\lim_{\Delta x \to 0}\frac{J_r - J_{r+\Delta r}}{\Delta r} = \frac{\partial J}{\partial r} = \frac{\partial}{\partial r}\left(DA\frac{\partial C}{\partial r}\right)$$

$$\frac{1}{A}\frac{\partial}{\partial r}\left(DA\frac{\partial C}{\partial r}\right) + \dot{k} = \frac{\partial C}{\partial x} \quad \text{Cartesian coordinate system}$$

$$\frac{1}{r}\frac{\partial}{\partial r}\left(Dr\frac{\partial C}{\partial r}\right) + \dot{k} = \frac{\partial C}{\partial x} \quad \text{Cylindrical coordinate system}$$
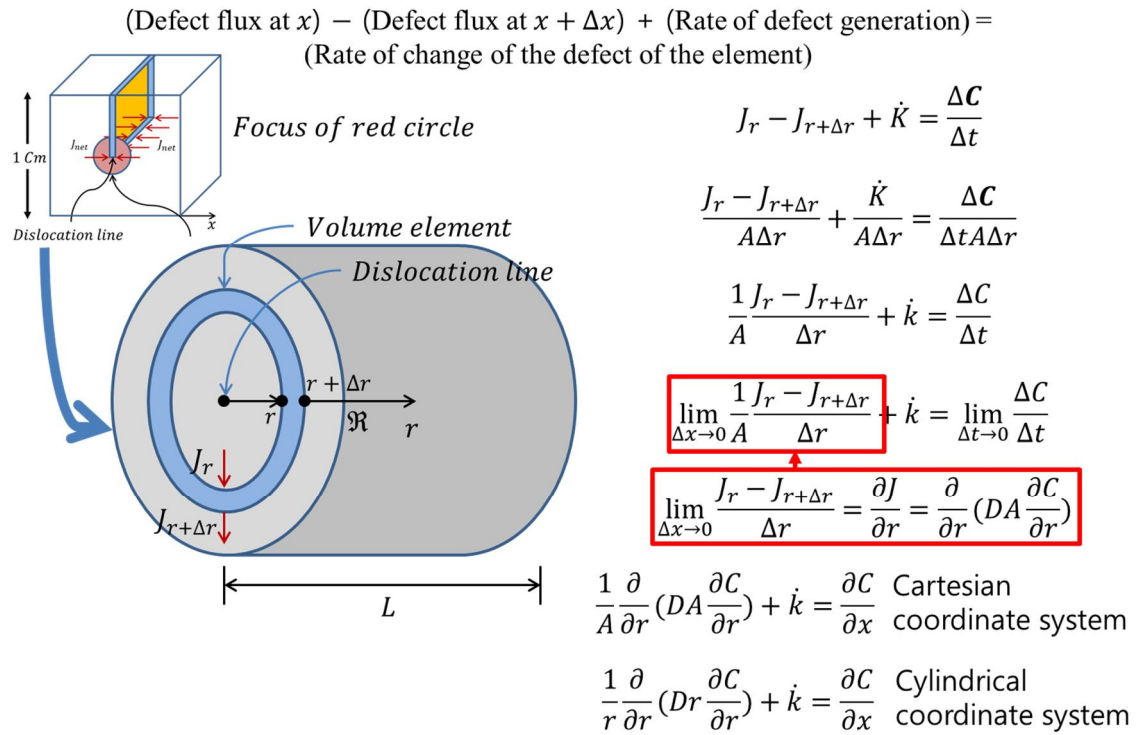
Figure III.3.4 Cylindrical mass balance system for dislocation sink strength

III.3.4 The connection between sink size and RIDI

Radiation-induced dimensional instability in cladding materials is mainly caused by defect and sink reaction. Hence RIDI could be fully explained with sinks growth and nucleation behavior. Before to directly consider the various effect (i.e. stress and alloy) on rate theory, the relationship between RIDI and sink size was reviewed to verify its methodology.

From traditional reaction mechanisms which are well explained in the previous section, diffusion's limited reaction is applied to calculate defect abortion rates. Hence, sink size could be derived by sink strength and which means that atom is accumulated at a certain type of sink. Since atomic accumulation is directly proportioned with dimensional change, RIDI could be simply calculated by sink size change.

There is various type of sinks such as void, dislocation, and precipitation etc. For the sake of simplification, these representative irradiation sinks are classified as disk and sphere. From blow equation, sink number density and sink change could be derived. To calculate all defect absorption rate from each sink, total number density has to be derived. Total number density is

$$\rho_{disk} = 2\pi \, r_{disk} N_{disk}$$
<div align="right">Equation   III.3.7</div>

$$\rho_{void} = \rho_{ppt} = N_{sph}$$
<div align="right">Equation   III.3.8</div>

Here, $r_{disk} \; and \; N_{disk}$ are the radius of sink and number density of sink, which has disk morphology. From these density equations and sink strength equation, reaction probability of defect and sink or total defect accumulation rate could be calculated

$$\frac{dS_x}{dt} = \rho_x \left(Z_x^i D_i C_i - Z_x^v D_v C_v \right)$$
<div align="right">Equation   III.3.9</div>

here, S_x is the total number of defects in sithe nk, $Z_x^{i \; or \; v}$ is the vacancy and interstitial bias factor of any given sink, $C_{v \; or \; i}$ is vacancy or interstitial concentration in the iron matrix (cm^{-3}), $D_{v \; or \; i}$ is the diffusion coefficient of vacancy or interstitial in the matrix ($cm^2 s^{-1}$). Since interstitial and vacancy are recombined at sinks, reaction rate should be expressed by net defect flux ($Z_x^i D_i C_i - Z_x^v D_v C_v$). (In Eq., interstitial flux is positive and that of vacancy is negative for interstitial net defect flux. However, the type of net defect flux could be changed by sink type i.e., void will be expressed

by vacancy net defect flux because void is composed by vacancy).

As assumed, there is two types of sink. In case of a disk type of sinks such as dislocation line and loop, it induced the irradiation creep and growth. If defect diffusivity is not biased, irradiation creep and growth do not occur. However, in case of zirconium, diffusion is biased as DAD hence irradiation growth occurs without external stress. In case of stainless steel, irradiation creep is only occurred by external stress. Therefore, irradiation growth and creep could be calculated by the general equation of strain rate. The equations are

$$\frac{d\varepsilon}{dt} = \rho bv$$

Equation III.3.10

where, ϵ is the elongation (cm), and v is the dislocation velocity (cm^{-2}s^{-1}). In this equation, most import parameter is dislocation velocity which physical meaning is exactly same of defect flux (i.e. reaction probability between defects and sinks). Hence the equation of dislocation velocity is

$$v = \frac{1}{b}(z_i^j D_i C_i - z_v^j D_v C_v)$$

Equation III.3.11

Therefore, from that equation, irradiation growth and creep are calculated. In case of irradiation swelling, it could be calculated as below equation

$$\frac{dV}{dt} = \Omega 4\pi r_{sph}(z_v^j D_v C_v - z_i^j D_i C_i)$$

Equation III.3.12

From Eqs., not only dimensional instability but also microstructure characteristic, i.e. number density and radius of sink can be calculated. Although microstructure can't be fully explained in detail, the average radius of the sink would be derived as below equation [32]:

$$\frac{dr_{sph}}{dt} = \frac{\Omega}{r_{sph}}\left(Z_{sph}^i D_v C_v - Z_{sph}^v D_i C_i\right)$$

Equation III.3.13

In case of disk type, the total number defect in disk type of sinks is used to drive change of radius. This method is well-described in a previous work [46]. Therefore, the equation for the radius of a disk type of sink is below.

31

$$r_{disk} = \sqrt{(S_{disk} / \pi b N_{disk})}$$

<div align="right">Equation
ffffffffffIII.3.14</div>

III.3.5 Stress effect on RIDI with the traditional method

It is worth noting that stress-induced preferred dislocation loop nucleation and growth has been already considered. In 1973, Brailsford simply showed that irradiation creep and swelling will be explained by two mechanisms, i.e. stress induced preferred nucleation (SIPN) and stress-induced preferred growth (SIPG) [33]. However, in this study, SIPN was not considered because it was revealed that SPIN has little effect compared with SIPG.

In the preview section, RIDI is formulated by using the net defect flux which is the origin of RIDI. Hence in applied stress condition, defect absorption equation should be modified to consider the stress effect by adopting SPIG. Specifically, SIPG was accounted by modifying the reaction probability between defect and sinks.

To modify reaction probability, the SIPG mechanism should be reviewed. Firstly, it was developed to explain the diffusional creep mechanism in thermal creep behavior. Brailsford borrows this concept and then applied irradiation situation. In the thermal creep mechanism, especially in diffusional creep, stress effect was accounted by modifying the bulk defect concentration (equilibrium concentration). In detail, bulk defect concentration would be changed by depending on the direction of applied stress. This is the key idea of diffusional creep mechanism. In tensile stress field, bulk vacancy concentration will be decreased as blew equation.

$$C_v^j = C_v^0 \exp(-\frac{\sigma b^3}{kT})$$

<div align="right">Equation III.3.15</div>

In 1972, Brailsford uses the concept of diffusional creep. Bulk defect concentration was assumed that it is affected by the emission of vacancy from sink to free matrix. Hence bulk defect concentration has a negative effect on vacancy absorption rate to sink.

The difference between diffusional creep and Brailsford's irradiation model is the consideration of the interstitial atom. In his model dislocation loop growth was explained by stress preferential induced attraction (SPIA).

Therefore, Brailsford just combine two phenomena. In traditional diffusion creep equation, it can be interpreted that vacancy is simultaneously absorbed and emitted by sink. Therefore, vacancy absorption rate, which considers stress effect, should be expressed more precisely as below equation.

$$A_v = z_v^j D_v C_v - z_v^j D_v C_v^j$$
<div align="right">Equation III.3.16</div>

Here, C_v^j is the bulk defect concentration near the sinks, C_v^0 is the bulk defect concentration, and b is the Burgers vector (cm) hence vacancy absorption rate decrease with increasing of the bulk defect concentration. From this equation, SPIA is could be expressed as below equation by considering interstitial flux and bulk defect concentration which is reflect stress effect on creep.

$$J = \rho_j (z_i^j D_i C_i - z_v^j D_v C_v + z_v^j D_v C_v^j)$$
<div align="right">Equation III.3.17</div>

Unfortunately, this Brailsford approach does not account the vacancy formation from the free matrix which has a positive effect on vacancy absorption rate. Moreover, one thing remained which is not considered in Equation III.3.15 is stress effect on the diffusion coefficient. It is obvious that self-diffusion is a function of applied stress. However, until now, the stress effect on defect diffusivity and defect generation in the free matrix were not considered. Those phenomena are important especially at high temperature which is SFR condition.

In this study, to account the stress effect on diffusivity, activation energy is modified as same approach method in diffusional creep model.

$$D_v = D_v^0 \exp(-\frac{\sigma b^3}{kT})$$
<div align="right">Equation III.3.18</div>

Here, D_v is the vacancy diffusion coefficient in stress applied condition, D_v^0 is vacancy diffusion coefficient in non-stress applied condition. This kind of approach was already adopted in zirconium and its based alloy [2]. However, this approach was not extended to iron and its based alloy.

III.3.6 Stress effect on RIDI with a recent method

To establish the sink strength in the previous section, the defect absorption rate is calculated by

solving the isotropy diffusion equation. However, to consider the stress effect, reaction probability has to be modified as the anisotropy diffusion equation. It is not a simple task to generate and solve the anisotropy diffusion equation. Therefore, in the traditional method, sinks are characterized as two-part depending on stress direction. In the recent method, the sink will be treated as two parts depending on stress direction. However, there is the difference between traditional and recent method, that is diffusion tensor. From diffusion tensor, more accurate analysis become a possible.

As discussed in previous section, MD simulation is powerful tool and stress effect on diffusivity did not consider. Hence stress effect on diffusivity could be calculated by MD simulation. Fortunately, recently, many MD simulation has been conducted to account the various effect on defect behavior. C.W. Kang and M. Banislaman is most representative researcher [37].

The most important progress on stress effect on diffusivity in MD simulation is an analysis of cluster behavior. In non-stress applied condition, cluster diffuse in an arbitrary way. However, in applied stress condition, clusters diffuse in one diction. In the traditional approach, only point defect behavior could be analyzed, hence this information is much valuable information.

Not only qualitative information but also quantitative data could be obtained by following the trajectory of atom position. From this information, Mean Square Displacement (MSD) could be derived to obtain the diffusion tensor.

III.3.7 Alloy effect on RIDI with the traditional method

Alloy plays many roles in metallurgy, i.e. improve mechanical, physical, and, corrosion properties. Specifically, in cladding materials, alloy improves the radiation resistant properties. There is two mechanisms that alloy effect on metal properties, i.e. alloy change the defect diffusion behavior and make precipitation, which acts as a trap for point defect and mobile dislocation.

However, in the early stage of nuclear engineering, there is no research tool to analyze the alloy effect on defect diffusivity. Hence only precipitation effect could be treated because precipitation could be observed by experimental equipments such as TEM or SEM.

During the process to optimize the cladding materials, the iron-based alloy is chosen from austenite steel to ferritic-martensitic steel. Meanwhile, it was revealed that precipitation reduced the irradiation swelling. To explain this phenomenon, one assumption was suggested that precipitation play neutral sinks. In detail, it was assumed that precipitation could provide recombination site as a point defect trap because precipitation is not composed with a lattice defect, but it composed with other alloy

elements and a different structure. What means is if interstitial is absorbed nearby precipitation, compressive potential field is generated and then vacancy is absorbed favorably. This mechanism could be applied for vacancy absorption nearby precipitation.

Therefore, the bias factor of precipitation should be changed by considering net defect flux. This kind of approach is well-described in Brailsford's paper [47].

$$Z_{ppt}^{v} = \frac{D_i C_i}{D_v C_v}$$ Equation III.3.19

This traditional method could explain why precipitation improves the irradiation swelling. However, all alloy element does not form the precipitation. Solution-state of alloy play on the improvement of RIDI needs state of art simulation tools.

III.3.8 Alloy effect on RIDI with a recent method

Recently by using first principle and MD simulation, the reaction between defects and alloy have been revealed. The materials design company is the most advanced research group in this study region. Not only point defect but also the stability of extended defects which is affected by alloy had been researched. Nb effect on interstitial diffusivity in Zr-Nb was simulated and express as MSD [35]. Firstly, in first principle simulation, one lattice atom is extracted and then the alloy element is created. By relaxation process, each alloy element characteristic could be expressed by each energy state such as formation migration and binding energy.

Alloy play not only substantial but also an interstitial role. Hence alloy is inserted in any interstitial site, and then same type information of could be revealed. Form this result, MD simulation could simulate the relationship between point defect and alloy. Finally, it was confirmed that interstitial diffusion by MSD

III.3.9 Cascade effect on defect generation rate and sink density

Not only defect generation rate but also sink density was affected by cascade annihilation. Garner show the experimental evidence of cascade annihilation effect [48]. In case of solution annealed materials, it could be analyzed that neutron bombardment only increase the sink density. However, in case of 20% cold-worked specimen, sink density is decreased by radiation damage. Hence both mechanism of defect generation and annihilation should be considered in rate theory. The modified rate equation is needed for consideration of cascade annihilation. The modified equation is expressed

as shown as Figure III.3.5. Defect generation and sink strength is modified from normal equation. From the experimental result, sink annulation rate (c_k) could be derived.

$$\frac{dC_v}{dt} = K_o - K_{iv}C_iC_v - K_{vs}C_vC_s^T$$

$$\frac{dC_i}{dt} = K_o - K_{iv}C_iC_v - K_{is}C_iC_s^T$$

$$\frac{dC_v}{dt} = (K_o-C_0) - K_{iv}C_iC_v - (K_{vs}C_vC_s^T - C_k)$$

$$\frac{dC_i}{dt} = (K_o-C_0) - K_{iv}C_iC_v - (K_{is}C_iC_s^T - C_k)$$

Figure III.3.5 Modified master equation by considering the cascade annihilation of sink

III.4   Computer code implementation

The python 2.0.7 language is used for the rate theory modeling [49]. In detail, python library module (Scipy) is used to solve the simultaneous ordinary differential equation, i.e. master equation of the rate theory [50]. Generally, Scipy module is used to solve the linear algebra, integration, special functions and image processing with efficient numerical routines.

Among the various module in Scipy, the scipy.integrate.odient is numerical integrate a system of ordinary differential equations in Scipy routines. From this system, the defect concentration could be integrated by numerical method.

To adopt the scipy.integrate.odient, time step function should be defined. In scipy.integrate.odient, integration time step is defined as "array" in python. Hence in this study, time step was defined by using "for" statement. Interval of time was given as 0.25 (0.25, 0.50, 0.75…). The region of time was defined that irradiation damage started from the 10^{-7} to 10^{9}. Since time is accounted from 10^{-7}, primary radiation damage did not consider. Hence defect generation rate was input parameter in this study.
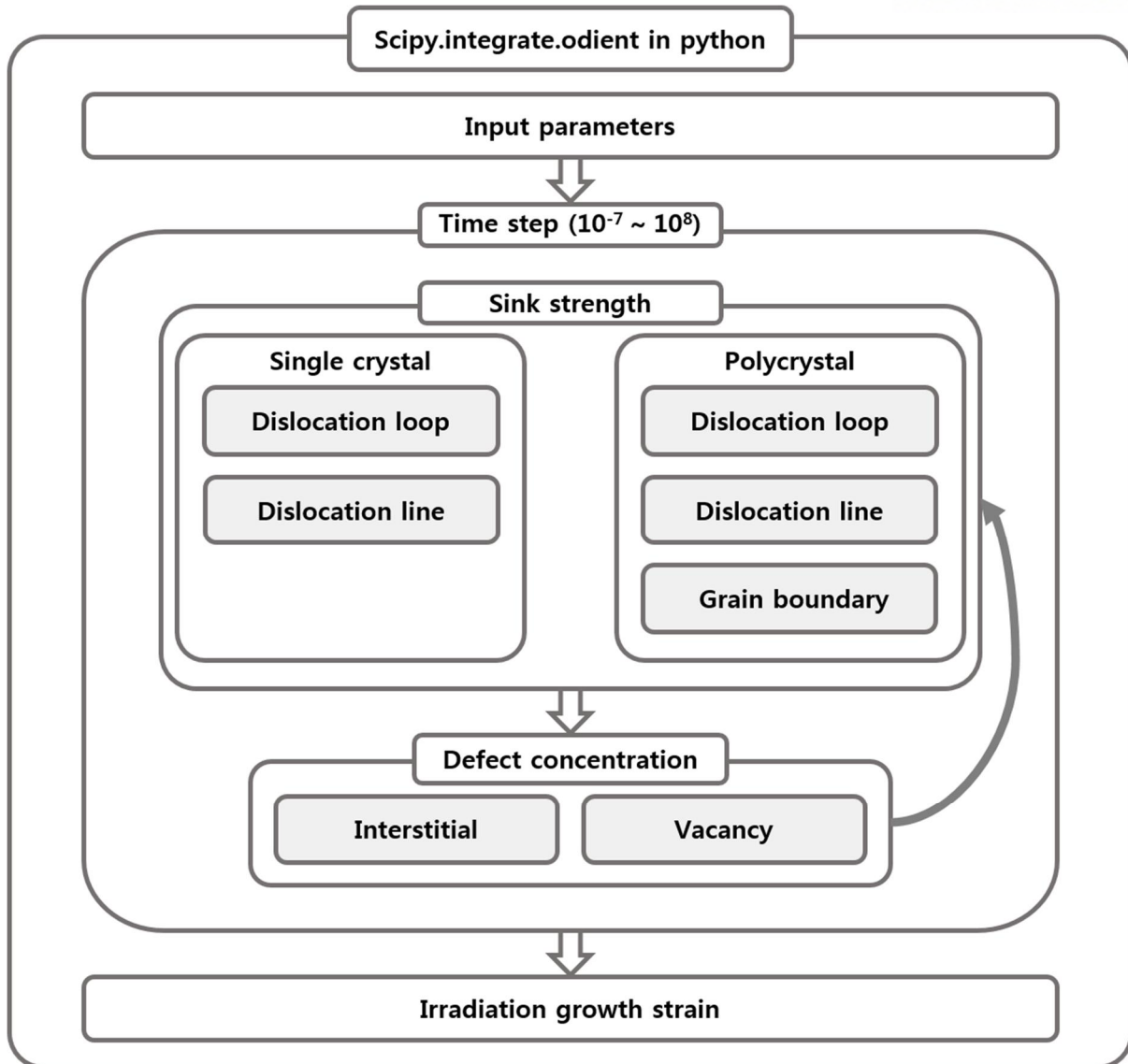
Figure III.4.1 Schematic diagram of code implementation

IV Results – Zirconium and its alloys

IV.1 The methodology of irradiation growth modeling

In case of zirconium, irradiation growth and creep are two representative RIDI mechanism. To eliminate the texture effect, irradiation growth was firstly simulated from a single crystal, and then polycrystal is examined. To calculated irradiation creep, stress was considered by modifying the diffusion coefficient. Finally, the alloying elements effect was simulated. The detail approach method and equations were introduced in rationale chapter. Hence in this chapter, the equation for specific systems (such as single crystal and polycrystal) are briefly described.

IV.1.1 Rate equation of single crystal & polycrystal

In case of single crystal zirconium, dislocation loop and dislocation line are the main sinks in the matrix. Hence, sinks in the defect rate equations could be simply composed by dislocation loop and line. The initial dislocation line density was obtained from experimental observation as shown in Table IV.2.1. Each sink is characterized by <a> and <c> axis because the origin of irradiation growth was assumed as DAD phenomenon.

$$\frac{dC_{sv}}{dt} = K_o - K_{iv}C_iC_v - \rho_{ilp}Z_{ilp}^vC_vD_v - \rho_{vlb}Z_{vlb}^vC_vD_v - \rho_{dp}Z_{dp}^vC_vD_v - \rho_{db}Z_{db}^vC_vD_v \qquad \text{Equation IV.1.1}$$

$$\frac{dC_{si}}{dt} = K_o - K_{iv}C_iC_v - \rho_{ilp}Z_{ilp}^iC_iD_i - \rho_{vlb}Z_{vlb}^vC_iD_i - \rho_{dp}Z_{dp}^iC_iD_i - \rho_{db}Z_{db}^iC_iD_i \qquad \text{Equation IV.1.2}$$

$$\rho = \rho_{dp} + \rho_{db} + 2\pi r_v N_v + 2\pi r_i N_i \qquad \text{Equation IV.1.3}$$

where K_o is defect production rate. K_{iv} is recombination rate which mean vacancy and interstitial are combine and go to perfect lattice atom. ρ_{ilp}, ρ_{dp}, ρ_{vlb} and ρ_{db} are each sink density. Z_{ilp}^i and Z_{ilp}^v are interstitial and vacancy bias factor of interstitial loop, Z_{dp}^i athe nd Z_{dp}^v are interstitial and vacancy bias factor of dislocation line, Z_{vlb}^i and $Z_{vlthe\ b}^v$ are interstitial and vacancy bias factor of vacancy loop, Z_{db}^i and Z_{db}^v are interstitial and vacancy bias factor of dislocation line. C_{si} and C_{sv} are defect concentration of interstitial and vacancy in single crystal matrix, D_i and D_v are the diffusion coefficient in the matrix.

The first term on the right-hand side of Equation IV.1.1 is the defect generation rate; the second is the recombination rate; the third is the vacancy absorption rate of <a> interstitial loops, which are parallel to the prism plane; the fourth is the vacancy absorption rate of <c> vacancy loops, which are parallel to the basal plane; the fifth is the vacancy absorption rate of <a> dislocation lines, which are perpendicular to the prism plane; the last is the vacancy absorption rate of <c> dislocation lines, which are perpendicular to the basal plane. The master equation of vacancies follows the same method as that of interstitials. The constants are listed in Table IV.2.1.

In case of polycrystal zirconium, not only dislocation loop and line but also GB should be considered as the main sink in the matrix. Therefore, the rate equations are more complex than a single crystal case. Using single crystal defect rate equation, defect rate equation could be simply expressed.

$$\frac{dC_{pv}}{dt} = \frac{dC_{sv}}{dt} - k_{gp}^2 Z_{gp}^v C_v D_v - k_{gp}^2 Z_{gp}^v C_v D_v$$

Equation IV.1.4

$$\frac{dC_{pi}}{dt} = \frac{dC_{si}}{dt} - k_{gp}^2 Z_{gp}^i C_i D_i - k_{gb}^2 Z_{gb}^i C_i D_i$$

Equation IV.1.5

$$k_{gb}^2 = 6 \times \sqrt{\rho} / d_{gb}$$

Equation IV.1.6

where C_{pi} and C_{pv} is defect concentration of interstitial and vacancy in polycrystal matrix. k_{gp}^2 and k_{gb}^2 are grain boundary sink strength. Z_{gp}^i and Z_{gp}^v are interstitial and vacancy bias factor of grain boundary in prism. Z_{gb}^i and Z_{gb}^v are interstitial and vacancy bias factor of grain boundary in basal plane.

In the polycrystal equation, the sink strength of the grain boundary was calculated using Brailsford and Bullough's method. The constants are listed in Table IV.2.1. it is assumed that the dislocation line density does not change because dislocation loops absorb all the defect flux. The loop number density is hard to calculate by a theoretical method because there is no general equation for loop nucleation and growth equation under radiation. Therefore, the experimental value of the loop number density was used.

As described in Equation IV.1.4 and Equation IV.1.5, vacancy dislocation loops in the prismatic plane are not considered in this study because the consideration of co-existence of vacancy and interstitial is

needed to modify the fundamental assumption of SRT. Since SRT assumes that all sink is homogeneously distributed, and these sinks receive same defect flux, the expression of co-existence of vacancy and interstitial dislocation loops are neglected in this study. However, since the reaction probability was calculated by SRT using average defect flux value of each sink, vacancy loops in the prismatic plane could be neglected without having any problem in the situation where the sinks are distributed homogeneously.

IV.2   Fundamental parameters

The experiment of irradiation growth has been done many researchers after Buckly [12]. From these experiments, qualitatively mechanisms are suggested by using microstructure analysis and then, defect rate theory is used to the calculation of defect concentration for quantitatively modeling. Historically, Hesketh [51] and Carpenter [52] set up firstly theoretical growth modeling by experiment database. After that, theoretical modeling base on rate theory developed by Dollins [53], Fainsteins - Dedraz [54], MacEWEN [55] and Bullough [56] who adopt rate theory. However, these papers, published in the 1980s, had two limitations. First mobile defects are only composed only point defect. Second point defect has isotropic diffusion. From these assumptions, calculation results could not fully explain the microstructural characteristic.

In the after of 1980s, noticeable theoretical modeling paper is about to sink strength in zirconium was published by Woo [2]. He considered difference of the interstitial diffusion coefficient <a> axis and <c> axis. Therefore, the bias factor could be developed at each sink in the zirconium matrix. Until now this modeling gives a fundamental base with PBM approach in the growth research area.

Recently, a computer simulation was developed, and theoretical analysis was advanced. From these evolutions, irradiation growth modeling is researched again to fundamental understanding. Christien [57] had been theoretically modeled with Frenkel pair three diffusion model in a single crystal. And after that Golubov [58] also predict with theoretical modeling in a single crystal with PBM modeling. More specifically, in Christien work, he assumed that main sink is dislocation loop and line. <a> elongation occurs by <a> dislocation loop growth. <c> shortening occurs by agglomeration of vacancy loop. From Christien an equation, irradiation growth result show good agreement of experimental data. In case of Golubov, elongation is calculated by account reaction kinetics of 1-D interstitial cluster in steady state.

To simulation irradiation growth, basic parameters are adopted from these literature studies. The diffusion coefficient is the most important parameter as a fitting parameter. Hence, from the Christien study, the value of the diffusion coefficient is adopted. The bias factor is adopted from Woo's researched. The experimental result such as dislocation number density is accounted from Northwood study as shown in Table IV.2.1.

Table IV.2.1 Input parameters

Input parameter		Symbol	Unit	Value	Reference/comment
Defect generation rate		G	dpa s^{-1}	10^{-7}	[16]
Recombination radius		r_{iv}	cm	10^{-7}	[57]
Burgers vector		b	cm^{-2}	3.23×10^{-8}	[59]
Diffusion coefficient	Vacancy	D_v	cm^2 s^{-1}	3.0×10^{-17}	[57]
	INTERSTITIAL	$\overline{D}_i$	cm^2 s^{-1}	1.0×10^{-6}	[57]
Sink strength	<a> loop	ρ_{ilp}	cm^{-2}	$2\pi r_i N_i$	[58]
	<c> loop	ρ_{vlb}	cm^{-2}	$2\pi r_v N_v$	[58]
	<a> dislocation line	ρ_{dp}	cm^{-2}	Single: 7.25×10^6	[36]
				Cold: 20×10^9	[36]
	<c> dislocation line	ρ_{db}	cm^{-2}	Single: 2.25×10^6	[36]
				Cold: 5×10^9	[36]
	<a> GB	$(k_{GB}/2)$	cm^{-2}	$6 \times \sqrt{\rho} \div d_{gb}$	[60]
	<c> GB	$(k_{GB}/2)$	cm^{-2}	$6 \times \sqrt{\rho} \div d_{gb}$	[60]
Average strain factor	<a> loop	A_{ilp}	Constant	0.5	[53]
	<c> loop	A_{vlb}	Constant	1.0	[53]
	<a> dislocation line	A_{dp}	Constant	0.5	[53]
	<c> dislocation line	A_{db}	Constant	1.0	[53]
	<a> GB	A_{GBp}	Constant	0.5	Assume in this work
	<c> GB	A_{GBp}	constant	0.5	Assume in this work
Bias factor	<a> loop	Z_{ilp}^i	Constant	1	[61]
	<c> loop	Z_{vlb}^i	Constant	0.586	[2]
	<a> dislocation line	Z_{dp}^i	Constant	1.56	[2]
	<c> dislocation line	Z_{db}^i	Constant	0.586	[2]
	<a> GB	Z_{gp}^i	Constant	1.56	[2]
	<c> GB	Z_{gb}^v	Constant	0.586	[2]

IV.3   Irradiation growth modeling of single crystal

The strain rate is determined not only by defect flux but also average strain. The concept of the average strain was first suggested by Dollins. Before this concept was suggested, irradiation growth was assumed to be directly proportioned with the growth of dislocation line and loop size. However, dislocation has each directionality. Since depending on dislocation direction, irradiation growth should be changed.

IV.3.1 Average strain value for single crystal

In Dollins's work, the direction of dislocation loops and lines was accounted to calculate the irradiation growth of a single crystal in any given direction. As shown in Figure IV.3.1, depending on the directionality of dislocation loop, irradiation growth could be changed. For example, if the dislocation is growth in b_1 direction, there is no strain change in the perpendicular direction of b_1. Since dislocation loop is randomly distributed, average stain value is deduced by 0.5.
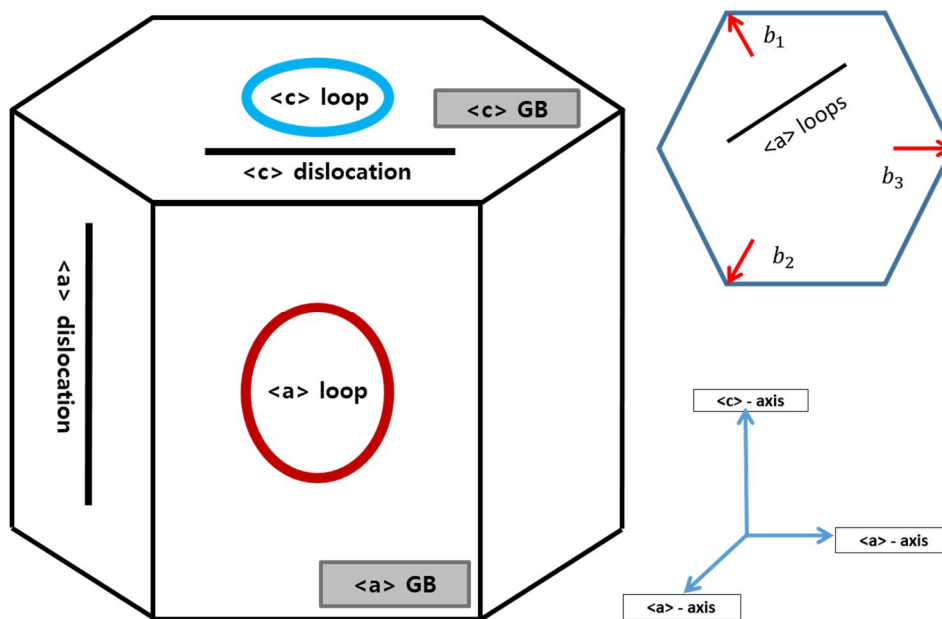

Figure IV.3.1 Schematic of main sinks in zirconium by SRT

Hence, from this quantitative analysis, irradiation growth by dislocation lines and loops could be expressed in terms of an average strain value. Therefore, the average strain factor effect was considered in the irradiation growth equation for single-crystals.

IV.3.2 Strain equation for single crystal

After the definition of average stain value and anisotropy factor, the irradiation growth strain rate was calculated using the dislocation climb mechanism.

$$\frac{d\varepsilon}{dt} = \rho b V \qquad\qquad \text{Equation IV.3.1}$$

$$V = \frac{1}{b}\left(Z_i D_i C_i - Z_v D_v C_v\right) \qquad\qquad \text{Equation IV.3.2}$$

where ϵ is the elongation (cm), ρ is the dislocation density (cm^{-2}), b is the Burgers vector (cm), v is the dislocation velocity (cm^{-2}s^{-1}), and z_i and zv are the interstitial and vacancy bias factors of dislocations, respectively.

Physically, Equation IV.3.1 expresses all the dimensional changes that could explain the creep- and stress-induced strain. These phenomena occur in one direction. However, irradiation growth occurs in various directions because the defect flux originates in neutron bombardment. Therefore, this general equation is limited to the calculation of each sink strain. Because of the anisotropy of the interstitial diffusion coefficient, the defect flux is specified for each sink. (For vacancies, the diffusion coefficient is always isotropic because the activation energy is much higher than that of interstitials.) From these equations, irradiation growth could be calculated for a specific sink type.

The bias factor is also considered to affect the capture efficiency because it determines the reaction probability of defect and sinks reactions. In an hcp system, the bias factor depends on the DAD because the crystal structure is anisotropic. Therefore, the detailed irradiation growth equation of a single crystal is expressed for each sink type:

$$\frac{d\varepsilon_a^{ilp}}{dt} = A_{ilp}\rho_{ilp}\left(Z_{ilp}^i D_i C_i - Z_{ilp}^v D_v C_v\right) \qquad\qquad \text{Equation IV.3.3}$$

$$\frac{d\varepsilon_a^{dp}}{dt} = A_{dp}\rho_{dp}\left(Z_{dp}^i D_i C_i - Z_{dp}^v D_v C_v\right) \qquad\qquad \text{Equation IV.3.4}$$

$$\frac{d\varepsilon_c^{vlb}}{dt} = A_{vlb}\rho_{vlb}\left(Z_{vlb}^v D_v C_v - Z_{vlb}^i D_i C_i\right)$$

Equation IV.3.5

$$\frac{d\varepsilon_c^{db}}{dt} = A_{db}\rho_{db}\left(Z_{db}^i D_i C_i - Z_{db}^v D_v C_v\right)$$

Equation IV.3.6

$$\frac{d\varepsilon_a}{dt} = \frac{d\varepsilon_{ilp}}{dt} + \frac{d\varepsilon_{dp}}{dt}$$

Equation IV.3.7

$$\frac{d\varepsilon_c}{dt} = \frac{d\varepsilon_{vlb}}{dt} + \frac{d\varepsilon_{db}}{dt}$$

Equation IV.3.8

where ε_a^{ilp}, ε_a^{dp}, ε_a^{vlb}, and ε_a^{db} are the irradiation growth strain induced by interstitial dislocation loops in the prism plane, dislocation lines parallel to the prism plane, vacancy dislocation loops in the basal plane, and dislocation lines parallel to the basal plane, respectively, and A_{ilp}, A_{dp}, A_{vlb}, and A_{db} are the corresponding average strain factors for each sink.

IV.4   Irradiation growth modeling of polycrystal

In the growth equation for polycrystal zirconium, the grain boundary sinks and grain orientation (texture) are considered. Therefore, irradiation growth of polycrystal zirconium is expressed differently from that of single crystals.

IV.4.1 Anisotropy factor for polycrystal

For polycrystals, the effect of texture (the anisotropy of each grain direction) should be considered in the strain equation, and then the growth strain rate could be calculated by each sink type. For single crystals, irradiation growth could be simply expressed by average strain value, the dislocation loop density because a-axis elongation and c-axis shortening are caused directly by dislocation loops. However, in case of polycrystal, anisotropy factor is needed to consider the texture because polycrystal irradiation growth indirectly is proportional to sink radius. F-factor is about the resolved fraction of basal poles in any given direction. Therefore, by using F-factor, anisotropy factor ($G_{poly} = 1 - 3F_d$) is considered for irradiation growth. For example, if the texture is homogeneously distributed, F-factor has 0.33, and then irradiation growth will not be occurred because anisotropy factor is 0

IV.4.2 Strain equation for polycrystal

The average strain factor of grain boundaries is also considered after the <a>- and <c>-axis growth strain rate is calculated to determine the growth in a certain direction. The average strain factor of grain boundaries is 0.5 because anisotropic grain boundary distribution is assumed for sufficiently high annealing. Therefore, the growth strain rate equations including the texture are expressed as

$$\frac{d\varepsilon_a^{gp}}{dt} = A_{gp}k_{gp}^2\left(Z_{gp}^i D_i C_i - Z_{gp}^v D_v C_v\right)$$

Equation IV.4.1

$$\frac{d\varepsilon_d}{dt} = G_{poly}\times(\frac{d\varepsilon_a^{ilp}}{dt}+\frac{d\varepsilon_a^{dp}}{dt}+\frac{d\varepsilon_a^{gp}}{dt})$$

Equation IV.4.2

where ε_d is irradiation growth strain in the direction of interest of polycyrstal; and ε_a^{gp} are the irradiation growth strain induced by grain boundaries in the prism of single grain; A_{gp} are the average strain factors for grain boundaries in the prism of single grain;

From the anisotropy factor, the relationship between radiation growth of single crystal and polycrystal

could be defined. In tradition, anisotropy factor was simply calculated by F factor ($G_{poly} = 1 - 3F$). However, recent studies reported that irradiation growth of polycrystal could not be simply calculated by simple anisotropy factor because the difference of each grain orientation induced the grain-interaction. Therefore, the grain-interaction could make a change of irradiation growth depending upon specimen texture. Therefore, in this study, grain-interaction accounted from Woo's research.

IV.5   Results of irradiation growth modeling

The irradiation growth strain is calculated by the SRT and general dislocation climb equation. The results for both single-crystal and polycrystal zirconium are examined in terms of the defect concentration, defect flux, sink strength, and growth strain. The effect of dislocation lines and loops on growth was verified for single-crystal zirconium. The effect of grain boundaries on growth was confirmed for polycrystal zirconium. For annealed polycrystals, the grain boundary effect was an important parameter for dislocation lines and loops. In contrast, the grain boundary effect was negligible for cold-worked polycrystal zirconium. Finally, for verification, the calculation results are compared with experimental data.

IV.5.1 Single crystal

The defect concentration shows typical low-sink-density behavior in single-crystal zirconium. Initially, the defect concentration increases because reaction probability is too low to recombine or interact with sinks. Next, the interstitial defect concentration decreases and the vacancy concentration increases because of rapid interstitial diffusivity. From this region, the defect reacts with the sink, and the sink density is changed. Finally, point defects are in a steady state because the production rate could be compensated by the recombination rate (10^{-8} dpa). Figure V.4.2 (a) shows the defect concentration of single-crystal zirconium.
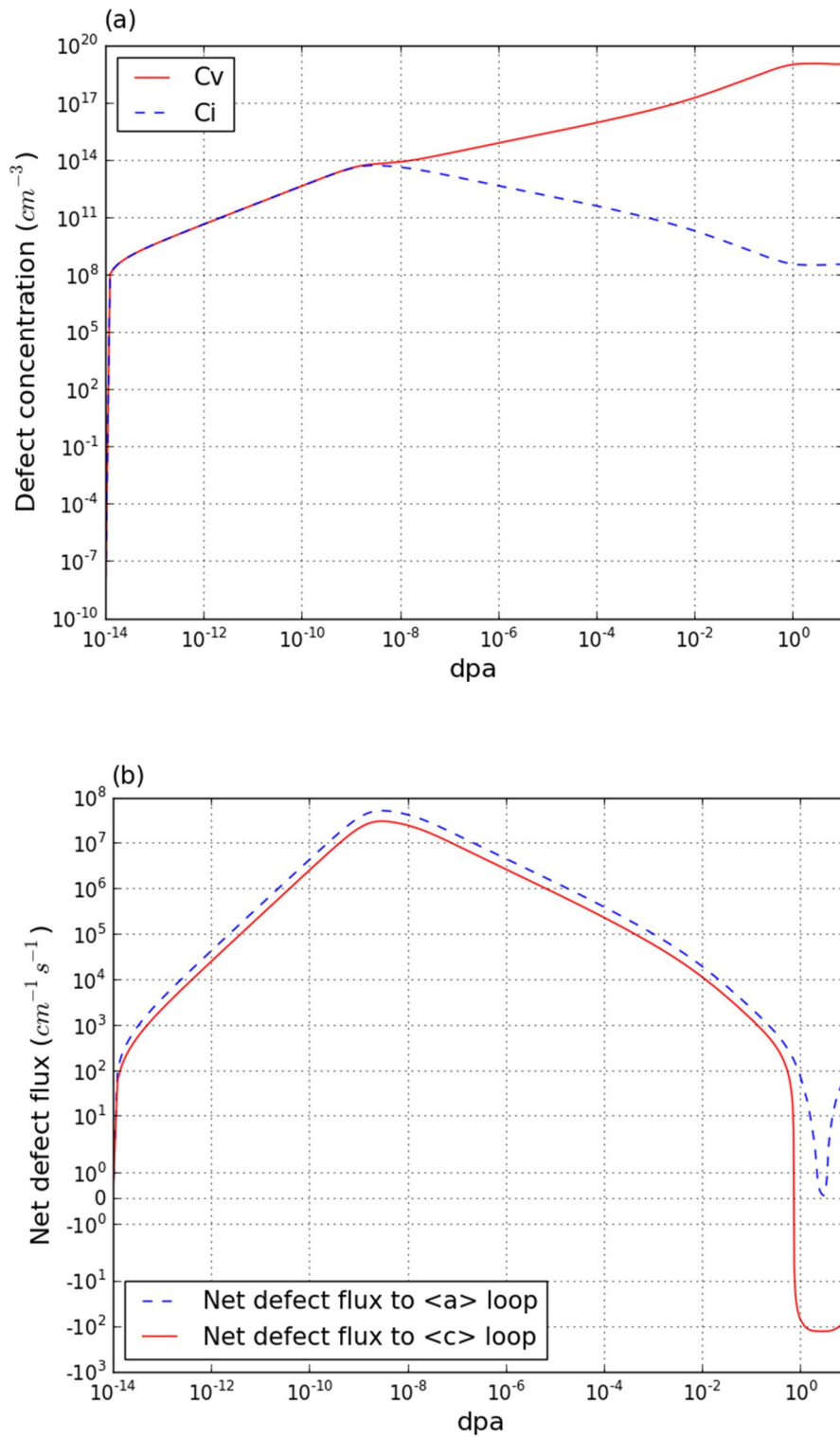
Figure IV.5.1. Radiation-induced (a) point defect concentrations, and (b) net defect flux to dislocation loops in single-crystal zirconium at 553 K

From the calculated defect concentration, the interstitial net defect fluxes to the major sinks are calculated. In single-crystal zirconium, these are the <a> and <c> dislocation loops. Figure V.4.2 (b) shows the interstitial net defect flux to the sinks. The defect flux initially increases at 10^{-9} dpa and immediately afterward decreases up to 1 dpa. In this early stage, net defect flux occurs during a very short time. Therefore, sinks are not developed significantly, i.e. the effect of initial regime on irradiation growth is negligible. Actually, the growth is affected in the steady-state net flux region, i.e. the high-dpa region. The net defect flux to <a> dislocation loops become positive, whereas the that of vacancy become negative. It is obvious behavior because DAD assumption already indicate that interstitial defects are accumulated in <a> dislocation loops, and vacancies are reacted with <c> dislocation loops. In this irradiation growth model, two types of dislocation loops are examined and calculated. The method of calculating the dislocation density follows that of Barashev. The number density and radius of dislocation loops are used to calculate the dislocation density. Figure IV.5.2 (a) shows the number density of dislocation loops. The value of the former is obtained from an experimental database, and then the radius is calculated using the the total number of defects:

$$\dot{S}_v = 2\pi r_v N_v (D_v C_{sv} - D_i C_{si})$$

Equation   IV.5.1

$$r_v = \sqrt{(S_v / \pi b N_v)}$$

Equation   IV.5.2

where S_v is the total number of vacancies in the vacancy dislocation loops. The change in Sv could be calculated from the defect flux because the reaction probability is proportional to the circumference of the dislocation loops and the defect flux. The radius of interstitial dislocation loops can be calculated using the same equation as that used for vacancies. Figure IV.5.2 (b) shows the radius of the dislocation loops. For interstitial <a> loops, the radius increases dramatically in the early dpa region. Subsequently, the radius is in the steady state. For <c> dislocation loops, the radius increases linearly from 3 to 7 dpa. However, there is no general information about the number density of <c> dislocation loops. The early-stage research presented only the ratio of the number densities of dislocation loops. Fortunately, the presence of <c> dislocation loops was analyzed by Holt and Gilbert in order to understand breakaway phenomena. In zircaloy-2, <c> dislocation loops do not appear before the 3 dpa region.

Figure IV.5.2 (c) shows the change in the dislocation loop density versus the dpa. Initially, the <a> dislocation loop density increases dramatically, whereas that of <c> type loops increases above <3> dpa. Next, the density of both types of dislocation loops shows a saturation region. The <a> dislocation loops are generated by the net interstitial defect flux behavior. However, <c> dislocation

loops generation and growth are caused by the net vacancy flux. These behaviors exactly follow the model structure. Discontinuities behavior of dislocation loops is caused by the limitation of the SRT model. Dislocation loop number density was based on the experimental result. It seems that there is a discrepancy between the defect concentration/defect flux (shown in Figure V.4.2) and the number density of dislocation loop (shown in   Figure IV.5.2 (c)).
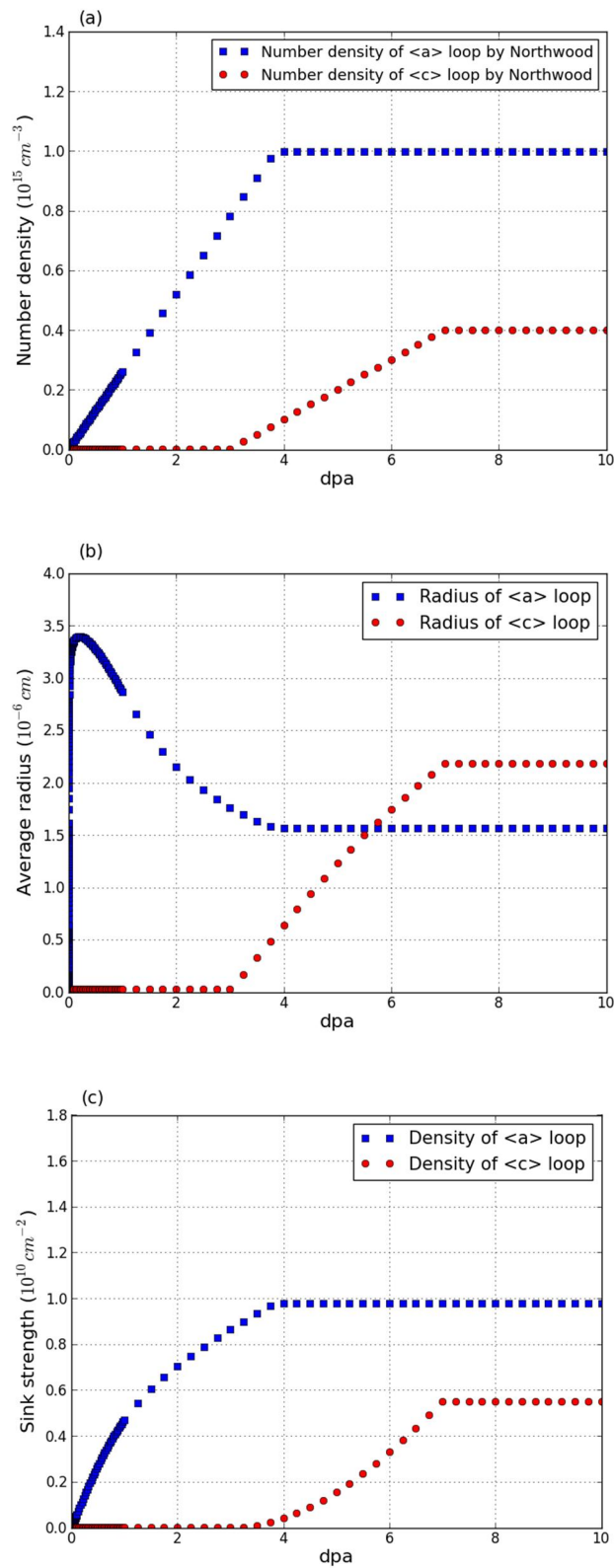
Figure IV.5.2. Sink information of (a) number density, (b) average radius, and (c) sink strength in single-crystal zirconium at 553 K

Finally, irradiation growth can be calculated using the defect concentration and sink density results. The results are compared with experimental measurements by Carpenter [11] in Figure IV.5.3. Although the experimental values of the growth strain were higher than the calculation data at 2^{-6} dpa, the overall growth tendency is similar to that of the experimental database and other irradiation growth models [7,8]. The modeled result shows a breakaway phenomenon, which is in good agreement with experimental data.
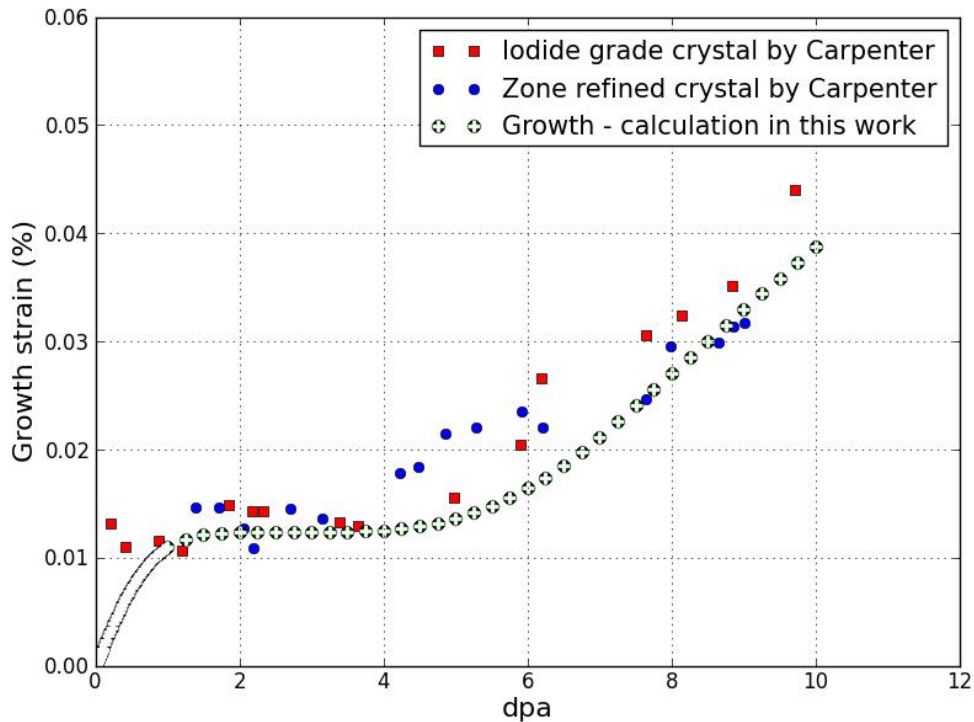
Figure IV.5.3. Modeled and experimental irradiation growth strain in single-crystal zirconium at 553 K

For single-crystal zirconium, dislocation loops have a stronger effect on irradiation growth than any other sink. Therefore, the strain should be analyzed by dislocation behavior. As described in previous section, dislocation density depends on the diffusivity, point defect concentration, initial dislocation line density, and bias factor. Among these four parameters, only the point defect concentration is dependent variable. Other parameters are independent variable. However, point defect is also determined at by other three parameters, i.e. diffusivity, initial dislocation line density, and bias factor. Therefore, fundamental research has to be carried out about the basic parameters such as diffusivity, bias factor, and initial dislocation density. Hence, in discussion chapter, each parameter is examined to further understanding.

In this study, number density of dislocation loops is the obtained from experimental results [17,18]. However, Christien and Barbu theoretically calculate the number density of dislocation loops by CDM. Nevertheless, those researchers did not verify the number density of dislocation loops with experimental results.

IV.5.2 Cold worked polycrystal

In cold-worked polycrystal zirconium, the defect concentration shows typical high-sink-density behavior. As in single-crystal zirconium, the interstitial defect concentrations initially increase 10-11 up to 10^{-12} dpa. However, in cold-worked polycrystal zirconium, interstitial defect concentrations initially increase 10^{-10} up to 10^{-12} dpa. Next, the effect of the recombination rate can be neglected because of the high sink density. Therefore, the rate of decrease of the interstitial concentration is smaller than that in single-crystal zirconium. Finally, interstitial and vacancy concentrations are in a steady state. Figure IV.5.4 (a) shows the defect concentrations in cold-worked polycrystal zirconium. The net defect flux to the sinks is analyzed for <a> dislocation lines, <c> dislocation lines, and grain boundaries. Figure IV.5.4 (b) shows the net defect fluxes to these sinks. The defect fluxes to sinks show quasi-steady-state regions instead of peaks, unlike the behavior in single-crystal zirconium. This phenomenon is caused by the high sink strength (the sink strength is enough to consume the defects at an early stage). Subsequently, as in single-crystal zirconium, the defect fluxes decrease. After 10^{-2} dpa, the net defect fluxes show a final steady-state region. Finally, these constant net defect fluxes determine the irradiation growth strain. Therefore, irradiation growth is accelerated by these constant fluxes to sinks.
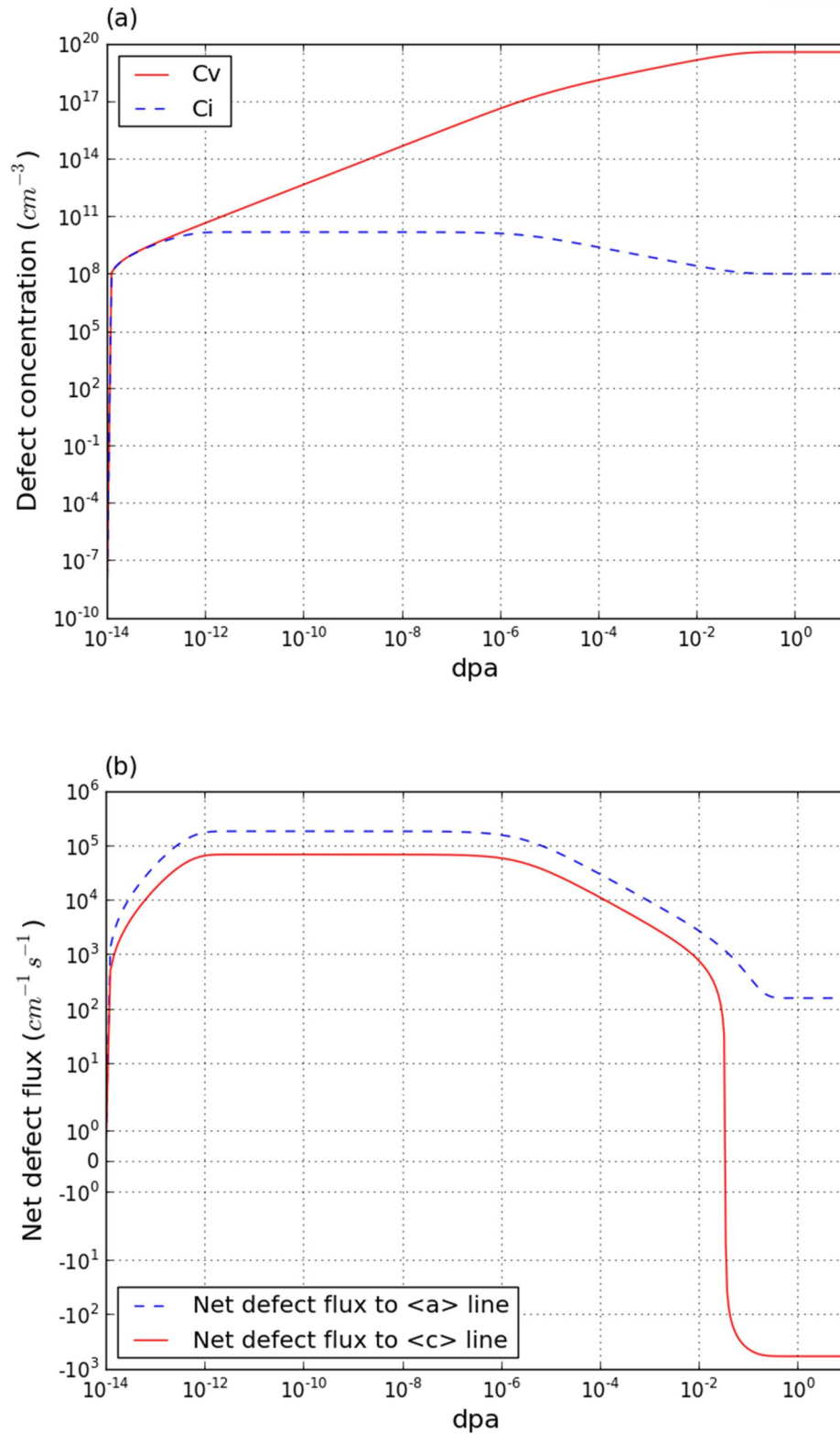
Figure IV.5.4. Radiation induced (a) defect concentrations, and (b) net defect flux to dislocation line in cold-worked polycrystal zirconium at 553 K

Because the major sinks in cold-worked polycrystal zirconium are dislocation lines and grain boundaries, three types of the sink are examined. Figure IV.5.5 shows the dislocation line density and grain boundary sink strength versus the dpa. The dislocation line density was assumed to be a time-independent parameter. Therefore, the dislocation line density is constant with respect to the dpa. (Physically, the dislocation line density in cold-worked zirconium is already sufficiently developed. Therefore, it could not be increased because dislocation lines develop into network dislocations.) The grain boundary sink strength function depends on the dislocation line density. Therefore, the sink strength of grain boundaries also constant with respect to dpa.
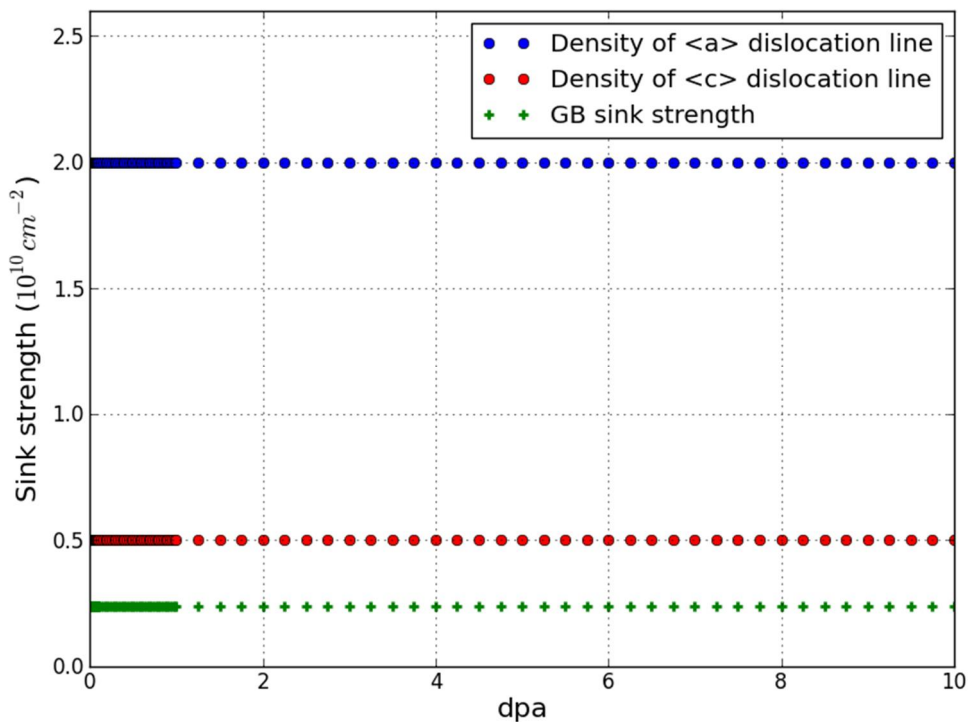
Figure IV.5.5. Sink strength in in cold-worked polycrystal zirconium at 553 K

Figure IV.5.6 presents the model results for cold-worked polycrystal zirconium. The irradiation growth strain of cold-worked polycrystal zirconium is also quite similar to experimental results. In this case, dislocation line sink effects are dominant. As result, irradiation growth exhibits very simple behavior, i.e. a linear increase with dpa. The results for cold-worked polycrystal zirconium were compared to experimental data of cold-worked zircaloy because of an absence of that of cold-worked polycrystal zirconium data. In cold-worked polycrystal zirconium, dislocation lines are the most powerful factor in irradiation growth modeling.
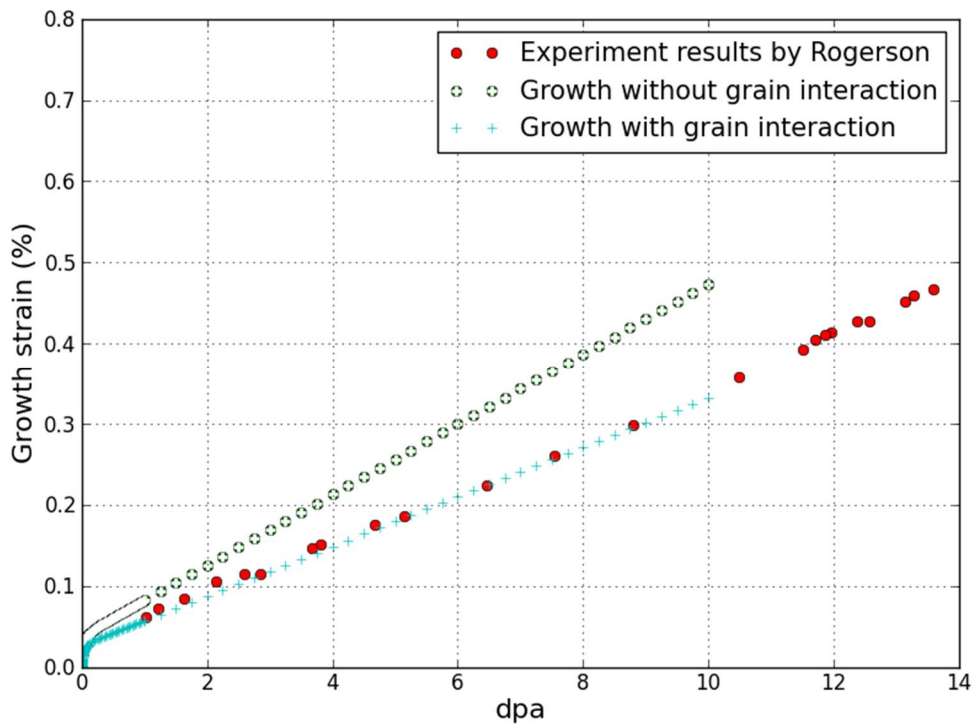
Figure IV.5.6. Modeled and experimental irradiation growth strain in cold-worked polycrystal zirconium at 553 K

IV.5.3 Annealed polycrystal

In annealed polycrystal zirconium, the defect concentration shows intermediate-sink-density behavior. As in the single-crystal and cold-worked cases, the defect concentration initially increases. Its subsequent behavior is similar to that in the cold-worked case. However, the quasi-steady-state region shows a much higher concentration because of the lower sink density. Figure IV.5.7 (a) shows the defect concentration in annealed polycrystal zirconium.

For the behavior of the net defect fluxes to sinks, three types of defect are also analyzed because the major sinks are dislocation loops and grain boundaries. Figure IV.5.7 (b) shows the net defect fluxes to sinks. As in cold-worked polycrystal zirconium, the sink strength is high enough to cause a steady state at low dpa (before 10^{-8}). However, the induced dislocation density in cold-worked polycrystal zirconium is much higher than that in annealed polycrystal zirconium. Therefore, the defect flux is much higher in annealed polycrystal zirconium than in cold-worked polycrystal zirconium.
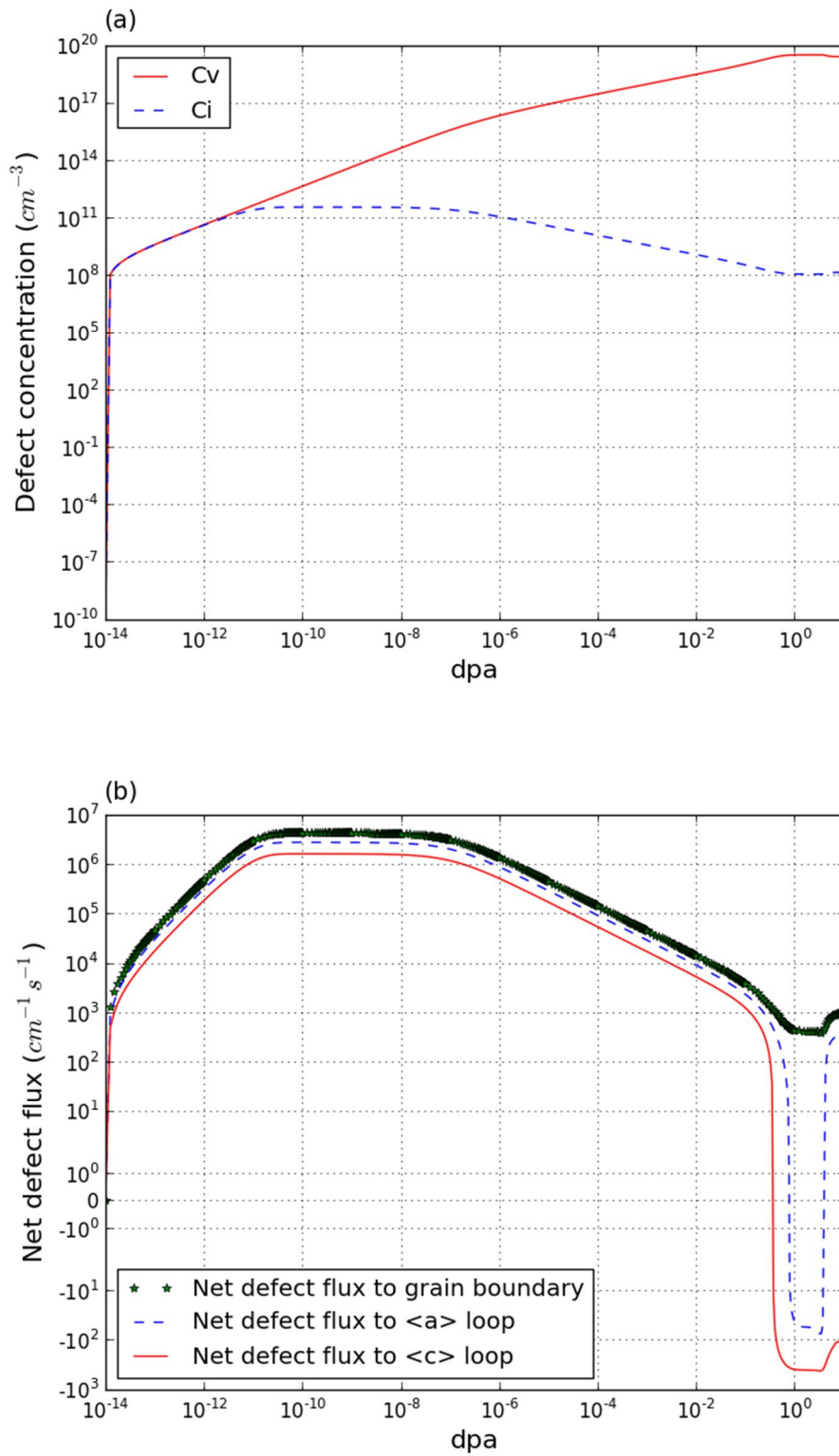
Figure IV.5.7. Radiation-induced (a) defect concentrations, and (b) net defect flux to dislocation loops and grain boundary in annealed polycrystal zirconium at 553 K

In annealed polycrystal zirconium, the major sinks are <a> and <c> dislocation loops and grain boundaries. Therefore, these three types of the sink are examined. Dislocation loop examined the same method of a single crystal. Figure IV.5.8 (a) shows the number density of dislocation loops. The value of the former is obtained from an experimental database, and the radius is calculated using the change rate of the total number of defects. Figure IV.5.8 (b) shows the dislocation loop radius. Unlike the case for the single crystal, the <c> dislocation loop radius is much larger than the <a> dislocation loop radius. Figure IV.5.8 (c) shows the dislocation loop density and grain boundary sink strength versus the dpa. The grain boundary sink strength increases with increasing dpa because it depends on the dislocation line and loop density. The <a> dislocation loop density has the shape of a semicircle before 4 dpa, after which <a> dislocation loops are saturated. The increase in the <c> loop density resembles an exponential model. However, <c> dislocations have a much higher sink strength than <a> dislocation loops. This result does not match the experimental results well.
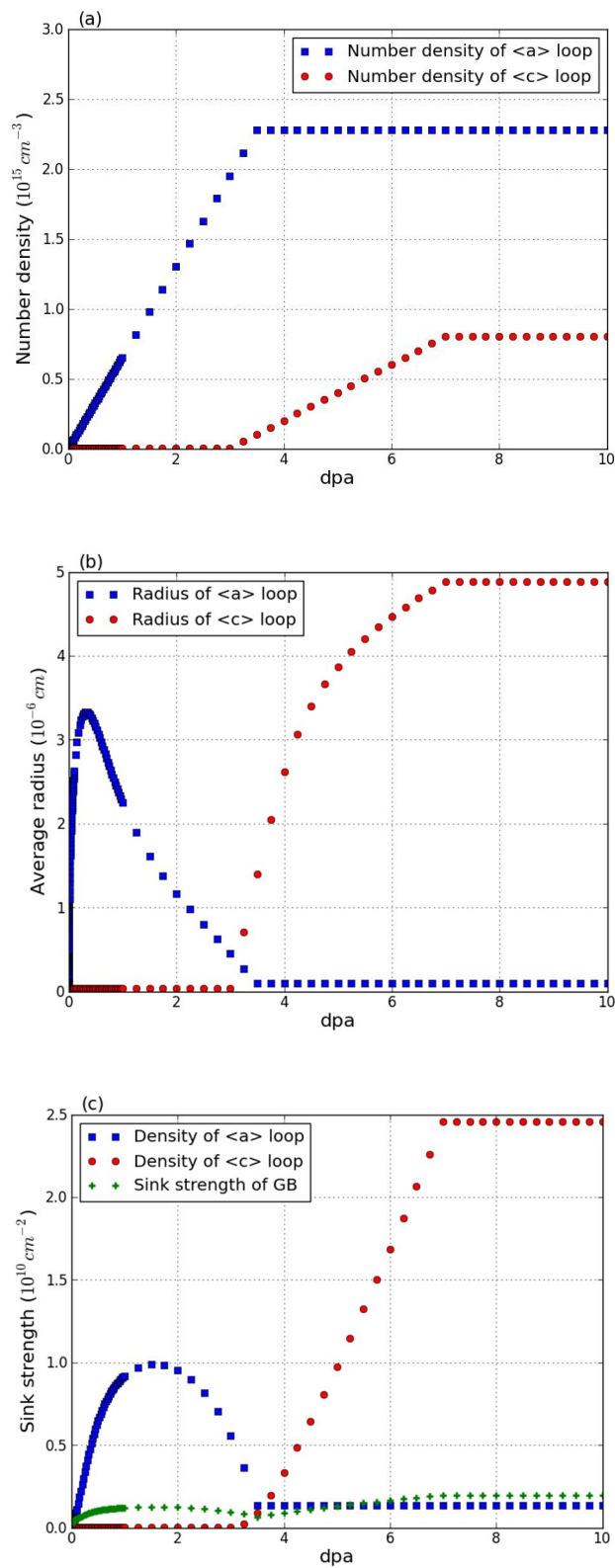
Figure IV.5.8. Sink information of (a) number density, (b) average radius, and (c) sink strength in annealed polycrystal zirconium at 553 K

Figure IV.5.9 shows the modeled growth in annealed polycrystal zirconium. Both results show high growth strain initially. However, after 1 dpa, the calculated strain shows a much slower increase. This discrepancy between the calculation and measurement increases with increasing dpa.

The strength model for grain boundaries is based on the dislocation line and loop densities. The dislocation lines are assumed to be constant with respect to the dpa. Therefore, the primary reason for the disagreement of annealed polycrystal zirconium is dislocation loops behavior.

In this model, the sink strength of dislocation loops is calculated using experimental data on the number density. The behavior of the sink strength depends strongly on the number density. However, there are no precise experimental data in the given dpa region. Therefore, cascade annihilation of sink, which is referred in rationale chapter, could be another possibility to overcome the discrepancy.

Other possibility could be reason of discrepancy, may be new mechanism for the grain boundary strength should be suggested. However, there is currently no general theory or simulation result for the grain boundary sink strength.
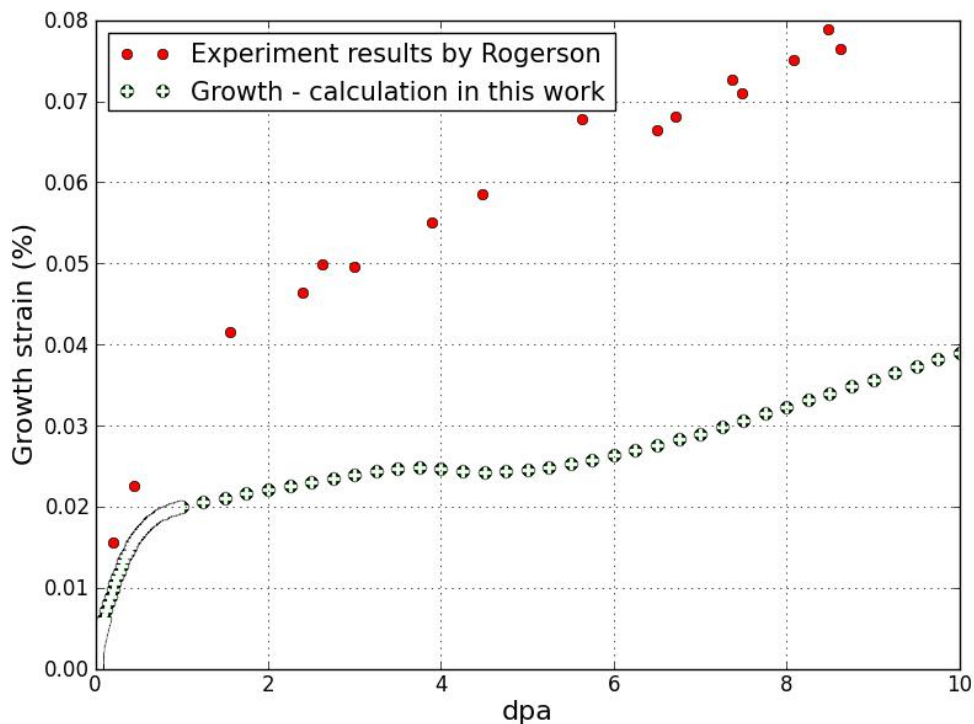
Figure IV.5.9. Modeled and experimental irradiation growth strain in annealed polycrystal zirconium at 553 K

IV.6   Stress effect on zirconium

In previous section, strain equations were derived by considering each sink effect on the irradiation growth. As same method, each sink effect on irradiation creep was expressed. For the simplification, dislocation is assumed that it is distributed isotopically. Hence, initial dislocation density, which is perpendicular with stress applied direction, was assumed 1/3 of total dislocation density. The detailed irradiation creep equation is:

$$\frac{d\varepsilon_a^{lp}}{dt} = A_{lp}\rho_{lp}\left(Z_{lp}^i D_i C_i - Z_{lp}^v D_v C_v\right)$$

Equation   IV.6.1

$$\frac{d\varepsilon_a^{dp}}{dt} = A_{dp}\rho_{dp}\left(Z_{dp}^i D_i C_i - Z_{dp}^v D_v C_v\right)$$

Equation   IV.6.2

$$\frac{d\varepsilon_p}{dt} = \frac{d\varepsilon_{lp}}{dt} + \frac{d\varepsilon_{dp}}{dt}$$

Equation   IV.6.3

where ε_a^{lp} are the irradiation creep strain induced by interstitial dislocation loops, and dislocation lines where stress is applied in the perpendicular direction. ε_p is the total irradiation creep strain along stress applied direction, respectively.

To account the stress effect on defect evolution, we need to know only three fundamental parameters such as migration, formation, and binding energy. However, until now there is no extensive study about migration, formation, and binding energy of zirconium under the stress condition.

The originality of this study is the modifying of Brailsford method. In Brailsford method, only vacancy emission of dislocation loop was considered. However, stress effect on diffusion coefficient and defect formation energy do not account. Those phenomena are important especially at high temperature. In this study, to account the stress effect on diffusivity, activation energy is modified as same approach method in diffusional creep model. In detail, as described rationale chapter, stress effect also considered by modified Arrhenius formulation.
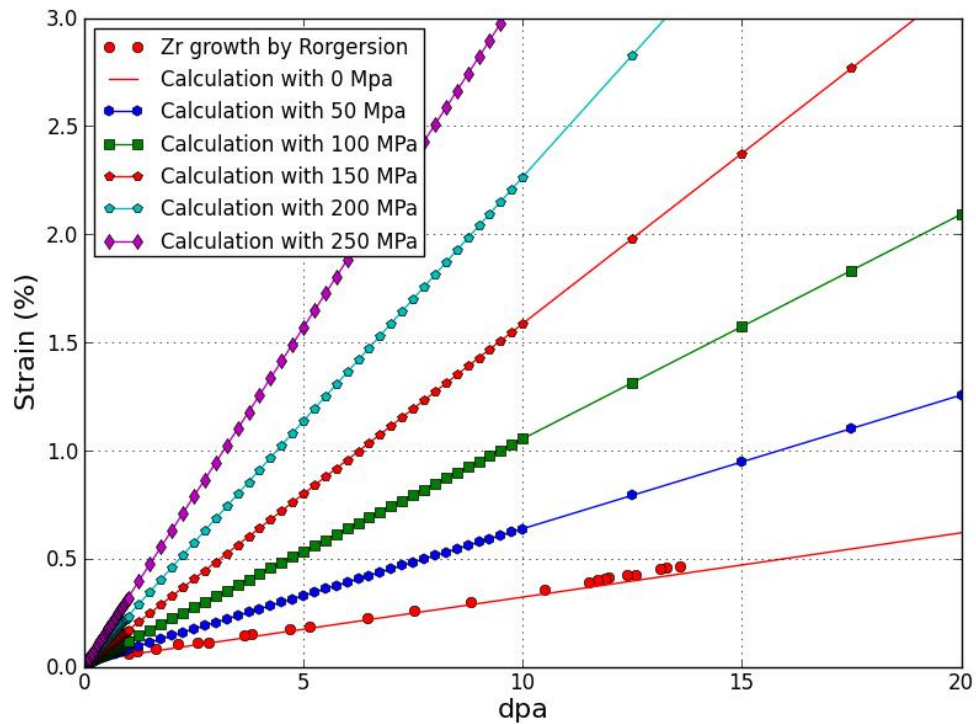
Figure IV.6.1 Stress effect on irradiation creep in cold-worked polycrystal zirconium at 553 K

In case of cold-worked zirconium alloy, it was assumed that dislocation density is already saturated. Hence sinks number density and radius behavior are not analyzed. However, in case of stainless steel, sink behavior should be analyzed because stainless steel is more ductility than zirconium. therefore, more detail analysis will be conducted in the iron-based alloy.

IV.7   Alloy effect on zirconium

To consider the alloy effect in the conventional way as described in the rational chapter, the number density of precipitation is an essential parameter. Nevertheless, there is no information of number density of precipitation because the quantitative analysis to analyze the number density of precipitation needed a lot of TEM observation. Only limited information is possible, i.e. precipitation radius and fraction were observed.

As a result, in this study, alloy effect on RIDI was considered in the other way which has never been considered in rate theory for RIDI, i.e. solid solution effect was considered. Recently correlation between the defect and alloy element has been revealed. From ab-initio, the activation energy of defect, which is nearby alloy element, have been calculated and then diffusivity was calculated by MD simulation. Hence alloy effect on RIDI could be derived by modifying the defect diffusivity in rate theory. In detail, Christensen [35] calculate the interstitial diffusivity within 0.5 % of Nb and 2.5 % Sn and in zirconium matrix. Hence Christensen reveals that Nb decreases the interstitial diffusivity nearly 1/5.64 at 500 K and 1/5.88 at 700 K with 0.5 % Nb in zirconium. Also, the same method was applied to account the Sn effect. Sn shows the high dependency with temperature and relatively less effect than Nb. Interstitial diffusivity is decreased about 1/4.05 at 500 K and 1/1.38 at 700 K with 2.5 Sn.

This information was adopted in rate theory and then irradiation growth was predicted as shown in Figure IV.7.1 and Figure IV.7.2. By adding 0.5 % Nb in cold-worked zirconium, 0.2 % strain is obtained whilst cold-worked pure zirconium shows nearly 0.3 % strain at 10 dpa. Since there was no experiment about irradiation growth of Zr-0.5% Nb, Zr-2.5Nb experimental results was compared with simulation results.

There is a discrepancy of Nb percentage between simulation and experiment. Through the Zr + Nb phase diagram, it was confirmed that 0.5 % Nb is at the boundary between α-Zr and α-Zr + β-Nb at 500 K. Hence 0.5 % Nb is maximum solubility limited at a given temperature. It can be interpreted that Christensen wants to confirm the maximum Nb effect as a solute.
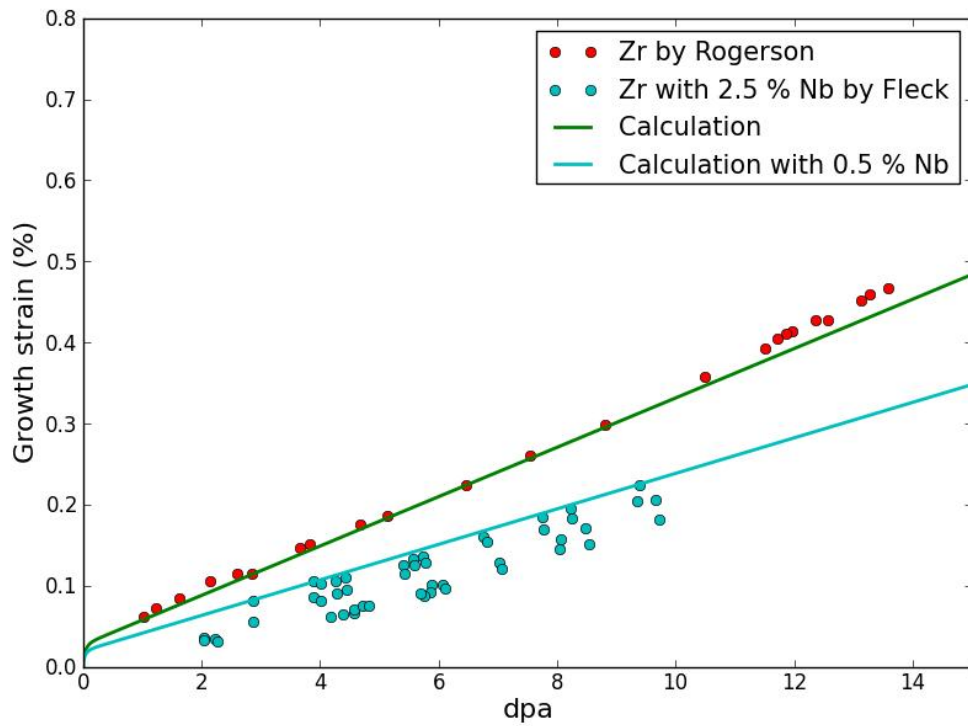
Figure IV.7.1. Nb effect on irradiation growth in cold-worked polycrystal zirconium at 553 K
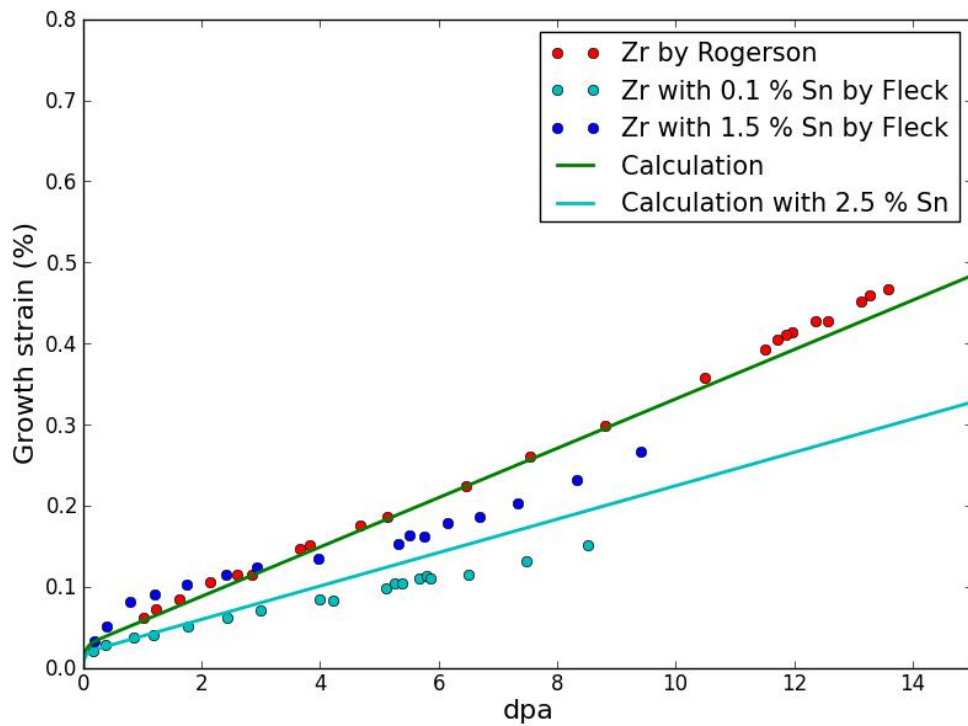
Figure IV.7.2. Sn effect on irradiation growth in cold-worked polycrystal zirconium at 553 K

IV.8   Limitation of SRT frame and PBM approach as a possible breakthrough

Irradiation growth and creep of zirconium were predicted by DAD assumption with SRT approach. However, recently, MD and ab-initio study show that DAD assumption is not true, and then suggest that the origin of irradiation growth is 1-D diffusion of the interstitial cluster.

In case of a bcc structure, the interstitial cluster could be mobile in <111> direction. In one <111> plane, there is three mobile directions. And there is 4 families of <111> plane. Hence total 12 isotropic diffusions could be possible. However, in case of zirconium, interstitial cluster only could mobile on prism plane of hcp structure. Therefore, it was suggested that irradiation growth is originated by anisotropic diffusion of the interstitial cluster rather than DAD.

Recently, Goloubov and Barashev use the PBM approach to consider the anisotropic diffusion of the interstitial cluster. They successfully predict the irradiation growth behavior of single crystal. However, they neglect the recombination and cluster evolution. Hence the only possibility of PBM is verified as replacement of DAD assumption.
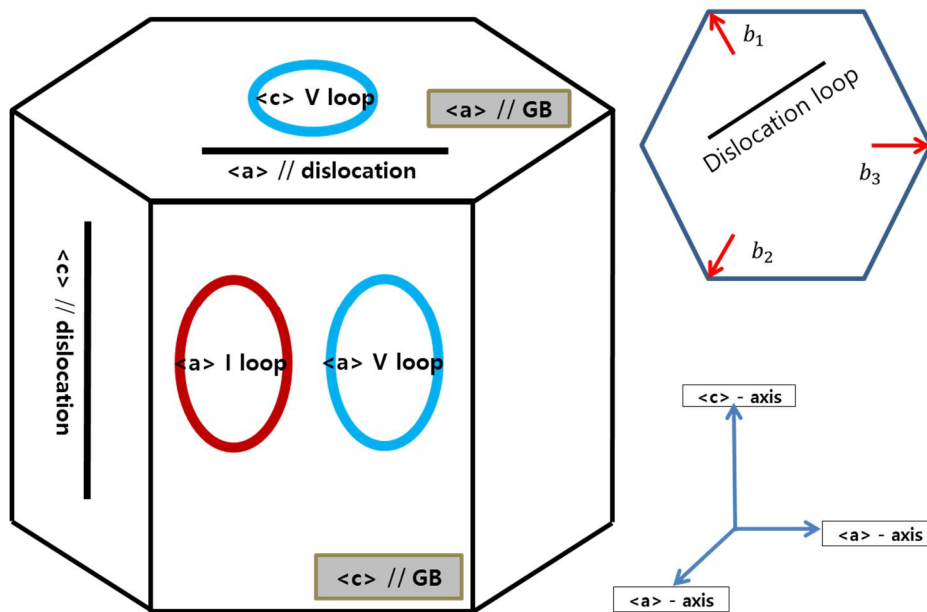
Figure IV.8.1. Schematic of the main sinks in zirconium by PBM

Therefore, in this study, from the equation which described in rationale chapter, PBM equation is developed with 6 major sinks as shown in Figure IV.8.1. Therefore, the master equation was established, and the defect absorption rate was calculated. However, since many energy parameters were not determined for PBM. Simulation results are failed as shown in Figure IV.8.3.
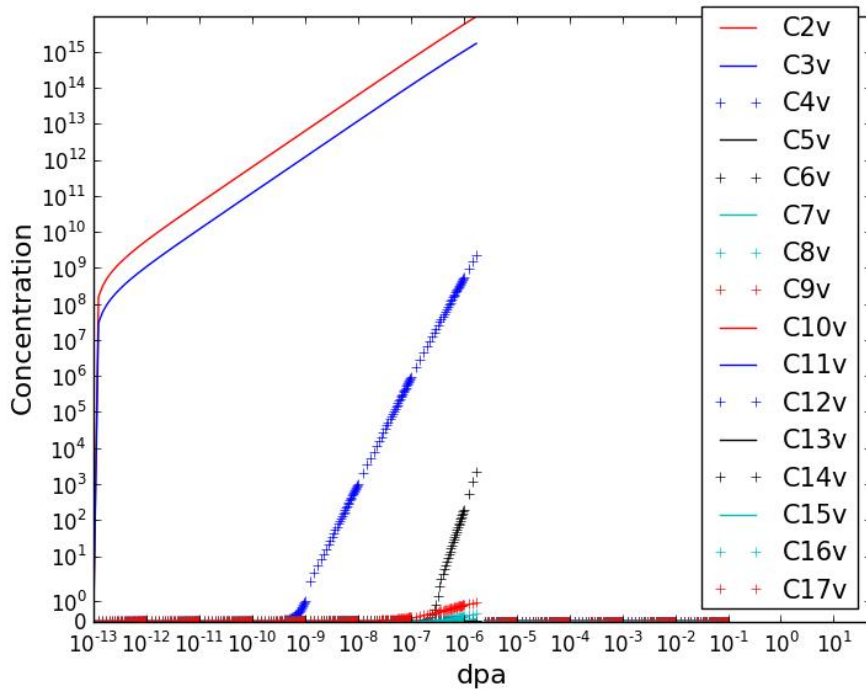
Figure IV.8.2 Vacancy cluster concentration in cold-worked polycrystal zirconium at 553 K by PBM
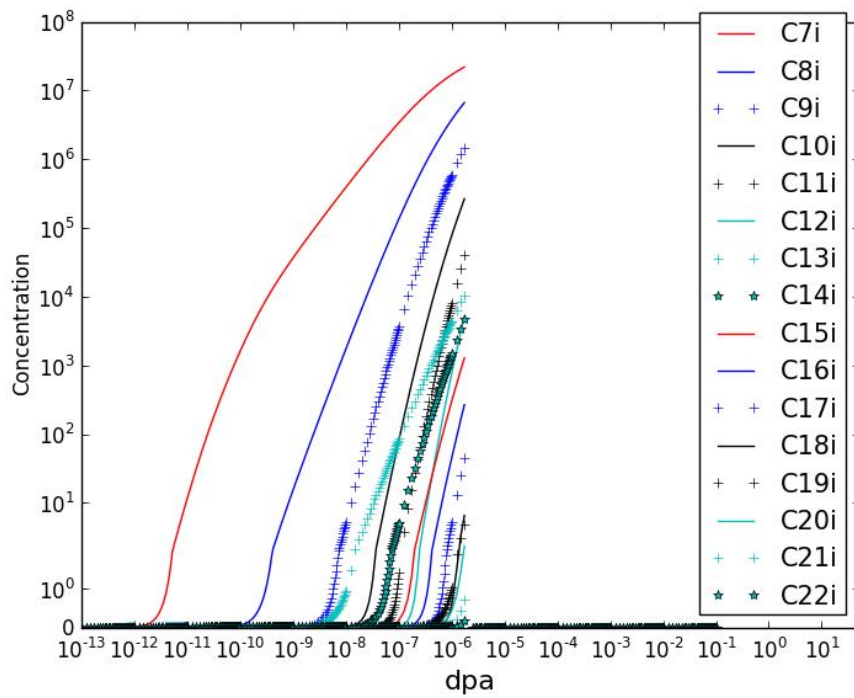
Figure IV.8.3 Interstitial cluster concentration in cold-worked polycrystal zirconium at 553 K by PBM

V   Results – Iron and its alloys

V.1   Methodology of iron-based alloy modeling

As mentioned in introduction chapter, the iron-based alloy is isotropic materials hence there is no texture such as zirconium. Since zirconium alloy has directionality, single crystal should be examined to analyze the texture effect on irradiation growth. However, iron-based alloy shows isotropic volume change, texture effect does not need to be verified. Hence irradiation swelling of single crystal had not been researched to confirm texture effect. Therefore, in this study, irradiation swelling of polycrystalline is directly calculated.

Iron-based alloy has many phases such as ferritic, austenitic, and cementite etc. Among various phase, austenite and ferrite are a most famous phase which is used for cladding materials. At the early stage of nuclear engineering, it was revealed that austenitic steel has a fundamental weakness about irradiation swelling. Hence high chrome ferritic-martensitic steel is chosen for SFR cladding materials [62]. In this point, simulation targeting structure is a bcc ferritic structure

V.1.1 Rate equation of pure iron

Unlikely zirconium case, iron-based alloy does not need to consider the texture, hence rate theory and strain equation are simple. What is really needed to accurately calculate the irradiation swelling is advanced rate theory equation, which could consider the complex defect behavior. As introduced in rationale chapter, CDM approach is applied for iron-based alloy,

$$\frac{dC_i}{dt} = K_o - K_{iv}C_iC_v - \sum_n \rho_n Z_n^i C_i D_i + \left(E_i^2 + \beta_v^2\right)C_{2i} + E_i^3 C_3 + E_i^4 C_{4i} \qquad \text{Equation V.1.1}$$

$$\frac{dC_{2i}}{dt} = \eta G_{dpa}\frac{f_{icl}^2}{2} + \beta_i^1 C_i / 2 + \left(\beta_v^3 + E_i^3\right)C_{3i} - \left(\beta_v^2 + \beta_i^1 + E_i^1\right)C_{2i} \qquad \text{Equation V.1.2}$$

$$\frac{dC_{ni}}{dt} = \eta G_{dpa}\frac{f_{icl}^n}{3} + \beta_i^{n-1} C_{n-1} + \left(\beta_v^{n+1} + E_i^{n+1}\right)C_{n+1} - \left(\beta_v^3 + \beta_i^3 + E_i^3\right)C_n \qquad \text{Equation V.1.3}$$

$$\frac{dC_{4i}}{dt} = \eta G_{dpa}\frac{f_{icl}^4}{4} + \beta_i^3 C_{3i} - \left(\beta_v^4 + \beta_i^4 + E_i^4\right)C_{4i} \qquad \text{Equation V.1.4}$$

where $C_{xv \ or \ xi}$ is vacancy or interstitial cluster concentration in the iron matrix (cm^{-3}), K_0 is the defect generation rate (cm$^{-3}s^{-1}$), which means vacancy and interstitial are combined to be a perfect lattice atom. G_{dpa} is the cluster defect generation rate (cm$^{-3}s^{-1}$), f_{cl}^x is the fraction of cluster, η is the cascade efficiency, K_{iv} is the recombination rate (cm^3s^{-1}), ρ_n is the density of sink of n type in the iron matrix (cm^{-2}), $Z_n^{v \ or \ i}$ is the vacancy or interstitial bias factor of sink on n type in the iron matrix, which is a dimensionless number, β is the point defect absorption constant, E is the point defect emission constant, ρ_n is the density of a specific sink such as dislocation line, dislocation loop, and void. Unfortunately, these methods are needed specialized numerical ODE solver and simulation time. Hence in this paper, the master equation is expended only up to fifteen to the simplified calculation.

V.2   Fundamental parameters

In the early 2000s, important papers were published by various authors. H. Duparc uses CDM approach as rate theory to predict the radius and number density of interstitial and vacancy loops. Calculated results were compared with the experimental result under 1 MeV electron by high voltage microscope [63]. This study object is the verifying the irradiation hardening of pressure vessels by CDM. In this study, the diffusivity of point defect was used as a fitting parameter to calibrate with experimental and simulations results. From the calibration, it was revealed that interstitial has $D_0^i = 4 \times 10^{-4}$ and $E_m^i = 0.3$, respectively, a vacancy has $D_0^v = 1$ and $E_m^v = 1.3$

By C.C. Fu, valuable information on the properties of defects, i.e. migration, formation or binding energy could be obtained by comparison between simulation and experiment [64]. In detail, the multi-simulation method was adopted, that is, kMC and ab-initio were used to simulate the resistivity experiments. In detail, defect concentration is predicted by following Takaki's discussion depending on temperature. In Takaki's discussion, various regimes of temperature were characterized by defect behaviors; In case of the stages (I) (23 - 101 K), recombination of the Frenkel pair is derived by specific geometries; In the stage (ID2), (107.5 K), correlated recombination is caused by free migration of the interstitial; In the stage (IE) (123–144 K) recombination is introduced interstitial diffusion, migration energy is 0.27 ± 0.04 eV; In stage (II) (164–185 K), di-interstitial could also have effects on reaction kinetic with $E_m^{2i} = 0.42 \pm 0.03$ eV; In stage (III) (220–278 K), vacancy attributes recombination, with $E_m^v = 0.55 \pm 0.03$ eV; In the stage (IV) (520–550 K), dissociation is taken accounted of consideration. From these information, stress or alloy effect was not considered. Therefore, from these fundamental parameters, RIDI was calculated with various stress and temperature conditions.

Table V.2.1 Input parameters

Input parameter		Symbol	Unit	Value	Ref
Temperature		T	K	673	
Hoop stress		σ	MPa	200	
Iron density		ρ	g cm^{-3}	7.85	-
Burgers vector		b	cm^{-2}	3.23×10^{-8}	-
Recombination radius		r_{iv}	cm	0.65×10^{-7}	[63]
Surface tension		γ	eV cm^{-3}	10.04×10^{17}	[65]
Defect generation rate		G	dpa s^{-1}	8.45×10^{-7}	[66]
Interstitial fraction		f_{i1}	-	0.594	[67]
Di-interstitial clustering fraction		f_{i2}	-	0.334	[67]
Tri-interstitial clustering fraction		f_{i3}	-	0.0723	[67]
Vacancy fraction		f_v	-	0.625	[67]
Di-vacancy clustering fraction		f_{v2}	-	0.292	[67]
Tri-vacancy clustering fraction		f_{v3}	-	0.0825	[67]
Di-vacancy binding energy		E_{2v}^B	eV	0.3	[64]
tri-vacancy binding energy		E_{3v}^B	eV	0.37	[64]
tetra-vacancy binding energy		E_{4v}^B	eV	0.62	[64]
Di-interstitial binding energy		E_{2i}^B	eV	0.8	[64]
tri-interstitial binding energy		E_{3i}^B	eV	0.92	[64]
tetra- interstitial binding energy		E_{4i}^B	eV	1.64	[64]
Vacancy formation energy		E_v^f	eV	2.07	[64]
Vacancy migration energy		E_v^m	eV	0.3	[63]
Interstitial migration energy		E_i^m	eV	1.3	[63]
Sink strength	\<a\> loop	ρ_{ilp}	cm^{-2}	$2\pi r_i N_i$	[57]
	\<a\> dislocation line	ρ_{dp}	cm^{-2}	1×10^{11}	Assume in this work
	Void	ρ_{db}	cm^{-2}	$4\pi r_{void}\rho_{void}$	[32]
Bias factor	Dislocation line	Z_{ilp}^i	Constant	1.1	[63]
	Dislocation loop	Z_{vlb}^i	Constant	1.0	[63]
	Void	Z_{dp}^i	Constant	1.0	[63]

V.3   Irradiation swelling modeling

In the case of iron, the rate of irradiation swelling could be calculated directly by considering the defect absorption rate. In case of zirconium, the concept of the average strain is needed to consider the texture. Hence the equation to calculate the irradiation swelling is very simple to compare with zirconium case. As described in the rationale chapter, irradiation swelling was calculated by defect absorption rate of the void as described in Equation V.3.1.

$$\frac{dV}{dt} = \Omega 4\pi r_{void}(z_v^j D_v C_v - z_i^j D_i C_i) \qquad \text{Equation V.3.1}$$

V.4   Results of irradiation swelling modeling

To validate the simulation model, the temperature dependence of irradiation swelling of pure iron polycrystalline was calculated and compared with experimental data at 1 dpa [68]. Although cluster was calculated only up-to fifteen, experimental number density does not need because it was assumed that most large cluster is directly developed as sinks such as dislocation loop and void. From concentration of number density, sink radius was calculated and then, void swelling is derived.

V.4.1 Pure iron

Figure V.4.1 and Figure V.4.2 shows point defect concentration and number density of cluster defects. The defect concentration of pure iron show typical high-temperature behavior, both point and cluster defects are saturated at 10^{-6} dpa. As written by G.S. Was in fundamental of radiation materials, this fast saturation is occurred by fast recombination and absorption phenomena [8].

The common phenomenon of these defects' behavior is the saturation. In case of a point defect, the saturation behavior was determined by recombination and absorption rate. More exactly, generation rate was balanced with recombination rate when each type of defect flux ($Z_x^i D_i C_i$ or $Z_x^v D_v C_v$) were equally absorbed at sinks. However, in the cluster, saturation the mechanism is different from that of point defect. In case of cluster defects, saturation is derived by absorption and emission of point defects. However, in the cluster, saturation the mechanism is different from that of point defect. In case of cluster defects, saturation is derived by absorption and emission of point defects. One thing to be noted in this paper is large vacancy cluster concentration eventually overwhelm the that of a small cluster. This phenomenon is caused by a characteristic of capture efficiency and emission rate because larger cluster has larger surface, which mean larger absorption rate.

From defect concentration, cluster number density is derived by calculating the absorption rate as shown in Figure V.4.1 and Figure V.4.2. The absorption rate is derived by following the rule, which was used to calculate the sink strength. In case of emission, simple Arrhenius formulation is used. Number density shows the same trend of cluster defects because number density is obtained from the largest cluster concentration. Base on the result of number density, the radius of sinks was calculated and expressed in Figure V.4.3. One thing to be noted here is larger vacancy cluster overwhelm the small cluster.
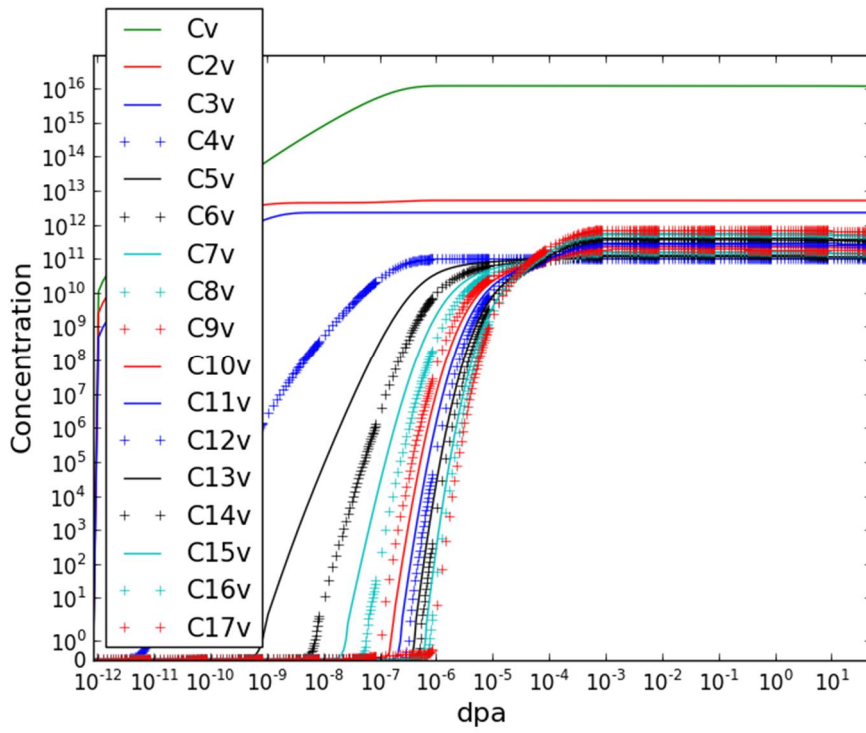
Figure V.4.1 Vacancy and its cluster concentrations in iron at 700 K
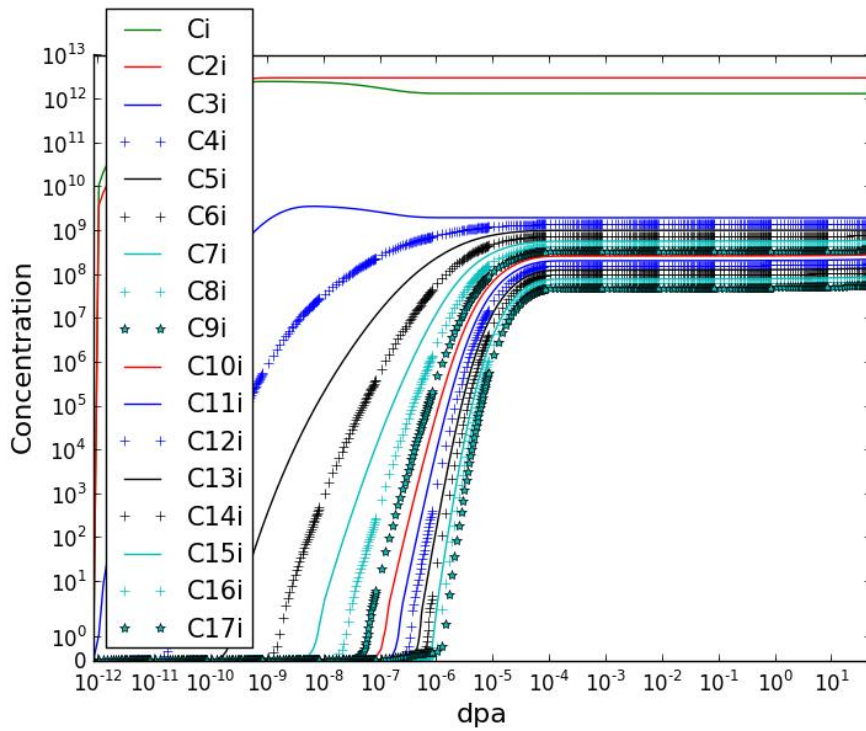
Figure V.4.2 Interstitial and its cluster concentrations in iron at 700 K

Both sink radius was increased at 10^{-6} dpa because number density is too low, and then until 10^{-4} dpa, both radiuses were decreased. The discrepancy between two sinks happens after 10^{-4} dpa. In case of the void, the absorption rate is much higher than emission rate hence radius growth with given number density. However, in case of dislocation loop were dissolved at SFR condition. To verify the radius behavior with linear scale, Figure V.4.4 was added.
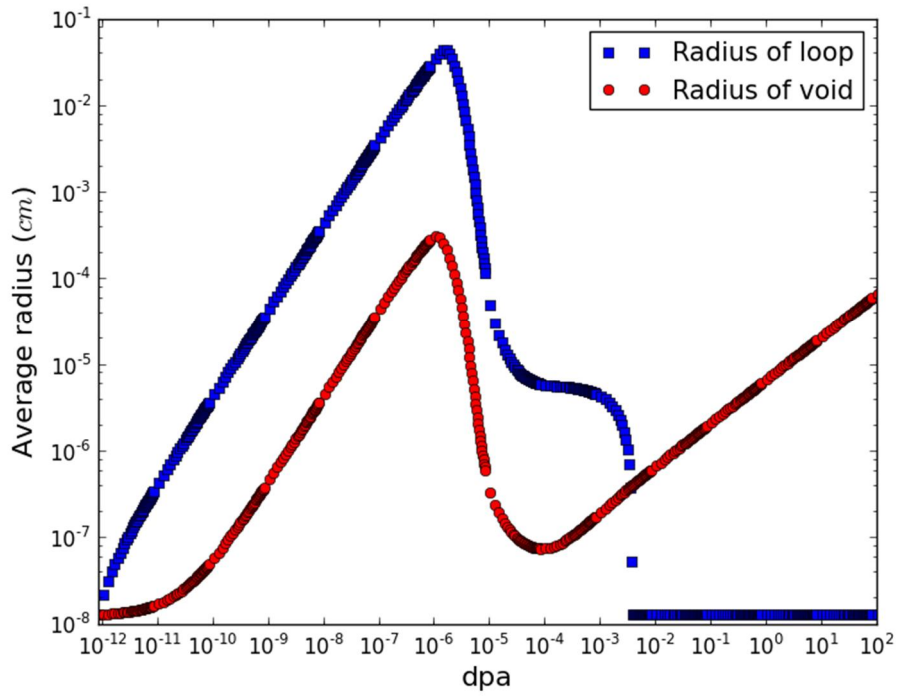
Figure V.4.3 Dislocation loop and void radius in iron by logarithmic scale at 700 K
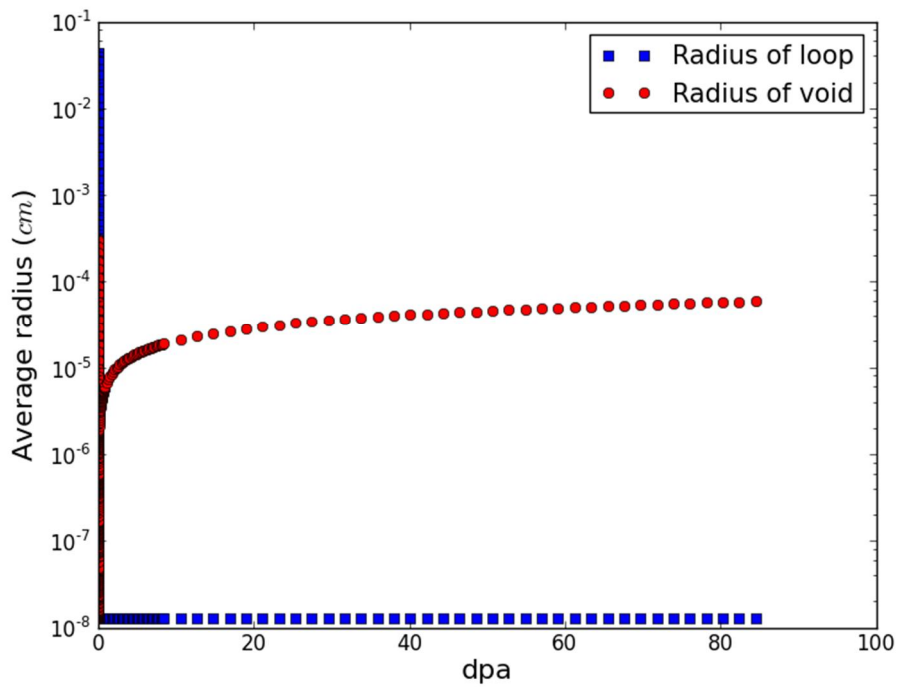
Figure V.4.4 Dislocation loop and void radius in iron by linear scale at 700 K

Finally, irradiation swelling was calculated and described by Figure V.4.5. The irradiation swelling depending on dpa shows exponential shape. It is predictable behavior because radius is increased as exponentially with saturated number density. This behavior was already confirmed in experiment result in EBR II or FFTF [6].
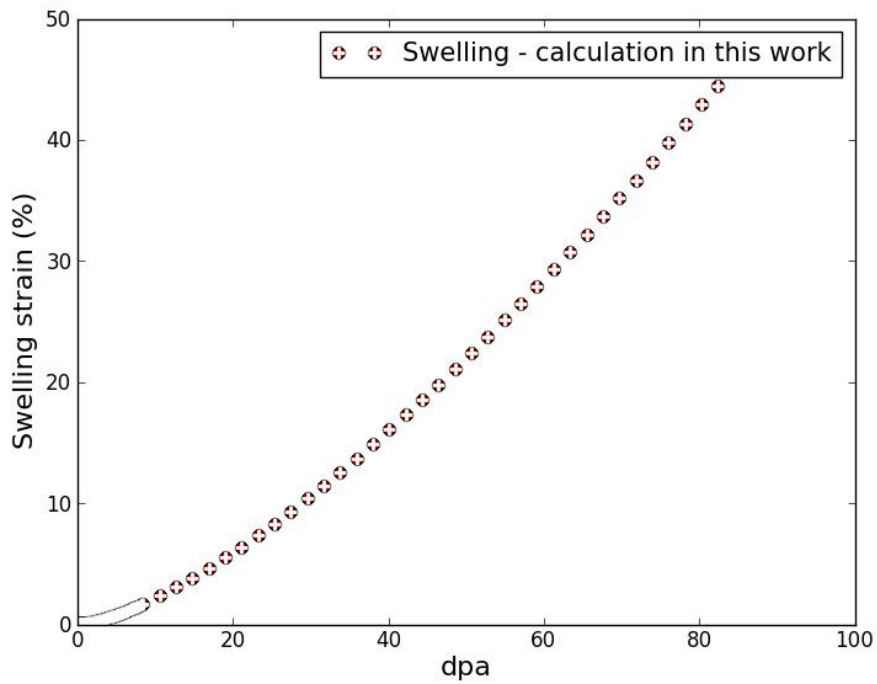
Figure V.4.5 Irradiation swelling behavior in iron at 700 K

V.5   Stress effect on iron

Just like zirconium case, dislocation climb mechanism is applied to calculated irradiation creep. From the general climb equation, irradiation creep equation is derived by the same method of zirconium. The detailed irradiation creep equation is expressed for each sink type:

$$\frac{d\varepsilon_a^{lp}}{dt} = A_{lp}\rho_{lp}\left(Z_{lp}^i D_i C_i - Z_{lp}^v D_v C_v\right)$$

Equation V.5.1

$$\frac{d\varepsilon_a^{dp}}{dt} = A_{dp}\rho_{dp}\left(Z_{dp}^i D_i C_i - Z_{dp}^v D_v C_v\right)$$

Equation V.5.2

$$\frac{d\varepsilon_p}{dt} = \frac{d\varepsilon_{lp}}{dt} + \frac{d\varepsilon_{dp}}{dt}$$

Equation V.5.3

where ε_a^{lp} and ε_a^{dp} are the irradiation creep strain induced by interstitial dislocation loops, and dislocation lines where stress is applied in the perpendicular direction. ε_p is the total irradiation creep strain along stress applied direction, respectively.

In zirconium results chapter, stress effect was accounted by modifying the Brailsford model. However, as described in the rationale chapter, stress effect could be directly considered by MD simulation. Hence the MD simulation method was adopted to calculated interstitial diffusivity.

The supercell 8x8x12 results with 1536 Fe atoms and periodic boundary condition is applied. To account stress effect, isothermal Uniaxial deformation along [100], [010], [110] or [111]. The cell stretching along [111] direction leads to shrinkage in both [1-1 0] and the [1 1-2]. The stretching along [010] leads to shrinkage in both [001] and [100]. The stretching along [100] leads to shrinkage in both [010] and [001]. The stretching [110] leads to shrinkage along [001] and [1-10].

The equilibration step allows the lattice to expand to a temperature of 800 K ~ 900 K with a pressure of 0 kbar at each simulation cell boundary using isothermal-isobaric NPT ensemble. Then, the simulation cell is deformed in the x-direction, to maintain a constant strain, while the lateral boundaries are controlled using the canonical (NVT) ensemble. By assuming 1-time step is equal to 1 fs we evaluate the diffusivity for 1 ns.

In case of migration energies, MD simulations are performed at temperatures over the temperature range, which are high enough to obtain sufficient defect mobility. The potential model used embedded atomic potential developed by Mendelev as it shows the potential was obtained by fitting to both ab initio total energy calculation results and experimentally measured properties [69].

We need to get the deviation time between the position of a particle and some reference position. It is the most common measure of the spatial extent of random motion and can be thought of as measuring the portion of the system "explored" by the random walker, this is called the MSD.

By getting the MSD results from MD calculation for 1 ns of run, the diffusion coefficient calculated using the Equation V.5.4 as shown below.

$$D_N(T) = \frac{\overline{R^2}(T)}{2n_d t} \qquad \text{Equation V.5.4}$$

Where $R^2(T)$ is the mean square displacement nd is the dimensionality of the diffusion process. From the extracted the trajectories of the single interstitial diffusivity, the OVITO is used for visualization the dimensionality of the diffusivity. t is the simulation time. The migration energies represent difference of total energy between the initial SIAs configuration and the SIAs at saddle.

The MD approach does not preselect migration paths hence the n_d value was determined from the extracted trajectories of diffusion of the defects for 1 ns simulation using the OVITO code, and the migration energies are obtained from temperature dependence equation. The migration energies are extrapolated from Arrhenius expression, Equation V.5.5

$$D_N(T) = D_{0,N} e^{-\frac{E_m}{kT}} \qquad \text{Equation V.5.5}$$

where k is Boltzmann's constant, E_m is the migration energy, and $D_{0,n}$ is a pre-factor. Table V.5.1 shows interstitial diffusivity by stress applied directions.

Table V.5.1 Diffusion coefficient by stress effect by MD simulation

Stress direction	Migration energy (eV)	Do pre-factor (cm^2/s)	Diffusion coefficient (cm^2/s)
<100>	0.121413223	0.0004246	8.4375×10^{-5}
<110>	0.448910772	0.0001709	2.24905×10^{-4}
<111>	0.114562858	0.0004690	9.24655×10^{-5}

From the calculation interstitial diffusivity, the concentration of defect and cluster, radius, and swelling is recalculated. The hole results on stress condition show the same tendency of that of non-stress condition. However, the strain rate was rapidly increased. In this study, the purpose of research is establishing the prediction model for the long fuel cycle condition. Hence, 600 MPa is applied and show ridiculous behavior because strain rate was so high. After 1 dpa, simulation was broken because of limitation of calculating power
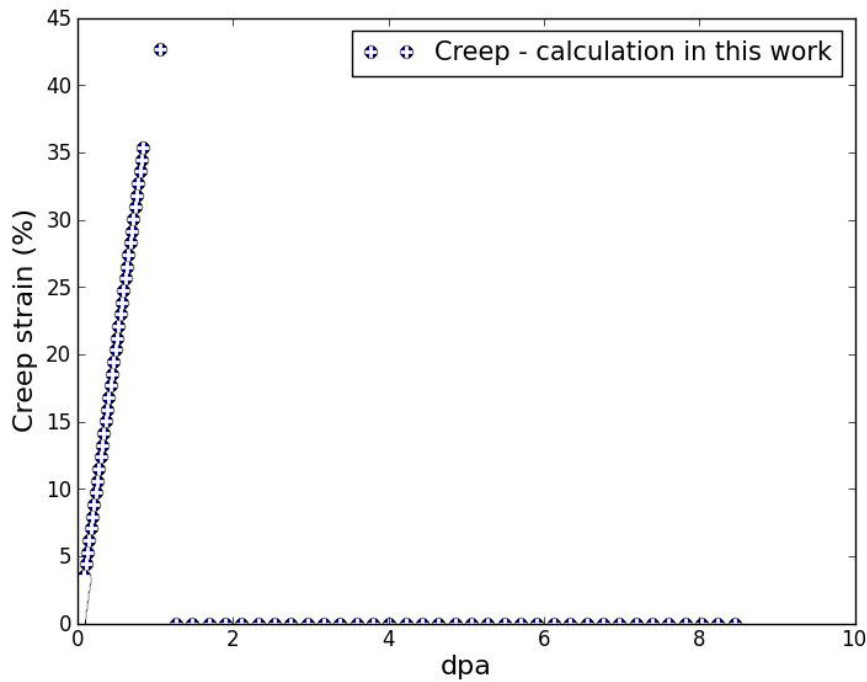
Figure V.5.1 Stress effect on irradiation creep in iron at 873 K and 600 MPa.

V.6   Alloy effect on iron

In case of zirconium alloy, solute state of alloy effect was considered. However, in case of an iron-based alloy, precipitation effect was considered by the traditional method. In case of precipitation, it has unique property compared with other sinks because precipitation is not composed with a lattice defect, but it composed with other alloy element with a different structure. Hence precipitation could provide recombination site as a point defect trap. Therefore, the bias factor of precipitation should be changed by considering net defect flux. This kind of approach is well-described in Brailsford's paper [47]. From established irradiation swelling model, precipitation effect was considered, and then defect concertation and swelling was calculated as shown Figure V.6.1.
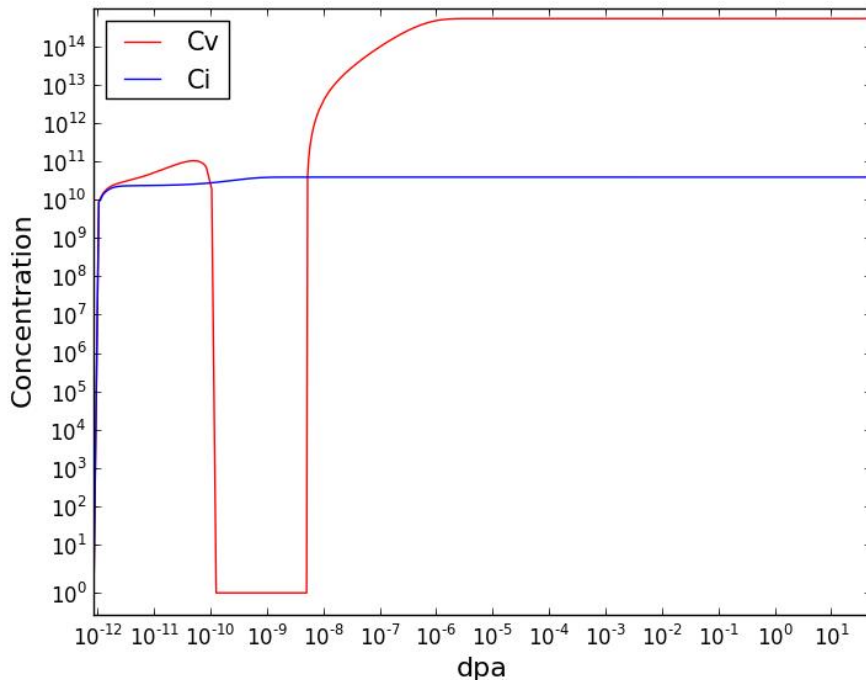
Figure V.6.1 Precipitation effect on point defect concentration in iron at 700 K

One thing to be noted is vacancy concentration behavior in the early stage ($\sim 10^{-8}$) is abnormal. This phenomenon is caused by a bias factor of precipitation. Since precipitation provides recombination site, vacancy flux has to be compensated with interstitial flux. As result, vacancy concentration is decreased as shown in Figure V.6.1. (To prevent vacancy defect has minus value, code structure was modified.)

82
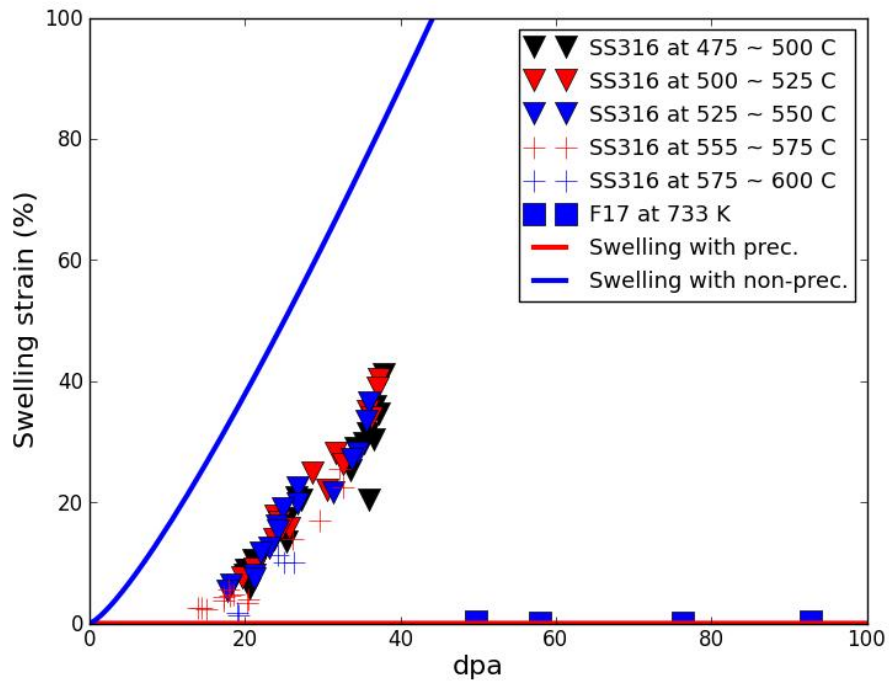
Figure V.6.2 Precipitation effect on irradiation swelling in iron

In Figure V.6.2, the comparison result of swelling with non-precipitation and precipitation is described. In case of precipitation case, total concentration is lower than that of the non-precipitation case. Nevertheless, the general behavior of radius and swelling did not change. However, total swelling is much decreased. When it compares with experimental results, swelling rate of non-precipitation has the same slope with SS316 steel. In case of the swelling rate of precipitation, F17 experimental results are well matched. Since precipitation number density and size were adopted from microstructure analysis of F17, it is obvious behavior.

V.7   Cascade effect on iron

As presented in rationale chapter, cascade annihilation effect on sink was accounted by fitting method of experiment result. By Garner, it was experimentally observed that network dislocation density of iron-based alloy is saturated nearly 10^{11} cm^2 no matter how fabrication process is applied to specimen.

Hence to account sink annihilation, dislocation loop radius equation is modified. In detail, annihilation factor was considered in dislocation loop density equation. It was assumed that annihilation rate is proportion with total density. The annihilation rate was redetermined by 40%. As results, irradiation swelling rate was decreased.
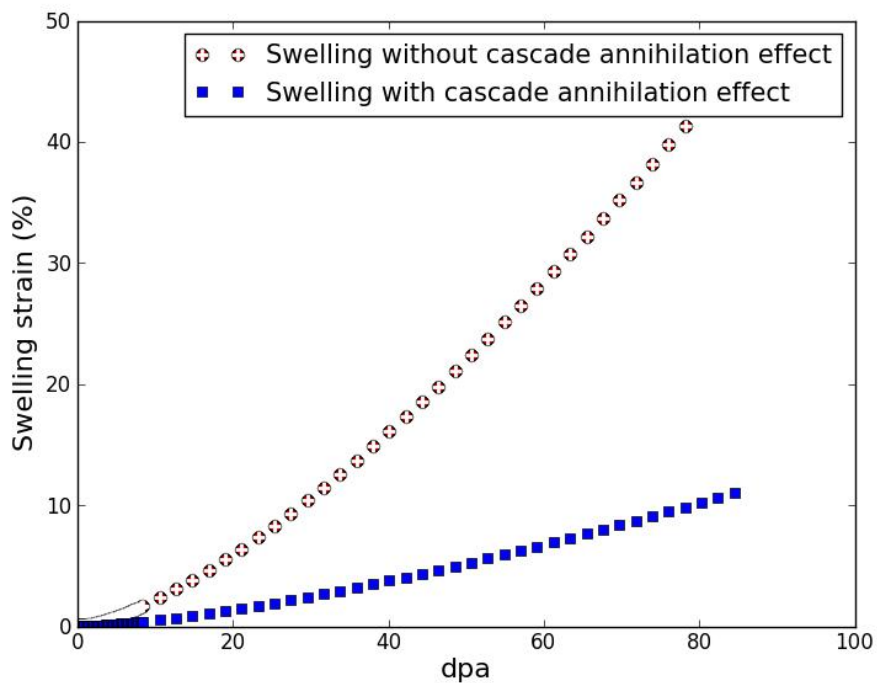
Figure V.7.1 Cascade annihilation effect on irradiation swelling in iron at 700 K

V.8   Limitation of CDM frame and PBM approach as a possible breakthrough

In the previous section, irradiation swelling and creep could be analyzed with the CDM approach. However, as referred in rationale chapter, void lattice ordering had been founded many years ago. Which phenomenon could not be explained by traditional rate theory such as CDM. Not only just this void lattice ordering, High swelling rates in low dislocation density and void swelling near grain boundary are typical examples, what traditional rate theory could not be used. Hence, Singh and Woo suggested new rate theory, which calls PBM by considering cascade. At firstly it was assumed that SIAs cluster will survive after cascade relaxation and react with a mobile sink. Recently it was revealed that 1-D mobile SIAs cluster with sinks is the main reaction mechanism. Until now, PBM is the most advance rate theory to explain radiation damage phenomenon including microstructure.

However, as shown in this Table V.8.1, PBM do not use to predict irradiation degradation, a simple cluster dynamic model is adopted for many authors. Because PBM has critical limitations. Actual cladding material, void lattice ordering does not occur. And Singh-Foreman catastrophe does not occur.

Nevertheless, it is deniable that all study has the same limitation that neglecting the 1-D SIAs. Hence the point is what kind of mechanism is applied to change the frame from PBM to CDM. In another way, the specific mechanism has to be considered in rate theory. Although many authors in Table V.8.1 do not consider specific mechanism which can neglect PBM, all of them insist that that atomic simulation could be the solution to overcome the limitation of rate theory.

Table V.8.1 Various rate theory study about iron-based alloy steel

	E.M. Getto, (2016), USA	A. Gokhman (2011), Ukraine	E. Meslin (2008), France	A. H. Duparc (2002), France
Model	CDM	CDM	CDM	CDM
Temp.	440 ~ 480 ℃	300 ℃	200 ~ 400 ℃	300 ~ 600 ℃
Materials	F/M steel & HT-9	Fe-12.5 Cr alloys	Pure iron	Fe-0.13 Cu alloys
Pressure	Non	Non	Non	Non
Source	Iron+ (ions)	Neutron	Kr+ (ions)	Electron
Target subject	Cladding for FBR	Cladding for FBR	PBV for PWR	PBV for PWR
dpa	180 ~ 650	0.6, 1.5		
Code	DLSODE (Fortran)	LSODA (Fortran)		

Recently, there are many MD and ab-initio study about stress and alloy effect on defect behavior. Because the strain field is distorted mainly by stress and alloy element. Which is never systemically organized in rate theory. Therefore, it is natural to think about that stress effect on SIAs in PBM could give hint to interpret this frame change. Stress effect on frame change is not new idea. It already suggested by ORNL research team. They suggested that the correlation between dislocation and void could be the reason of unsaturated void growth. Hence verification of external stress effect on PBM could be indirect evidence of Barashev suggestion [26]. Moreover, quantitatively analyze is possible to derive how much energy is needed to frame change from PBM to CDM.

Hence irradiation swelling was predicted by establishing the PBM master equation. As expected, irradiation swelling is saturated with steady-state defect concentration as shown in Figure V.8.1. In the experiment, pure iron swelling is much higher than that of simulation. Moreover, recent experimental research suggests that pure iron also depends on dpa. Therefore, more fundamental study about defect reaction mechanism with sink should be needed a more fundamental study.
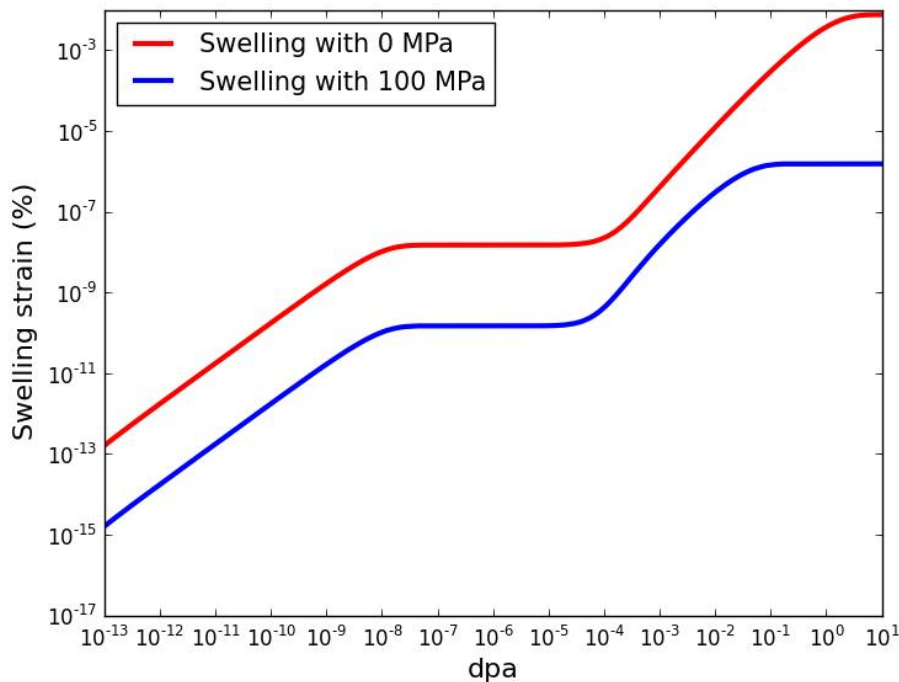
Figure V.8.1 Stress effect on irradiation swelling behavior in iron by PBM

VI Discussion

In this study, RIDI behavior of zirconium and iron-based alloy were analyzed. The modeling of RIDI was derived by combing the rate theory and results of state of art simulation. As results, more improved understanding could be possible by considering alloying element and stress effects.

However, although, as referred in rationale chapter, all simulation has certain limitations because various assumption and its induced limitation are still a barrier to grasp the fundamental understanding. Therefore, in this discussion chapter, among the various limitations, major issues were treated, and then path forward was dealt.

VI.1 Parametric study

Various parameters are used in rate theory to calculate the defect generation rate, defect recombination rate, and defect absorption rate. Among various parameters in master equations, independent variables are defect generate rate, defect diffusivity and each sink bias factor. In case of sink density and concentration is a dependent variable. Hence in this section, those parameters were examined to define the limitation of this thesis and to see the possibility to improve it's limitations.

VI.1.1 Defect generation rate

Defect generation term is the most important parameters to determine RIDI as input data. Hence dpa is suggested and calculated, based on the NRT method, to unify the degree of radiation damage with various neutron spectrum by different reactor type. However, detail calculation sequence of dpa is not suggested. It is specious that same calculation methodology is adopted to obtain dpa for each experiment.

Fortunately, in case of zirconium, experimental data of irradiation growth was researched by one extensive experimental project from NRL of UKAEA. In NRR programs, the same reactor (DIDO) was used, hence direct comparison by each experimental result was possible [70]. At that time, experimental results were presented by fluence. Recently F. Christien represents these results with dpa by assuming that 1 dpa has the same effect with 7×10^{24} fluence in DIDO reactor without any proof [57]. From the F. Christen simulation result for single crystal zirconium, diffusivity was used as fitting parameters. Therefore, the simulation result should be well matched with experimental results.

However, in case of an iron-based alloy, irradiation swelling is independently researched by many research groups with various reactors. Although experimental results are expressed by dpa, it cannot be assured that every researcher used a standardized method for calculating the dpa. Following the Garner's statements, some experimental results show the incorrect calculation of dpa [48].

VI.1.2 Diffusivity

As referred in the previous section, defect generation rate is the most important criteria. However, diffusivity and concentration also determine the recombination rate and absorption rate. Since defect concentration is also determined by diffusivity, diffusivity is the only independent variable.

In case of zirconium, after the 1980s, only two research groups have used the rate theory, i.e. F. Christien in France and S.I Golubov in the U.S.A. Both research groups use the diffusion coefficient

as a fitting factor [58]. In the results chapter, diffusivity values of zirconium were adopted from F. Christien. Hence these values are needed to be validated with experimental and simulation results. In detail, since the only the fitting value of diffusivity is applied to predict the irradiation growth of zirconium, dislocation radius should be compared between calculation and experimental results. Moreover, simulation results of diffusivity were not suggested for zirconium in CANDU reactor condition. Therefore, extensive study is suggested for the fundamental understanding.

In case of iron-based alloy, the situation is better than zirconium case, because C.C. Fu simulation results were used as diffusivity value [64]. Moreover, C.C. Fu simulation result for diffusivity had been calibrated by comparing the microstructure analysis. In A.H. Duparc study, 1 MeV irradiations is used as a microscope for experimental observation. It was revealed that interstitial migration energy should be modified from C.C. Fu simulation results, i.e. migration energy should be increased from 0.3 to 1 eV and binding energy of di-interstitial should be decreased from 0.9 to 0.2 eV. Therefore, the calculation result of this study could be more reliability when it compared with that of Duparc results.

In case of E. Meslin, to calibrate the diffusion coefficient, point defect clustering is simulated and its results were comprised by experimental data under cascade damage conditions [71]. The difference of H. Duparc study is considering of cascade phenomenon [63]. Various activation energy is obtained from C.C. Fu simulation results. Migration energy of interstitial and its cluster are $E_m^i = 0.34$, $E_m^{2i} = 0.34$, $E_m^{3i} = 0.42$; Respectively, vacancy type cluster has $E_m^v = 0.67$, $E_m^{2v} = 0.62$, $E_m^{3v} = 0.35$, and $E_m^{4v} = 0.48$. Not only E. Meslin, there are many studies about radiation effect on materials. However, it is believed that E. Mesline study is most extensive study because not only interstitial cluster but also vacancy cluster mobility is accounted.

VI.1.2.1   Stress effect on defects

In this study, stress effect was considered in both way; In a conventional way, modified Brailsford method is applied in zirconium; Recent MD simulation results were adopted in the iron-based alloy. However, these methods are needed to be verified.

As described in the rationale and results chapter, there are mis-concept in the Brailsford model, it was assumed that vacancy concentration in thermal equilibrium has an only negative effect on vacancy defect flux $J_v = \rho_j\left(z_v^j D_v C_v - z_v^j D_v C_v^j\right)$. However, the vacancy concentration in thermal equilibrium could be positive effect. Moa reover, recently, vacancy emission from sink is already the considered in rate theory as binding energy. Hence Brailsford model is modified as figure

Brailsford's model	This work
I defect flux is $J_i = \rho_j z_i^j D_i C_i$	I defect flux is $J_i = \rho_j z_i^j D_i C_i$
V defect flux is $J_v = \rho_j\left(z_v^j D_v C_v - z_v^j D_v C_v^j\right)$	V defect flux is $J_v = \rho_j\left(z_v^j D_v C_v + z_v^j D_v C_v^j\right)$
C_v^j is effective emission form dislocation loops	C_v^j is effective emission form dislocation loops
$C_v^J = C_v^0 exp\left(\dfrac{\sigma b^3}{kT}\right)$	$D_v^J = D_v^0 exp\left(\dfrac{-\sigma b^3}{kT}\right)$
$\therefore J_{total} = \rho_j(z_i^j D_i C_i - (z_v^j D_v C_v - z_v^j D_v C_v^j))$	$\therefore J_{total} = \rho_j(z_i^j D_i C_i - (z_v^j D_v C_v + z_v^j D_v C_v^j))$

Figure VI.1.1 Brailsford method vs modified Brailsford method

To validate modified method in iron-based alloy, calculation results are comprised with Brailsford method. As shown in Figure VI.1.2, irradiation creep does not occur in Brailsford model whilst modified model shows significant creep behavior with the same diffusion coefficient. However, both calculations are carried out by over-simplified CDM. Only up-to tri-vacancy and tri-interstitial cluster considered in the master equation. Therefore, the MD simulation result could not be verified. Three approaches should be validated with the same rate theory frame.

The limitation in both conventional and recent method to consider stress effect is only one type of defect is considered; In the conventional method, vacancy diffusivity is modified; In the recent method, only interstitial considered. Both point defect should be considered in rate theory.

Not only irradiation creep, but also irradiation swelling is affected by stress. However, stress effect on binding energy of cluster defects had not been researched. From the experiment, it was clear that irradiation swelling rate could be increased depending on temperature and stress. In this simulation, only irradiation creep is calculated when stress is applied. Hence both irradiation swelling and creep should be simultaneously verified.
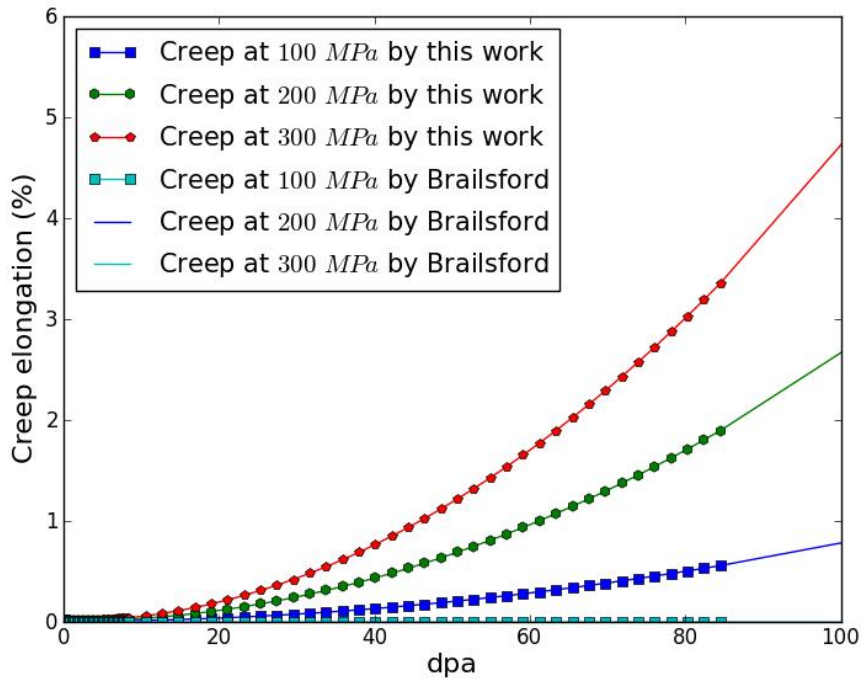
Figure VI.1.2 Calculation result by Brailsford method and modified Brailsford method in iron at 700 K

VI.1.2.2   Alloy element effect on defects

In conventional method to consider alloying element effect, the oversimplified assumption is applied. Since precipitates is treated as a neutrally-biased sink, defect flux of vacancy should be a negative value at the initial stage as shown in Figure VI.1.3. Which is an inevitable phenomenon to compensate with interstitial flux. Hence in this study, vacancy concentration behavior is controlled by "if" state in python code to be a positive value as shown in Figure VI.1.4. Nevertheless, vacancy absorption rate should be modified at the initial stage because the precipitate effect is so strong. The effective radius of the precipitation could be indirectly observed by TEM analysis. From the TEM analysis, highly distorted areas seem to have only two or three layers. Therefore, a modified approach is needed by considering the effective radius concept.
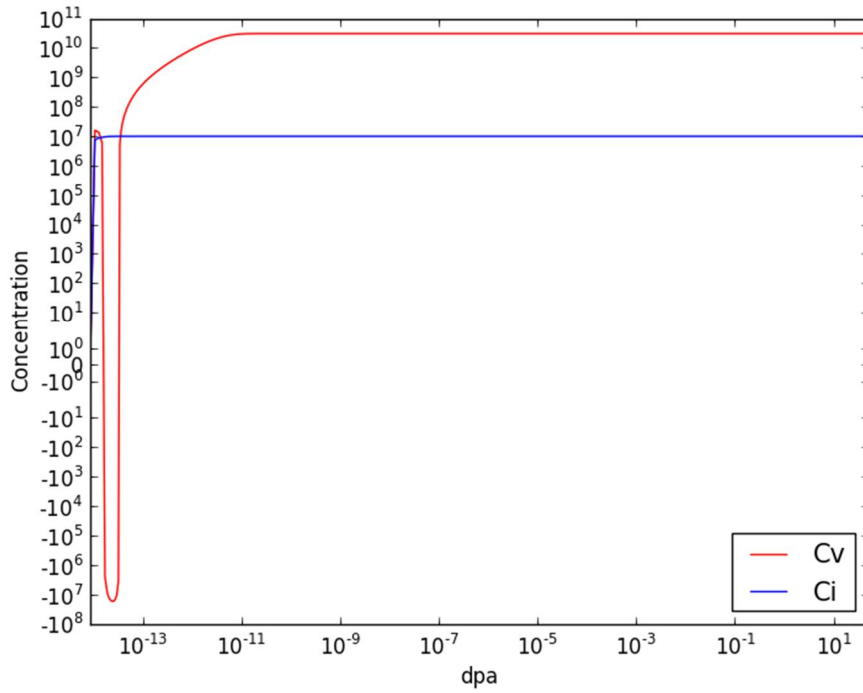
Figure VI.1.3 Defect concentration behavior in iron by a conventional method
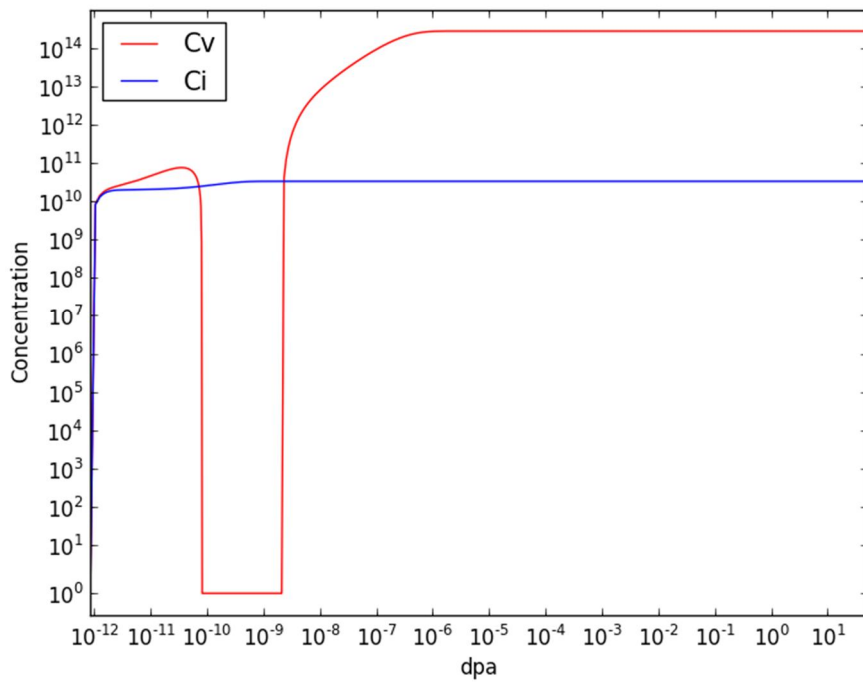
Figure VI.1.4 Defect concentration behavior in iron by this work

Not only the conventional method but also a recent method has certain limitation. In MD simulation, the correlation between defect and solution state of the alloying element was considered. However, alloying element changes the hole microstructure. Not only basic lattice structure, but also grain boundary size, texture, sink morphology and sink density etc. are affected by alloying element. However, MD simulation is not enough to consider hole microstructure information.

VI.1.3 Bias factor

The third limitation is bias factor, which is about capture efficiency. In the previous section, only bulk diffusivity was treated. However, defect behavior near the sink is totally different from the normal lattice matrix because sink distorts the matrix by strain field. Obviously, this strain field is not constant because sink morphology is changed by external stress and alloying elements. However, in this paper, the value was assumed constant regardless of environment condition. Despite this recognition, there is no general theory or systemically method to analyze the bias factor. Although, C.H. Wo. and G. Gosele use elegant elastic theory to obtain the bias factor [2, 34]. However, recent simulation result denied those results. Hence, direct observation of defect reaction with sink is presented by long-time atomic simulation from ORNL. Nevertheless, the bias factor could be derived directly from this observation. The methodology should be suggested to derive a bias factor from the direct observation. Because of reaction kinetics is the heart of defect reaction mechanism, capture efficiency should be systemically researched to establish the general model in radiation effect on metals.

VI.1.4 Sink density

Sink number density and radius were also important parameter to determine the defect absorption rate. Up to present, sink number density and radius were analyzed based on defect flux. There was no study about cascade annihilation of the sink. In this study, cascade annihilation of the sink was accounted by considering the saturation of sink density.

The different approach had been used in zirconium and iron-based alloy. In case of zirconium, number density was obtained from the experimental result because SRT is used. In case of ion-based alloy, number density was derived by CDM.

Since the experimental result of sink number density is used as input parameters in zirconium case, Therefore, cascade annihilation is already accounted. In detail, it was revealed that dislocation number density and radius were saturated at certain dpa [72]. In case of <a> dislocation, saturation is occurred at 4 dpa whilst <c> dislocation is saturated as 7 dpa. At that time, this saturation phenomenon was not

considered as cascade annihilation of the sink. Nevertheless, there was no recognition about cascade annihilation of the sink, it was successfully adopted in rate theory.

However, in case of iron-based alloy, CDM approach is adopted to explain the RIDI. Hence cascade annihilation of the sink could not be considered as experimental results. Therefore, to account cascade annihilation of the sink, a simplified approach is suggested

If it was assumed that all defect is annihilated in a cascade zone, the quantitative analysis could be possible. In this point of view, the cascade zone should be derived, and then the annihilation rate will could be derived. To derive the total size of cascade zone, depending on neutron spectrum, NRT method or MD simulation should be applied with all energy group.

VI.2   Path forward

In the previous section, the most important parameters are examined to confirm the limitation of each parameter. In this section, to see the other possibility of defect behavior, all defect reaction mechanism will be examined, and then new methodology will be examined for the improved understanding.

VI.2.1 Reaction kinetics of defects

From the PBM analysis, the defect reaction mechanism is expanded by 1-D diffusivity. Hence defect reaction mechanism could be summarized 3 by 3 symmetry table as shown below Table VI.2.1.

Table VI.2.1 Defect reaction kinetics

		Point defect (3-D mobile)		SIAs cluster (1-D mobile)	Sink (immobile)		
		I type	V type	I	I type	V type	Precipitate
Point defect (3-D mobile)	I type	The growth of SIAs cluster	Recombination	The growth of SIAs cluster	The growth of I type sink	Dissolution of V type sink	Recombination
	V type	Recombination	The growth of vacancy cluster	Dissolution of SIAs cluster	Dissolution of I type sink	The growth of V type sink	Recombination
SIAs cluster (1-D mobile)	I type	The growth of SIAs cluster	Dissolution of SIAs cluster	SIAs cluster reaction with SIAs cluster	The growth of I type sink	Dissolution of V type sink	Recombination
Sink (immobile)	I type	The growth of I type sink	Dissolution of v type sink	The growth of I type sink	Non		
	V type	Dissolution of I type sink	The growth of V type sink	Dissolution of V type sink			
	Precipitate	Recombination	Recombination	Recombination			

In Table VI.2.1, reaction kinetics could be characterized by five types of reactions. Among five reactions, 3-D mobile & 3-D mobile / 3-D mobile & immobile / 1-D mobile & immobile reaction were considered in rate theory, i.e. reaction 3-D mobile & immobile defect were considered in SRT and CDM and reaction 1-D mobile & immobile defect was considered in PBM. However, two reactions; 3-D mobile defect & 1-D mobile / 1-D mobile & 1-D mobile, were not considered in the reaction mechanism. Those two mechanisms also should be considered in rate theory.

VI.2.2 Frame of rate theory (SRT vs CDM vs PBM)

Recently many research activities on RIDI already have been done by using CDM. However, there is no guarantee that the accuracy of CDM is better than the old approach of using experimental sink densities and SRT. In this work, calculation results for single-crystal and cold-worked polycrystal zirconium without considering the cluster is quite similar to the experiment result. From this result, it is difficult to determine that cluster is the reason for the disagreement in radiation growth of annealed polycrystal. Moreover, straight-forward master-equation-based formulation in CDM requires microscopic information on the particle-cluster reaction (forward and backward) for each cluster size, such as association and dissociation enthalpies and entropies of clusters, which is difficult to get and many empirical assumptions have to be made. Hence, to develop this method, various parametric information should be calculated and reaction probability by considering atomic configuration should be obtained [40,41]. Also, CDM is based on the diffusion-controlled kinetics to explain reaction between defect and cluster. Diffusion-controlled kinetics is not suitable method to predict the reaction between defect and cluster. In case of small clusters, reaction-controlled kinetics is more suitable method to describe reaction probability. In case of PBM, reaction kinetic is more complex than CDM. In this situation, SRT is one of easy and simple tools to be applicable to and simulate various situation.

When PBM is compared with SRT/CDM, the frame is totally changed. In conventional way, the origin of RIDI was freely migrating point defect. However, in case of PBM, RIDI is affected by 1-D interstitial cluster. Hence, recently there are many studies about behavior of interstitial cluster. Nevertheless, there is no general explanation about 1-D interstitial cluster effect on RIDI.

VI.2.3 Cluster number density

In this study, only fifteen clusters ($2 \leq n \leq 15$) were accounted for cluster defect. Large Cluster (> 15) was assumed that it is directly developed as dislocation loop or void which has a uniform size. It is obvious that lager number of the master equation will be more sophisticated to analyze the radiation effect on materials. Nevertheless, the advance of the technic in grouping method, large calculation time and high-performance computing system is needed. Hence in this study, a limited number of the

cluster were considered. As result, the simulation result is limited in its accuracy. However, an ode15s module in MatLab provides unlimited number of the master equation. Therefore, more accurate simulation is possible if Matlab module is possible in python.

VI.2.4 He effects on iron-based alloy

He transmutation play the important role in RIDI because the stability of the void is determined by implantation of He in vacancy cluster. However, in this study, He reaction between void did not consider. Recently thermal stability of vacancy cluster and void are researched by OKMC. Hence by adopting this research results, RIDI prediction could be more realistic for an engineering application.

VI.2.5 Stochastical fluctuation

The rate theory is based on a deterministic method based on the mean field which means that rate theory could not consider the heterogeneous generation and growth of sinks and defects in the matrix. Hence sink size and morphology are uniform and microstructure characteristic could not be accounted.

Stochastic fluctuations can be an alternative method to explain the deviate between calculation results and the experimental database [73]. In this approach, thermal and other noises could be taken into account in reaction probability. Because of the complexity of CDM and PBM approach, classical rate theory based on stochastic fluctuation could be more suitable for anisotropy materials. However, in order to adopt this method, stochastic concept should be defined and understood in materials perspective. This academic background is beyond this study.

VI.2.6 Residual stress

In this paper, residual stress effects on the anisotropy factor were neglected in annealed polycyrstal. However, Causey et al. revealed profound effects of residual stress in radiation growth [23]. In the specific case, radiation growth occurs in opposite direction to relax residual stress. After the relaxation, the strain shows a common tendency. To describe this effect, the upper-bound model was used since this model base on the numerical method. Unfortunately, there is no available data about residual stress of the specimen, which was used for in this paper. Moreover, single crystal compliances also should be calculated by Hill's criteria and Eshelby model in hexagonal structural slip system. This method also will be adopted in the next research step.

VII Conclusion

In this study, stress, alloy and cascade annihilation effects were considered with conventional and recent method to improve the fundamental understanding of the RIDI. Stress effect was account by modifying the defect diffusivity. Brailsford method, modified Brailsford method and result of MD simulation are adopted to modify the diffusivity. In case of alloying element effect, precipitation effect was considered as conventional method, and then solute state effect on defect diffusivity was considered by MD simulation results. Cascade annihilation effect on sink was accounted by fitting method from the experimental result.

Since the 1960s, RIDI of structural materials has been the most important phenomena in nuclear reactors. However, there is no general model of RIDI, which could also explain microstructural changes, owing to lack of knowledge of the fundamental understanding of atomistic behavior.

Recently, not only rate theory but also various simulation tools were developed to analyze the RIDI. Molecular dynamic simulation and kinetic Monte Carlo simulation are representative simulation tools. Although those various research tools with significant progress in computer performance, rate theory is still a favorite option to simulate radiation effect on materials since this method can give instinctive understanding with short computation time. Moreover, the scale of simulation time and simulation length is large enough to satisfy the engineering point of view whilst another simulation method still need a lot of limitation of time and length scale. Therefore, systematically organization of fragmented knowledge by combining state of art simulation method with rate theory would be valuable work.

Fortunately, in-situ experimental equipment, which could detect the sink development behavior, have been developed. From this advanced experimental equipment, validation of advanced rate theory could take one step further to grab fundamental understanding and engineering value.

So far, rate theory plays the assistant role to analyze the integrity of structural material by suggesting the radiation-induced degradation mechanism. However, recently, there is research trend to predict the life of structural materials by simulation approach. This means that the simulation approach could be the main method to determine the nuclear system design. In this point of view, the author thinks that the result of the study could give engineering contribution to nuclear society.

Therefore, the following summarizes is a part of effort to improved limitation of perception of RIDI by systematically organizing the fragmented knowledge of atomic behavior in various condition.

VII.1 Zirconium and its alloys

In order to maintain a consistent viewpoint, annealed single crystal, annealed polycrystal and cold-worked polycrystal were predicted with same SRT method, and then, stress and alloying element effect were verified by considering the modified diffusivity and precipitation. The simulation target environment was condition of pressure tube in CANDU reactor. So far, there was no research to predict both single crystal and polycrystal with same rate theory.

In case of single, the defect concentration shows typical low-sink-density behavior. Hence the defect flux initially increases at 10^{-9} dpa and immediately afterward decreases up to 1 dpa. From the defect flux, sinks radius was calculated. Initially, the <a> dislocation loop density increases dramatically, whereas that of <c> type loops increases above 3 dpa. Next, the density of both types of dislocation loops shows a saturation region. The <a> dislocation loops are generated by the net interstitial defect flux behavior. However, <c> dislocation loops generation and growth are caused by the net vacancy flux. Irradiation growth was calculated by sink development, and then calculation result was compared with experimental measurements by Carpenter. Although the experimental values of the growth strain were higher than the calculation data at 2^{-6} dpa, the overall growth tendency is similar to that of the experimental database and other irradiation growth models.

In cold-worked polycrystal zirconium, the defect concentration shows typical high-sink-density behavior. The dislocation line density was assumed to be a time-independent parameter. (Since the density of dislocation line in cold-worked zirconium is already sufficiently developed, there is no chance to develop the dislocation loop) The irradiation growth strain of cold-worked polycrystal zirconium is also quite similar to experimental results. In this case, dislocation line sink effects are dominant. Therefore, irradiation growth shows very simple behavior, i.e. a linear increase with dpa.

In annealed polycrystal zirconium, the defect concentration shows intermediate-sink-density behavior. Unlike the case for the single crystal, the <c> dislocation loop radius is much larger than the <a> dislocation loop radius. The <a> dislocation loop density has the shape of a semicircle before 4 dpa, after which <a> dislocation loops are saturated. However, <c> dislocations have a much higher sink strength than <a> dislocation loops. Calculation results show high growth strain initially. However, after 1 dpa, the calculated strain shows a much slower increase.

To account stress effect on diffusivity, activation energy is modified as same approach method in diffusional creep model. In detail, as described rationale chapter, stress effect also considered by modified Arrhenius formulation. In case of cold-worked zirconium alloy, it was assumed that dislocation density is already saturated. Hence, for the simplification, simulation was carried out only

in cold-worked zirconium case because sinks number density and radius behavior did not need to be analyzed. As results, strain rate of irradiation creep is accelerated depending of stress. At 10 dpa, irradiation growth shows 0.3 % strain, whilst 1.1 % strain of irradiation creep was obtained by 100 Mpa.

In this study, alloy effect on RIDI were considered in the other way, which has never been considered in rate theory for RIDI, i.e. solid solution effect was considered. In detail, Christensen [35] calculate the interstitial diffusivity within 0.5 % of Nb and 2.5 % Sn and in zirconium matrix. Hence Christensen reveal that Nb decrease the interstitial diffusivity nearly 1/5.64 at 500 K and 1/5.88 at 700 K with 0.5 % Nb in zirconium. Also, same method was applied to account the Sn effect. Sn shows the high dependency with temperature and relatively less effect than Nb. Interstitial diffusivity is decreased about 1/4.05 at 500 K and 1/1.38 at 700 K with 2.5 Sn. This information was adopted in rate theory and then irradiation growth was predicted. By adding 0.5 % Nb in cold-worked zirconium, 0.2 % strain is obtained whilst cold-worked pure zirconium shows nearly 0.3 % strain at 10 dpa. Since there was no experiment about irradiation growth of Zr-0.5% Nb and Zr-2.5Nb experimental results was compared and simulation results shows good agreement.

VII.2 Iron-based alloy

In case of iron-based alloy, the nucleation and growth behavior of sinks were simulated by CDM approach, and then stress, alloying element and cascade annihilation effect were considered. Unlike zirconium case, different method is applied to account stress and alloying element effect. In detail, Migration energy was derived by MD simulation and adopted in rate theory to account stress effect.

The defect concentration of pure iron show typical high-temperature behavior, both point and cluster defects are saturated at 10^{-6} dpa. This fast saturation is occurred by fast recombination and absorption phenomena [8]. From defect concentration, cluster number density is derived by calculating the absorption rate. Number density shows same trend of cluster defects because number density is obtained from the largest cluster concentration.

The both sink radius were increased at 10^{-6} dpa because number density is too low. And then until 10^{-4} dpa, both radiuses were decreased. The discrepancy between two sinks is happened after 10^{-4} dpa. In case of void, absorption rate is much higher than emission rate hence radius growth with given number density. However, in case of dislocation loop were dissolved at 700 K condition.

Base on the result of number density, the radius of sinks was calculated, and then irradiation swelling simulated. The irradiation swelling shows exponential shape by dpa. It is predictable behavior because radius increase as exponentially with saturated number density. This behavior was already confirmed in experiment result in EBR II or FFTF [6].

In zirconium results chapter, stress effect was accounted by modifying the Brailsford model. However, as described in rationale chapter, stress effect could be directly considered by MD simulation. Hence MD simulation method were adopted to calculated interstitial diffusivity. As result, stress effect on diffusivity was calculated. It was observed that diffusivity of interstitial has 8.437×10^{-5} cm^2/s at 873 K. This value was 11 times higher than non-stress applied condition (7.414×10^{-6} cm^2/s). From the calculation interstitial diffusivity, concentration of defect and cluster, radius, and swelling is recalculated. The purpose of research is prediction of ultra-long fuel cycle, 600 Mpa is applied. Up to the 10 dpa, irradiation creep shows 40% elongation with the stress applied direction.

In case of zirconium alloy, solute state of alloy effect was considered. However, in case of iron-based alloy, precipitation effect was considered by traditional method. From established irradiation swelling model, precipitation effect was considered, and then defect concertation and swelling was calculated. Since precipitation provide recombination site, vacancy flux has to be compensated with interstitial flux. As result, vacancy concentration is decreased. In case of precipitation case, total concentration is

lower than that of non-precipitation case. Nevertheless, general behavior of radius and swelling did not change. However, total swelling is much decreased. When it compares with experimental results, swelling rate of non-precipitation has same slope with SS316 steel. In case of swelling rate of precipitation, F17 experimental results are well matched. Since precipitation number density and size were adopted from microstructure analysis of F17, it is obvious behavior.

References

[1] B. N. Singh, S. I. Golubov, H. Trinkaus, A. Serra, Y. N. Osetsky, and A. V. Barashev, "Aspects of microstructure evolution under cascade damage conditions," *Journal of Nuclear Materials,* Article vol. 251, pp. 107-122, 1997.

[2] C. H. Woo, "Theory of irradiation deformation in non-cubic metals effects of anisotropic diffusion," *Journal of Nuclear Materials,* vol. 159, pp. 237-256, 1988.

[3] M. Kiritani, "Analysis of the clustering process of supersaturated lattice vacancies," *Journal of the Physical Society of Japan,* vol. 35, no. 1, pp. 95-107, 1973/07/15 1973.

[4] R. H. Johnson and G. W. Greenwood, "Deformation of uranium during alpha/beta cycles under small stresses and a quantitative interpretation of the mechanical weakness of metals undergoing phase transformations," *Nature,* vol. 195, p. 138, 07/14/online 1962.

[5] E. P. Wigner, "Theoretical physics in the metallurgical laboratory of chicago," *Journal of Applied Physics,* vol. 17, no. 11, pp. 857-863, 1946/11/01 1946.

[6] C. Cawthorne and E. J. Fulton, "Voids in irradiated stainless steel," *Nature,* Letter vol. 216, no. 5115, pp. 575-576, 1967.

[7] B. A. Loomis, T. H. Blewitt, A. C. Klank, and S. B. Gerber, "Elongation of uranium single crystals during neutron irradiation," *Applied Physics Letters,* vol. 5, no. 7, pp. 135-137, 1964.

[8] G. S. Was, "fundamentals of radiation materiasl science," 2007.

[9] K. Farrell, "5.07 - Performance of Aluminum in Research Reactors," in *Comprehensive Nuclear Materials*, R. J. M. Konings, Ed. Oxford: Elsevier, 2012, pp. 143-175.

[10] F. A. Garner, "Irradiation Performance of Cladding and Structural Steels in Liquid Metal Reactors," *Materials Science and Technology,* 2006.

[11] R. Krishnan and M. K. Asundi, "Zirconium alloys in nuclear technology," *Proceedings of the Indian Academy of Sciences Section C: Engineering Sciences,* journal article vol. 4, no. 1, pp. 41-56, April 01 1981.

[12] S. N. Buckley, Proc. Int. Conf. on Properties of Reactor Materials and the Effects of Radiation Damage, Butterworths, London, p. 413, 1962.

[13] V. FIDLERIS, "The irradiation creep and growth phenomena," *Journal of Nuclear Materials,* vol. 159, pp. 22-42, 1988.

[14] R. B. Adamson, *zirconium in the nuclear industry,* vol. ASTM 633 p. 326, 1977.

[15] A. Rogerson and R. A. Murgatroyd, "Effects of texture and temperature cycling on irradiation growth in cold-worked zircaloy-2 at 353 and 553 K," *Journal of Nuclear Materials,* vol. 80, pp. 253-259, 1979.

[16] A. Rogerson and R. H. Zee, "High fluence irradiation growth in single crystal zirconium at 553 K," *journal of Nuclear Materials,* vol. 151, pp. 81-83, 1987.

[17] A. Rogerson and R. A. Murgatroyd, "'Breakaway' growth in annealed zircaloy-2 at 353 K and 553 K," *Journal of Nuclear Materials,* vol. 113, pp. 256-259, 1983.

[18] A. R. Causey, "Acceleration of creep and growth of annealed zircaloy-4," *Journal of Nuclear Materials,* vol. 193, pp. 277-278, 1986.

[19] R. A. Holt, "In-reactor deformation of cold-worked Zr–2.5Nb pressure tubes," *Journal of Nuclear Materials,* vol. 372, no. 2, pp. 182-214, 2008/01/31/ 2008.

[20] E. A. Little, "Void-swelling in irons and ferritic steels: I. Mechanisms of swelling suppression," *Journal of Nuclear Materials,* vol. 87, no. 1, pp. 11-24, 1979/11/01/ 1979.

[21] D. S. Gelles, "Microstructural examination of several commercial alloys neutron irradiated to 100 dpa," *Journal of Nuclear Materials,* vol. 148, no. 2, pp. 136-144, 1987/04/01/ 1987.

[22] P. Dubuisson, D. Gilbon, and J. L. Séran, "Microstructural evolution of ferritic-martensitic steels irradiated in the fast breeder reactor Phénix," *Journal of Nuclear Materials,* vol. 205, pp. 178-189, 1993/10/01/ 1993.

[23] R. L. Klueh and A. T. Nelson, "Ferritic/martensitic steels for next-generation reactors," *Journal of Nuclear Materials,* vol. 371, no. 1, pp. 37-52, 2007/09/15/ 2007.

[24] L. K. Mansur, "Void swelling in metals and alloys under irradiation: an assessment of the theory," *Nuclear Technology,* vol. 40, no. 1, pp. 5-34, 1978/08/01 1978.

[25] R. Sizmann, "The effect of radiation upon diffusion in metals," *Journal of Nuclear Materials,* vol. 69-70, no. C, pp. 386-412, 1968.

[26] A. V. Barashev and S. I. Golubov, "Steady-state size distribution of voids in metals under cascade irradiation," *Journal of Nuclear Materials,* vol. 389, no. 3, pp. 407-409, 6/1/ 2009.

[27] T. R. Waite, "Theoretical Treatment of the Kinetics of Diffusion-Limited Reactions," *Physical Review,* vol. 107, no. 2, pp. 463-470, 07/15/ 1957.

[28] U. Gösele and A. Seeger, "Theory of bimolecular reaction rates limited by anisotropic diffusion," *The Philosophical Magazine: A Journal of Theoretical Experimental and Applied Physics,* vol. 34, no. 2, pp. 177-193, 1976/08/01 1976.

[29] S. J. Zinkle and B. N. Singh, "Analysis of displacement damage and defect production under cascade damage conditions," *Journal of Nuclear Materials,* vol. 199, no. 3, pp. 173-191, 1993/02/01/ 1993.

[30] M. J. Banisalman, S. Park, and T. Oda, "Evaluation of the threshold displacement energy in tungsten by molecular dynamics calculations," *Journal of Nuclear Materials,* vol. 495, pp. 277-284, 2017/11/01/ 2017.

[31] M. J. Norgett, M. T. Robinson, and I. M. Torrens, "A proposed method of calculating displacement dose rates," *Nuclear Engineering and Design,* vol. 33, no. 1, pp. 50-54,

1975/08/01/ 1975.

[32]   A. D. Brailsford and R. Bullough, "The rate theory of swelling due to void growth in irradiated metals," *Journal of Nuclear Materials,* vol. 44, pp. 121-135, 1972.

[33]   A. D. Brailsford and R. Bullough, "Irradiation creep due to the growth of interstitial loops," *Philosophical Magazine,* vol. 27, no. 1, pp. 49-64, 1973.

[34]   U. Gösele, "Anisotropic diffusion, long-range energy transfer and bimolecular exciton recombination kinetics," *Chemical Physics Letters,* Article vol. 43, no. 1, pp. 61-64, 1976.

[35]   G. D. Samolyuk, A. V. Barashev, S. I. Golubov, Y. N. Osetsky, and R. E. Stoller, "Analysis of the anisotropy of point defect diffusion in hcp Zr," *Acta Materialia,* Article vol. 78, pp. 173-180, 2014.

[36]   A. Rogerson, "Irradiation growth in zirconium and its alloys," *Journal of Nuclear Materials,* 1988.

[37]   C. Kang, Q. Wang, and L. Shao, "Kinetics of interstitial defects in α-Fe: The effect from uniaxial stress," *Journal of Nuclear Materials,* vol. 485, pp. 159-168, 2017/03/01/ 2017.

[38]   F. Christien and A. Barbu, "Modelling of copper precipitation in iron during thermal aging and irradiation," *Journal of Nuclear Materials,* vol. 324, no. 2-3, pp. 90-96, 2004.

[39]   W. Xu *et al.*, "In-situ atomic-scale observation of irradiation-induced void formation," *Nature Communications,* Article vol. 4, p. 2288, 08/05/online 2013.

[40]   A. Ervin and H. Xu, "Mesoscale simulations of radiation damage effects in Materials: A SEAKMC perspective," *Computational Materials Science,* vol. 150, pp. 180-189, 2018/07/01/ 2018.

[41]   Y. Zhang, H. Huang, P. C. Millett, M. Tonks, D. Wolf, and S. R. Phillpot, "Atomistic study of grain boundary sink strength under prolonged electron irradiation," *Journal of Nuclear Materials,* vol. 422, no. 1, pp. 69-76, 2012/03/01/ 2012.

[42]   M. Kiritani, "Microstructure evolution during irradiation," *Journal of Nuclear Materials,* vol. 216, pp. 220-264, 1994.

[43]   S. I. Golubov, A. M. Ovcharenko, A. V. Barashev, and B. N. Singh, "Grouping method for the approximate solution of a kinetic equation describing the evolution of point-defect clusters," *Philosophical Magazine A,* vol. 81, no. 3, pp. 643-658, 2001/03/01 2001.

[44]   S. I. Golubov, B. N. Singh, and H. Trinkaus, "Defect accumulation in fcc and bcc metals and alloys under cascade damage conditions - towards a generalization of the production bias model," *Journal of Nuclear Materials,* Article vol. 276, no. 1, pp. 78-89, 2000.

[45]   V. A. Borodin, "Rate theory for one-dimensional diffusion," *Physica A: Statistical Mechanics and its Applications,* vol. 260, no. 3, pp. 467-478, 1998/11/15/ 1998.

[46]   S. I. Choi, G.-G. Lee, J. Kwon, and J. H. Kim, "Modeling of sink-induced irradiation growth of single-crystal and polycrystal zirconiums in nuclear reactors," *Journal of Nuclear*

Materials, vol. 468, pp. 56-70, 2016.

[47]   A. D. Brailsford and R. Bullough, "Void growth and its relation to intrinsic point defect properties," *Journal of Nuclear Materials,* vol. 49&70, pp. 434-450, 1978.

[48]   F. Garner, "irradiation performance of cladding and structural steels in liquid metal reactors," in *Materials Science and Technology*: Wiley-VCH Verlag GmbH & Co. KGaA, 2006.

[49]   M. Luts, "Programming Python," ed: O'Reilly Media, 1996.

[50]   O. E. Jones E, Peterson P, et al., "SciPy: open source scientific tools for Python. 2001," 2012.

[51]   R. V. Hesketh, "Non-linear growth in zircaloy-4," *Journal of Nuclear Materials,* vol. 30, no. 1–2, pp. 219-221, 1969.

[52]   G. J. C. Carpenter and D. O. Northwood, "The contribution of dislocation loops to radiation growth and creep of Zircaloy - 2," *Journal of Nuclear Materials,* vol. 56, no. 3, pp. 260-266, 1975.

[53]   C. C. Dollins, "In-pile dimensional changes in neutron irradiated zirconium base alloys," *Journal of Nuclear Materials,* vol. 59, no. 1, pp. 61-76, 1976.

[54]   D. Fainstein-pedraza, E. J. Sawno, and A. J. Pedraza, "irradiation-growth of zirconium-base alloys," *Journal of Nuclear Materials,* vol. 73, pp. 151-168, 1978.

[55]   S. R. MacEWEN and G. J. C. Carpenter, "Calculations of irradiation growth in zirconium," *Journal of Nuclear Materials,* vol. 90, pp. 108-132, 1980.

[56]   R. Bullough and M. H. Wood, "Mechanisms of radiation induced creep and growth," *journal of Nuclear Materials,* vol. 90, pp. 1-21, 1980.

[57]   F. Christien and A. Barbu, "Cluster dynamics modelling of irradiation growth of zirconium single crystals," *Journal of Nuclear Materials,* vol. 393, no. 1, pp. 153-161, 2009.

[58]   S. I. Golubov, A. V. Barashev, and R. R. Stoller, "On the origin of radiation growth of hcp crystals" *ONRL,* 2011.

[59]   M. Griffiths, "A review of microstructure evolution in zirconium alloys during irradiation," *Journal of Nuclear Materials,* vol. 159, pp. 190-218, 1988.

[60]   A. D. Braislford and R. Bullough, "Void growth and its relation to intrinsic point defect properties," *Journal of Nuclear Materials,* vol. 69–70, no. 0, pp. 434-450, 1978.

[61]   F. Onimus and J. L. Béchade, "4.01 - Radiation Effects in Zirconium Alloys," in *Comprehensive Nuclear Materials*, R. J. M. Konings, Ed. Oxford: Elsevier, 2012, pp. 1-31.

[62]   D. S. Gelles, "Microstructural examination of neutron-irradiated simple ferritic alloys," *Journal of Nuclear Materials,* vol. 108-109, pp. 515-526, 1982/07/01/ 1982.

[63]   A.   Hardouin Duparc, C.   Moingeon, N.   Smetniansky-de-Grande, and A.   Barbu,

"Microstructure modelling of ferritic alloys under high flux 1 MeV electron irradiations," *Journal of Nuclear Materials,* vol. 302, no. 2–3, pp. 143-155, 2002.

[64]   C.-C. Fu, J. D. Torre, F. Willaime, J.-L. Bocquet, and A. Barbu, "Multiscale modelling of defect kinetics in irradiated iron," *Nature Materials,* vol. 4, no. 1, pp. 68-74, 2004.

[65]   K. Morishita, B. D. Wirth, T. Diaz de la Rubia, and A. Kimura, "Effects of helium on radiation damage processes in iron", *4th Pacific Rim International Conference on Advanced Materials and Processing*, 2001

[66]   J. A. Jung, S. H. Kim, S. H. Shin, I. C. Bang, and J. H. Kim, "Feasibility study of fuel cladding performance for application in ultra-long cycle fast reactor," *Journal of Nuclear Materials,* vol. 440, no. 1–3, pp. 596-605, 2013.

[67]   S. I. C. Kwang Beom Ko, Ji Hyun Kim, "Multi-scale Modeling Study of Irradiation Behavior of Reduced Activation Ferritic Martensitic Steels," *The 12th International Symposium on Fusion Nuclear Technology,* 2015.

[68]   F. A. Garner, M. B. Toloczko, and B. H. Sencer, "Comparison of swelling and irradiation creep behavior of fcc-austenitic and bcc-ferritic/martensitic alloys at high neutron exposure," *Journal of Nuclear Materials,* vol. 276, no. 1, pp. 123-142, 2000/01/01/ 2000.

[69]   M. J. Banisalman, S. Park, and T. Oda, "Evaluation of the threshold displacement energy in tungsten by molecular dynamics calculations," *Journal of Nuclear Materials,* vol. 495, no. Supplement C, pp. 277-284, 2017/11/01/ 2017.

[70]   A. Rogerson, "Irradiation growth in annf,aled and 25% cold-worked zircaloy-2 between 353 - 673 K," *Journal of Nuclear Materials,* vol. 154, pp. 276-285, 1988.

[71]   E. Meslin, B. Radiguet, and M. Loyer-Prost, "Radiation-induced precipitation in a ferritic model alloy: An experimental and theoretical study," *Acta Materialia,* vol. 61, no. 16, pp. 6246-6254, 2013/09/01/ 2013.

[72]   D. O. Northwood and W. Gilbert,"Neutron radiationdamage in zirconium and itsalloys," *Radiation Effects,* vol. 22, no. 139-140, 1974.

[73]   A. A. Semenov and C. H. Woo, "Stochastic fluctuations and microstructural evolution during irradiation by neutrons and heavy ions," *Journal of Nuclear Materials,* vol. 205, pp. 74-83, 1993/10/01 1993.

Acknowledgment

지난 석사 박사 시간을 되돌아보면, 너무나 많은 분들에게 큰 도움을 받았기에, 어떻게 감사의 인사 말을 전달해야 될지 잘 모르겠습니다. 그러나 제 나름의 기준을 작용하여, 고마운 분들에게 감사의 인사 말을 전하고자 합니다.

우선, 가족인 어머니, 누나에게 감사의 인사를 제일 먼저 드리고 싶습니다. 두 분이 제에게 주신 무한한 사랑과 배려, 인내심이 있었기에 지금의 제가 있을 수 있었다고 생각합니다. 항상 감사하게 생각 하고 있습니다. 특히나, 어머니. 어머니께서 주신 사랑은 다른 이를 포용할 용기를 주셨습니다. 어머님에게 배운 강인한 정신과 사랑은 남은 인생에서 가장 중요한 이정표로서 역할을 할 것입니다. 부디, 건강하게 오래 사셔서, 제가 은혜를 갚을 시간을 보다 많이 주시기를 간절히 기원합니다.

두번째로 김지현 지도 교수님께 감사의 인사를 올립니다. 교수님께는 비단 단순한 지식뿐만 아니라, 연구자로서 갖추어야할 근본 자세, 기본 양식 및 행동 지침에 이르기까지 이루 말할 수 없을 정도의 많은 가르침을 주셨습니다. 순간 이해할 수 없는 내용을 전해 주셨지만, 언제나 시간이 지나면 그 뜻을 헤아릴 수 있었습니다. 교수님께서 주신 가치를 사회에 환원하기 위해 열심히 노력하는 사람이 되고자 하겠습니다. 감사드립니다.

또한, 이번 박사 심사위원으로서 제 연구분야의 구체적이고 전반적 지도를 해 주신 안상준 교수님께 감사의 인사를 드립니다. 그러나 무엇보다 한 인간으로서, 수렁의 빠진 저의 삶의 태도를 구해주신 교수님께 무한한 감사의 인사를 드리고 싶습니다. 언제나 치열하게 사시는 교수님의 모습을 보며 항상 부끄러운 마음을 가지고 있습니다. 교수님께서 말씀해 주셨던 철학적이고 근본적 성찰을 항상 기억하고 있겠습니다.

KAERI 계신 권준현, 이경근 박사님에게 또한 감사의 인사를 드립니다. 두 분 박사님의 선행 연구가 없었다면, 지금의 제 박사 주제에 대한 구체적 연구는 주어진 박사 기간 동안 이루어 질 수 없었을 것입니다. 특히나, 바쁘신 와중에도 전화상으로, 또는 대면으로 연구의 뼈대와 세세한 연구내용을 봐주신 이경근 박사님께 다시 한번 감사의 인사를 드립니다. 박사님의 친절하고 구체적 가르침이 있었기에 박사학위까지 다다를 수 있었습니다. 또 다른 졸업 심사위원이 되어 주신 반치범, 박재영 교수님께도 감사의 인사를 전합니다.

대학원 생활을 하다 보면, 실제적인 연구의 내용들은 모두 연구실에서 이루어 지게 됩니다. 때문에, 울산과학기술대학교 102동 406호 및 112동 514호의 일원이었던 연구실 동료들에게도 감사의 인사를 전해야만 합니다. 김기동, 유승창, 김태용, 송인영, 이윤주, 함준혁, 이정환, 이정현, 고광범, 김종진, 신상훈, 최경준, 정주앙, 김태호, 김승현에게 감사를 표합니다.

다른 연구실이지만, 이승원형, 강사라누나, 김성만형, 박성대형, 조병진형, 탁태우형을 비롯한 선배님들로부터 많은 도움을 받았습니다. 언제나 칭얼댈 때마다 받아 주셔서 감사했습니다. 선배님들의 배려로 인해 저는 언제나 기댈 수 있는 곳이 있었습니다. 감사합니다. 또한, 동기인 유동한 형님을 빼 놓을 수는 없습니다. 힘들고 지칠 때 먹여 주시고 재워 주신 은혜 잊지 않겠습니다. 형님과 같이 보낸 석사 기간이 돌이켜 보면 가장 그리울 때가 많습니다. 같이 어려움을 헤매일 때, 언제나 든든한 벗이고, 가족이었습니다. 그리고, 후배님들에게 또한 감사의 인사해야만 합니다. 석사 기간 동안에는 이주영, 백제균, 정관윤, 조태원, 이철민, 신유경, 이희재, 공치동, 김원경, 이욱제, 곽재식, 정영신, 김미진, 김인국, 서석빈 후배들에게 많은 신세를 졌습니다. 여러분들의 지원이 있었기 때문에 지금의 제가 계속해서 연구를 하고 있다고 생각합니다. 또한, 박사기간 중에는, 안교수님 연구실의 이명규, 남창현, 정연송, 김건, 안정수, 김경훈, 하웅씨의 도움을 많이 받았습니다. 특히나, 박사 졸업기간에 많은 도움을 준 명규형에게 감사함을, 함께 시간을 많이 보내준 창현에게 고마움을 표합니다. 안전 연구실의 서정일, 박종우, 강정성, 최교수님 연구실의 정현준, 이찬기 후배님에게도 감사함을 표하고 싶습니다.

그리고, 힘들 때나 슬플 때 힘이 되어준 제 친구들을 언급하고 싶습니다. 부경대 동기인 민우, 유비, 상우, 명한, 영배, 광록이 힘들 때 마다 힘이 되어줘서 고맙다. 너희들이 없었다면, 험난한 대학원 생활 어떻게 견뎠을지 모르겠다. 특히 상우에게는 격 없이 칭얼대어서 미안한 마음이 크다. 주영형 밥 많이 사줘서 고마워요. 구영리에서 자주 만나요. 호상아 너도 박사 한다고 고생이 많다. 부산에서 보자. 중학교때부터 외로움을 서로 달래 주던 인우야. 어디를 가서도 네가 준 선물을 꼭 가지고 다니마. 항상 꾸준히 연락하자. 이번에는 내가 네 생일 선물을 챙겨 주고 싶다. 또한, 고등학교때부터 주말마다 내 곁을 지켜주던 영범아. 옆에 있어주어 고맙다. 네가 주말마다 내 옆에 있어주어 든든했다. 그리고 마지막으로 박사기간 동안 제 어린 마음을 배려해 주었던, 순수하고 마음씨 고운 친구 하림에게 감사의 인사를 전하고 싶습니다.

또한, 학교 심리건강센터에 계신 신지민 상담선생님에게도 감사의 인사를 드립니다. 선생님과 보낸 시간이 있었기에, 저 자신을 용서할 수 있었고, 덕분에 학위를 잘 마칠 수 있었습니다. 마지막으로 지금까지 제 연구가 수행될 수 있도록 허락해주신 모든 분들께 인사를 드립니다. 특히나, 연구 과제 행정일을 챙겨 주신 이남기 선생님, 친구처럼 친동생처럼 살뜰히 챙겨 주신 최은정 선생님 감사합니다. 또한, 도서관에 계신 권유리 선생님께 그간 보여주신 배려와 친절에 감사를 표하고 싶습니다. 학사일정을 챙겨 주신 박소희 선생님 감사합니다. 또한, 얼굴은 실제로 보지 못하였지만, 수 많은 선행 연구자 분들, 또한, 실제적으로 학위를 진행할 수 있게 해 주신 많은 행정 선생님에게도 감사의 인사를 전해 드립니다.

2019년 1월 7일, 밤 11시 12분, 형광등이 꺼지지 않는 112동 514호에서...
-최상일 올림-